



## Applications of diamond films: a review

Ramiz Zulkharnay & Paul W. May

To cite this article: Ramiz Zulkharnay & Paul W. May (2024) Applications of diamond films: a review, Functional Diamond, 4:1, 2410160, DOI: [10.1080/26941112.2024.2410160](https://doi.org/10.1080/26941112.2024.2410160)

To link to this article: <https://doi.org/10.1080/26941112.2024.2410160>



© 2024 The Author(s). Published by Informa UK Limited, trading as Taylor & Francis Group, on behalf of Zhengzhou Research Institute for Abrasives & Grinding Co., Ltd.



Published online: 07 Oct 2024.



Submit your article to this journal [↗](#)



View related articles [↗](#)



View Crossmark data [↗](#)

## Applications of diamond films: a review

Ramiz Zulkharnay  and Paul W. May 

School of Chemistry, University of Bristol, Bristol, UK

### ABSTRACT

Ever since methods to deposit diamond in the form of thin films by chemical vapour deposition (CVD) were developed in the 1990s, an astonishing variety of applications for this material has emerged. Indeed, the number and diversity of applications for CVD diamond are now so large that they merit a dedicated review in their own right, providing a comprehensive account of the huge variety of CVD diamond applications reported to date. This review discusses mechanical applications, as well as applications in electrochemistry, high-power electronic devices, quantum technology, thermal management, electron-emission devices, diamond composite materials, optics, radiation detectors, X-ray lenses, dosimeters, biomedical applications, diamond anvil cells, nuclear fusion applications, and nuclear betavoltaic batteries. Some applications for nanodiamond particles are also reviewed.

### ARTICLE HISTORY

Received 25 April 2024

Accepted 24 September 2024

### KEYWORDS

CVD diamond applications; electronic applications; mechanical applications; optical applications; quantum applications; review

## 1. Introduction

Diamond has long been renowned for its exceptional hardness, but it also has a remarkable range of other properties, including having the highest room-temperature thermal conductivity, high transparency from the UV through the visible region to the infrared, being the stiffest material, the least compressible, and is chemically and biochemically inert [1]. With such a diverse range of extraordinary properties, it is not surprising that diamond has often been referred to as “the ultimate engineering material” [2,3]. Historically, however, it proved very difficult to exploit many of these properties, due mainly to the fact that diamond was only available in the form of natural stones or grit, which were both scarce and expensive, and for which the only real application was to be cut and polished into gemstones for use as jewellery.

The invention of the high-pressure high-temperature (HPHT) method of diamond synthesis [4] in the 1950s allowed so-called “industrial diamonds” to be manufactured in large quantities. These diamonds ranged in size from nanometres to millimetres, but the high number of defects and their off-putting yellowy-brown discolouration precluded their use in jewellery at that time. Nevertheless, these HPHT diamonds could be used for a wide range of industrial processes which exploited diamond’s hardness and wear-resistance properties, such as cutting and machining mechanical components, and for polishing and grinding of optics. Over the next

70 years this became a hugely profitable industry, and the industrial diamond market remains highly lucrative today, with an estimated annual turnover of around \$15 billion dollars (USD) [5]. Over the past 50 years, improvements in the growth process have allowed high-quality HPHT diamonds to be fabricated with defect and dislocation densities comparable to or even better than CVD diamond, especially for larger stones [6,7]. The development of smaller high-pressure presses has allowed HPHT to become the method of choice to economically and rapidly fabricate large numbers of small, but gemstone-quality, single-crystal diamond stones for the jewellery market. Near-perfect HPHT diamond substrates, which have been laser cut from the as-grown material and polished smooth, are also finding lucrative applications as the seed crystals needed for other diamond growth methods (see below).

However, the major disadvantage of the HPHT process is that it still produces diamond in the form of single-crystal stones or grit, and this severely restricts the range of applications for which it can be used. This situation changed in the early 1980s, when work pioneered in Russia, Japan, and the United States [8], led to the development of a chemical vapour deposition (CVD) process for depositing diamond in the form of layers that were nm,  $\mu\text{m}$ , or even mm thick, on a variety of substrates. Research interest in CVD diamond skyrocketed, and the price for 1 carat (0.2 g) of CVD diamond in the form of a thin coating or as a freestanding plate fell below

**CONTACT** Paul W. May  [paul.may@bristol.ac.uk](mailto:paul.may@bristol.ac.uk)

© 2024 The Author(s). Published by Informa UK Limited, trading as Taylor & Francis Group, on behalf of Zhengzhou Research Institute for Abrasives & Grinding Co., Ltd. This is an Open Access article distributed under the terms of the Creative Commons Attribution License (<http://creativecommons.org/licenses/by/4.0/>), which permits unrestricted use, distribution, and reproduction in any medium, provided the original work is properly cited. The terms on which this article has been published allow the posting of the Accepted Manuscript in a repository by the author(s) or with their consent.

\$1 for the first time in the year 2000 [2]. Suddenly, CVD diamond became significantly more accessible, and engineers finally had diamond in a form which allowed them to exploit its vast array of outstanding properties in a wide variety of applications.

Led by US companies *Diamonex* and *Norton* [9], the first application of CVD diamond to be commercialised in the 1990s exploited its extremely high thermal conductivity in the form of heat spreaders to remove the localised heat from high-power electronic devices. These heat spreaders were made from freestanding plates of CVD-grown diamond which had been chemically removed from their Si substrate. The plates were then attached to the underside of the hot device on one side and to a heat sink, radiator or cooling system on the other, allowing rapid thermal transfer away from the device. CVD diamond-coated cutting, drilling and grinding tools were developed soon afterwards [10], as these were a natural follow-on from the HPHT tools already on the market.

But the dreams were always for diamond to break into the semiconductor market, and figures-of-merit were published demonstrating that diamond could, indeed, be the ultimate semiconductor material [11]. The first devices to come onto the market were surface acoustic wave (SAW) filters, which were developed by *Sumitomo* in Japan for use in mobile phones. These exploited the fact that diamond has the highest acoustic velocity of almost all materials ( $\sim 19 \text{ km s}^{-1}$ , or  $\sim 40$  times faster than that in air) [12]. The story of SAW filters parallels that of much of diamond technology. At first, there was a great deal of optimism about the remarkable properties of diamond enabling the SAW devices to have vastly improved performance over existing ones [13]. Then came the realisation that interfacing diamond with the surrounding materials (in this case the piezoelectric material needed to convert the SAW waves into voltages and back again), was not as easy as first thought [14], so optimising the device might take many years longer than hoped. Finally, as more time went by and only incremental progress was being made in solving these difficult problems, competing materials or technologies caught up with, and finally overtook diamond. CVD diamond was abandoned for SAW devices by most manufacturers in favour of new materials that had performance specifications that were inferior to diamond but were nevertheless still an improvement over previous generations of SAW devices. In short, the competing materials may not be the best, but they were “good enough” to do the job—without all the difficulties associated with using diamond.

This story was repeated many times for different potential diamond applications. Field-emission displays using diamond and/or carbon nanotube (CNT) electron emitters gained a lot of publicity in the late 1990s, but

these eventually lost out to liquid-crystal displays (LCD), light-emitting diode (LED) and organic LED (OLED) screens [15] due to their lower price, high reliability, and the fact that working LED/OLED televisions that were “good enough” for consumers arrived in the marketplace *before* diamond ones. Not surprisingly, research and development of diamond-based field-emission displays all but ceased in the early 2000s.

Diamond, along with its amorphous-carbon analogue, diamondlike carbon (DLC), had been proposed as an excellent bioinert, wear-resistant material with which to coat artificial load-bearing joint prostheses to increase their lifetime. However, there were problems with the early DLC coatings, which had poor adhesion and spread nanosized particulates into the body [16]. This led to a lack of trust in DLC (and by association, diamond) for medical applications by the medical community, who shunned diamond, preferring to stick with tried-and-trusted materials.

From about 2000 to 2010, the lack of success in identifying a practical room-temperature *n*-type dopant for diamond, along with seemingly only incremental progress in the development and commercialisation of large-area diamond substrates, stifled the development of diamond electronics. This roadblock coincided with reports that competing materials, such as SiC [17], GaN [18] (and more recently  $\text{Ga}_2\text{O}_3$  [19]), were going from strength to strength in terms of performance and available wafer sizes. In the same period, exciting new “wonder materials,” such as graphene, promised to outperform even diamond in some applications [20]. Reluctantly, the dreams of diamond being a universally useful semiconductor were scaled back, and diamond device research became focused only upon more specialised high-power, high-voltage and/or high-frequency applications. Even so, the continuing advances in competing materials began to threaten diamond’s dominance here as well. As a result, funding for diamond device research was channelled elsewhere (particularly into graphene research), and CVD diamond technology was starting to look like a “non-starter.”

However, around the year 2010, scientists, engineers, and importantly, funding agencies, started to realise that the various competing materials were also having significant problems of their own. Graphene, in particular, had been rather overhyped, and had received multi-millions of dollars in funding with few if any “killer applications” looking likely to reach the market in the near future [21]. It seemed that diamond was now back in the game!

This resurgence was helped by three main discoveries which reignited the enthusiasm for diamond technology. The first was the discovery that a common defect in diamond (the NV-centre) could act as a source of photons that were emitted one at a time with controlled and

known properties [22]. This led to the remarkable prospect that room-temperature quantum computing might become a reality in the near future. The second exciting breakthrough was the finding that boron-doped diamond (BDD) acted as superlative electrochemical electrodes, enabling a range of new potential analytical and biosensor applications [23]. Finally, the spectacular and highly lucrative success of CVD diamond gemstones in the worldwide jewellery market [24] helped expedite the long-hoped-for technological advances in diamond growth rate and large-area deposition. The availability of single-crystal diamond (SCD) wafers with larger areas that are more compatible with standard semiconductor materials triggered a revival of interest in diamond devices, with novel field-effect transistor (FET) architectures based on delta-doping and two-dimensional hole-gas conduction being developed. The medical world, too, lost some of its reticence about using diamond; applications, such as diamond-based neural implants, bionic eyes, brain-computer interfaces, and antimicrobial coatings started to be reported [25]. The nuclear industry started taking a deeper interest in diamond, particularly in fusion research, where diamond has been studied as a protective material for the plasma-facing surfaces inside a fusion reactor, or from which to fabricate the microwave-transparent windows required by gyrotrons to transmit continuously the 100's of megawatts of power needed to maintain a fusion plasma.

Although the exuberant hype of the 1990s has now been calmed somewhat by the sedative of realism, diamond technology is currently experiencing a renaissance in terms of the astonishing amount and surprising variety of new applications being reported. Indeed, the number and diversity of applications for CVD diamond have grown to such an extent that this subject has now been granted a review in its own right. Although this review provides a comprehensive account of the variety of CVD diamond applications reported to date, it obviously cannot cover them all. Indeed, just reporting the range and variety of CVD diamond electronic devices can fill an entire book [26], while excellent detailed reviews are available for most distinct CVD diamond application fields, such as electrochemistry [27], quantum information [28], and biomedical applications [25]. Likewise, detailed information about the growth of synthetic diamond gemstones, which have applications limited only to jewellery, can be found in several recent review papers [4,24,29] as well as a book written as a guide to workers in the gem trade [30]. In contrast, this review is intended to provide a glimpse of the “big picture”—an overview of the entire spectrum of diamond applications as they currently stand in mid-2024. Hopefully, this review may convince sceptical readers that diamond is *finally* living up to its promise as the ultimate engineering material.

## 2. Mechanical applications

### 2.1. Cutting milling and grinding tools

Because of the extreme hardness of diamond, its most widely known applications are those that improve the wear resistance and cutting ability of tools, such as saw-blades, drill bits, milling tools, wire-drawing dies, and grinders [31]. In addition, diamond's extremely high thermal conductivity removes damaging heat from the cutting edge, while its low coefficient of friction aids in the removal of the cut material. These impressive thermal and wear properties mean that diamond tools can run at high speeds that would destroy most other tools or coating materials. Alternatively, when used at normal speeds, diamond tools operate at a cooler temperature than other tool materials, reducing damage to heat-sensitive workpiece materials, as well as increasing tool lifetimes by as much as a factor of 10. Indeed, ever since so-called industrial diamond became available in the 1960s, it has been possible to buy diamond-coated tools at a local hardware store for surprisingly low prices. These tools are made using HPHT diamond crystals (or natural diamond offcuts from the jewellery industry) of size typically 2–30  $\mu\text{m}$ —which are either affixed individually as a coating onto the cutting surface or sintered together with ~5% of a metal binder (usually Co) to form polycrystalline diamond (PCD) composite blocks [32]. Other coating methods, such as electroplating or resin-bonding are also used but are less common [33].

The market for such diamond-cutting tools has been estimated at around \$10 billion (USD) in 2022 and is predicted to rise to close to \$20 billion by 2030 [5]. They are used in the construction industry for drilling and cutting of concrete and other hard materials. Diamond tools are also used in quarries for cutting and extraction of natural stone blocks, as well as shaping and polishing of the final stone products. Semiconductor wafers are diced into “chips” using diamond saws, while the transportation industry uses diamond tools for making and repairing infrastructure (cutting holes in roads to lay pipes, tunnel boring, *etc.*). The automotive and aerospace industries use them extensively for cutting specialised metals, alloys, and composites that incorporate problematic materials, such as Al-Si, Mg-Si, copper, graphite, carbon-fibre composites, metal matrix materials, green ceramics, fibre-reinforced plastics, and many non-metallic materials, such as wood, paper brick, cement, and printed circuit boards. Companies that drill for minerals, natural gas, and oil are huge users of diamond tools [34].

The advent of CVD diamond in the 1990s meant that tools could now be manufactured with cutting edges toughened by a conformal layer of diamond. The advantage of using CVD diamond coatings over “glued-on” HPHT grit or PCD blocks is that the CVD film is generally smoother, meaning the cuts have more precision, while

the coherent uniform nature of a CVD diamond coating affords it higher rigidity and higher thermal conductivity, enabling higher cutting speeds [35]. CVD diamond can also coat complex three-dimensional tool structures, allowing them to be used for micromachining applications, such as dental drills [36]. Larger diamonds with laser-cut holes are also used as dies for wire drawing [37].

Although the early problems of coating tungsten-carbide tools with CVD diamond have largely been solved [38], if used incorrectly, CVD diamond coatings deposited onto other tool materials can crack and delaminate. Currently, a lot of research effort is being put into solving the difficulties of depositing smooth, adherent diamond films onto metallic substrates, such as high-speed steel tools. These problems arise from the difference in the thermal expansion rates between the diamond and most other materials, as well as the limited choice of substrate material due to the high temperatures required for CVD. Another limitation of the use of diamond tools is that they cannot be used for non-ferrous metals, such as Co, Ni, Cr, V, and Fe (including most steels) due to their propensity to react with the diamond and form carbides at the high temperatures generated in the cutting process.

In 2022, CVD diamond-coated tools occupied only about 35% of the overall diamond-tool market [39], but that market is so huge that even this share is highly lucrative. HPHT diamond will still dominate the tool industry for many years to come, but as advances in deposition technology appear, CVD diamond might begin to take an increasingly larger share of the cutting-tool market.

## 2.2. AFM tips

In atomic force microscopy (AFM) a sharp tip, with a radius typically several nm to tens of nm, is located at the end of a stiff but flexible cantilever, usually made from Si or silicon nitride. The force interactions between the tip and the sample are recorded by monitoring the deflection of the cantilever using a laser, as the tip is scanned across the surface. The tip shape and radius predominantly determine the achievable lateral resolution. However, changes due to damage or wear of the tip frequently cause artefacts in AFM measurements [40]. This is a major problem in contact-mode imaging where the tip remains in continuous contact with the sample surface while it is dragged along. Adsorption of particles, molecules, or other nanoscale detritus onto the tip may also create imaging artefacts, *e.g.*, “multiple feature” images.

Such imaging artefacts can be minimised by using diamond AFM probes because these are less prone to wear and damage. For example, Agrawal *et al.* [41] demonstrated that AFM tips made from nanocrystalline CVD diamond are almost ten times more wear-resistant compared to commercially available silicon nitride AFM tips when imaging ultra-hard surfaces. Adsorption of particulates is also decreased on diamond AFM tips due

to the chemical inertness of diamond. Another advantage of diamond AFM probes is that, due to their high thermal conductivity, they can rapidly achieve thermal equilibrium conditions with the sample surface when in contact with it. This is important when analysing delicate biological samples which may be temperature sensitive.

Diamond AFM tips can be fabricated by coating a Si tip with a conformal layer of nanocrystalline diamond, or by using a SCD that has been etched to the correct shape and sharpness. Nowadays, such diamond AFM tips can be purchased commercially from a wide range of manufacturers.

Standard diamond AFM tips can be modified to provide extra functionality. Using electrically conducting BDD tips allows the AFM to be used for conductivity measurements with nanoscale lateral resolution, as well as acting as a micro- or nano-electrode in electrochemical analysis (see Section 3.3). Incorporating an NV-centre (see Section 5) into the end of the diamond tip allows a scanning AFM to be used for a variety of quantum sensing applications (see Section 5.3). A review of diamond AFM tips and their use can be found in Ref. [42].

## 3. Electrochemistry

Highly boron-doped diamond (BDD) exhibits electrical conductivity comparable to that of many metals, thus making it suitable as an electrode material for electrochemical redox reactions. Compared to conventional electrodes made from gold, platinum, or glassy carbon, those composed of or coated with BDD offer numerous advantages for electrochemistry [23,27,43]. Their primary benefit lies in the significantly broader operating range, enabling operation within potentials ranging from  $-1$  to  $+1.8$  V (see Figure 1). This facilitates the detection or analysis of redox species typically beyond the operating range of conventional electrodes [44]. Moreover, the signal response is flat within this operating window, which means there is virtually no background or

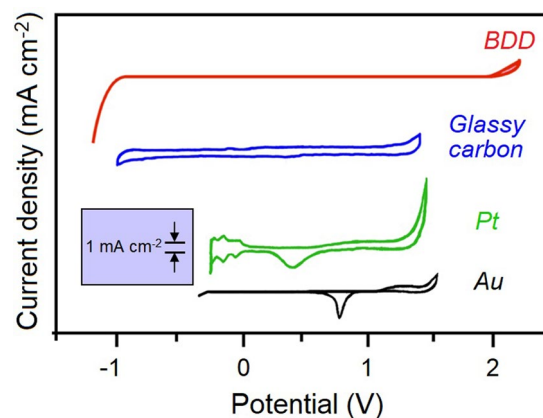


Figure 1. The potential windows of several different electrochemical electrodes. Redrawn using data from Ref. [44].

capacitance, allowing the BDD electrodes to be highly sensitive to small changes in analyte concentration. BDD electrodes are therefore able to detect compounds at nanomolar [*i.e.*, parts per billion (ppb)] concentrations, even when chemically similar species are also present (see Figure 2(a)). Moreover, BDD electrodes are chemically inert and resistant to corrosion under conditions of elevated temperatures and pressures, as well as in environments hostile to other electrode materials. Diamond is also recognised as being bioinert, *i.e.*, it does not elicit immune responses, including inflammation or rejection in living cells, allowing it to be used in various biochemical environments or inside living organisms. Additionally, BDD electrodes can be patterned into various micro- or nanosized structures, for example, nanowires [46], foams [47], fibres [48], and needles [45]. Such nanostructures can increase the active electrochemical surface area by up to 1000 times, together with an associated huge increase in sensitivity [45] (see Figures 2(b,c)). Furthermore, as well as BDD electrodes being mechanically robust, they exhibit significantly lower fouling propensity compared to traditional electrodes. Even in the event of fouling, they can be electrochemically cleaned *in situ* [49].

It must be emphasised, however, that there are many different varieties of BDD electrodes, and their electrochemical performance is critically dependent on various factors, such as the diamond grain size (*i.e.*, the number of grain boundaries and their  $sp^2$  carbon content), the roughness of the surface and its average crystallite orientation, as well as the B-doping level and uniformity, and surface functionality (*e.g.*, hydrophobic O-termination or hydrophilic H-termination) [27].

BDD electrode material or prefabricated BDD electrodes themselves can be purchased from several companies, including *Element Six* (UK) [50], *Condias* (Germany) [51], *Sumitomo Chemical* (Japan) [52], *Boromond* (China) [53], *sp<sup>3</sup> Diamond Technologies* (USA) [54], and nowadays are even available on *Amazon* [55]. Worldwide, there are currently around 50 research groups using BDD electrodes for a range of electrochemical applications.

### 3.1. Electrochemical analysis and assaying

A hugely important application for BDD electrodes is to determine the identity and concentration of contaminants or impurities in liquid samples, for example, pollutants in lakes and rivers. Conventional electrodes are often unsuitable for this purpose due to their catalysing the oxidation and/or reduction of water at lower potentials than those required to detect many target compounds. In contrast, with their much wider aqueous potential window, BDD electrodes play a key role here in enabling the detection in water supply systems of contaminants, such as heavy metals (Hg [56], Cd, Pb, Ni

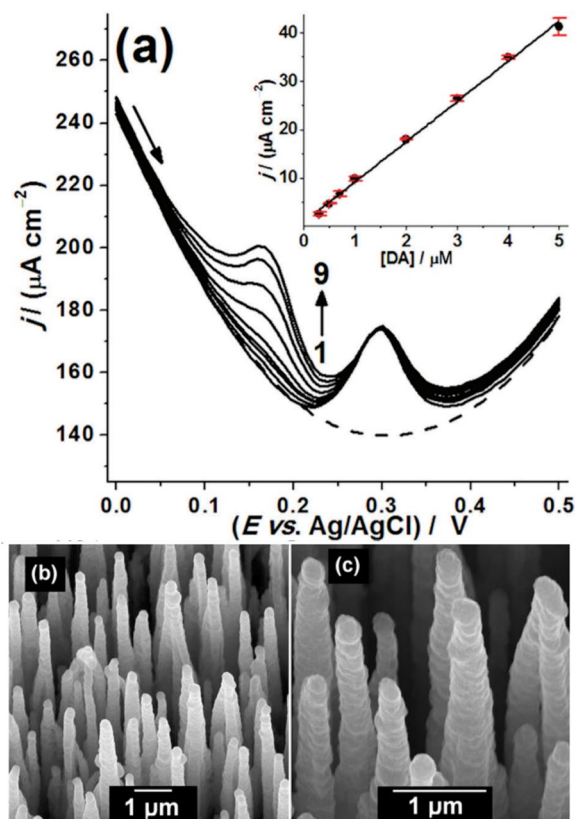


**Figure 2.** An example of nanostructured BDD electrodes being used for highly sensitive and selective electrochemical trace analysis in water. (a) Differential pulse voltammograms recorded for different concentrations (plots 1–9; 0–5  $\mu\text{M}$ ) of dopamine (DA) in the presence of 30  $\mu\text{M}$  uric acid—a chemically similar analyte. Inset: Current density  $j$  ( $\mu\text{A cm}^{-2}$ ) vs. concentration of dopamine ( $\mu\text{M}$ ) showing a linear response with concentration. (b,c) SEM images of nanostructured BDD needles on the surface of an electrode, with an electrochemically active area 220 times larger than that of a flat diamond electrode. Figures reprinted under CC BY 4.0 licence from Ref. [45] (published by the Royal Society of Chemistry).

[57], As [58]), polycyclic aromatics (PCAs) and pesticides [59], hormones and estrogenic compounds [60], explosives [61], neurotransmitters, such as dopamine [45], drugs (paracetamol, narcotics, pharmaceuticals) [62], and water-soluble nerve agents [61].

### 3.2. *In situ* medical diagnostics

Due to its bioinert properties, an important emerging application for BDD electrodes is for electrochemical measurements to be made *inside* a living organism. For this, micron-sized electrodes are needed [63], which are fabricated by coating a sharpened wire (usually made from W or Pt) with BDD. In neuroscience, these tiny BDD electrodes can be positioned inside a cell near the site(s) of the release and/or action of neurosignalling molecules, providing key information about the concentration changes of key molecules as a biological process occurs. For example, BDD microelectrodes have been used to measure the release of

noradrenalin from sympathetic nerves [64], as well as the release of serotonin from enterochromaffin cells in the small and large intestine during digestion [65]. However, one problem with using BDD for *in vivo* sensing is that BDD electrodes are rigid, which makes them difficult to implant into soft tissue. To solve this, a flexible microelectrode was fabricated by depositing BDD onto Parylene C [66]. This bendable electrochemical sensor can detect dopamine in the presence of ascorbic acid and has been used to record the neural activity inside a living rat. Such studies are still relatively new, but they hold significant promise for advancing future medical diagnostics.

### 3.3. Modified BDD electrodes

Alongside electrochemistry using planar macroscopic BDD electrodes, a relatively new and thriving field of study is the use of nanostructured or modified BDD electrodes. Examples of such BDD nanostructures include nanotextures, nanowires, networks, porous films, nanoelectrodes and undoped/BDD nanoparticles, and their uses are reviewed in detail in Ref. [67]. Likewise, BDD electrodes have been decorated with a range of metal nanoparticles for different analytical applications, reviewed in Refs. [43,68]. Often, the case here is that the metal nanoparticles are employed for studying specific analytes or performing bespoke tasks, such as catalysis, while the BDD electrode serves as a chemically inert yet electrically conducting support. Some recent representative examples of the use of nanoparticle-decorated BDD electrodes include the use of Pt for biosensors [69], Ag for analysis of ceftizoxime [70], Au for proton detection [71], tumour-marker sensing [72], and Hg analysis [73]), Ni as an immunosensor [74], and Bi for detection of Zn, Cd, and Pb ions [75].

### 3.4. CO<sub>2</sub> reduction

Another important application for BDD electrodes is to facilitate useful electrochemical reactions [43]. As mentioned above, to enhance the specificity of the reaction, high-surface-area catalytically active metal or metal-oxide nanoparticles are sometimes used to decorate the bare BDD electrodes. A key advantage of BDD electrodes in this context is their low background current, which mitigates the generation of H<sub>2</sub> gas resulting from the breakdown of the aqueous electrolyte, thereby preventing potential interference with the desired electrochemical reaction.

A topic currently generating much scientific interest is the capturing of carbon dioxide from the air and then converting it into chemically useful compounds, such as formaldehyde, formic acid or methanol [76]. This can be achieved using metal-nanoparticle-decorated BDD

electrodes. However, alongside the metal/electrode stability and reactivity (especially at low overpotentials), a key focus is the metal catalyst's ability to produce a single compound selectively and with high efficiency. For example, it was recently reported [77] that CeO<sub>2</sub>-decorated BDD electrodes allowed electrochemical reduction of CO<sub>2</sub> at overpotentials <50 mV with stable performance for many hours, producing formic acid with >40% Faradaic yield. When Pt-decorated BDD electrodes were employed to study the CO<sub>2</sub>-reduction reaction, its efficiency was found to depend upon the NaCl/KCl electrolyte composition and concentration [78]. Similarly, when BDD electrodes decorated with Ir were used to synthesise formic acid using a low overpotential of -1.7 V, a Faradaic efficiency of ~50% was achieved [79]. Cu-modified BDD electrodes have also been used to produce C<sub>2</sub>- and C<sub>3</sub>-containing molecules (such as ethanol, acetaldehyde, and acetone) by electrochemically reducing CO<sub>2</sub> at room temperature, with the concentration distribution of the three products depending upon the applied potential and the amount of Cu deposited [80].

### 3.5. Electrochemical water splitting (EWS)

EWS is the process whereby water is converted electrochemically into gaseous H<sub>2</sub> and O<sub>2</sub>. The process consists of two key inner-sphere reactions, the hydrogen-evolution reaction (HER) and the oxygen-evolution reaction (OER), which both involve the adsorption onto the electrodes of various reaction intermediates consisting of multi-step electron-transfer processes [81]. The H<sub>2</sub> gas that is produced can subsequently be reacted with oxygen in fuel cells to produce electrical power directly, or in combustion tanks to create heat and generate power indirectly *via* a turbine. Thus, critical to hydrogen power generation and the so-called "hydrogen economy" is the development of a cheap and efficient EWS process [82]. However, BDD's wide potential window—which is beneficial in electroanalysis—is detrimental to EWS, because a high overvoltage is now required for water splitting [83]. Ironically, diamond's chemical inertness means that the intermediate species involved in the HER and OER are less easily adsorbed onto the electrode surface, reducing the EWS catalytic efficiency on bare BDD electrodes [83].

However, when the BDD electrodes are decorated with nanoparticles, the situation changes, because the nanoparticles now serve as the catalyst and lower the overpotential required for EWS, while the BDD electrodes act as electrically conductive supports. For example, BDD electrodes coated with Ir-black powder are reported to increase the efficiency of the OER [84], while BDD electrodes decorated with CuO and ZnO nanoparticles improve the effectiveness of the whole EWS process [85].

A complementary method to EWS entails harnessing solar energy for the photocatalytic splitting of water. For this process, a suitable photoelectrode, such as Si, was employed to convert sunlight into electrical current, subsequently powering the EWS reaction [86]. However, a gradual degradation of the Si photoelectrodes was observed upon contact with the electrolyte. To mitigate this issue, the photoelectrodes were coated with a protective BDD layer decorated with a cobalt phosphate catalyst. The photocurrent generated by these protected electrodes was directed into the aqueous electrolyte and found to be sufficient to drive EWS—importantly *without* Si degradation. Likewise, nanostructured BDD electrodes coated by a thin layer of *n*-type photoactive TiO<sub>2</sub> developed a high photocurrent suitable for EWS [87]. BDD electrodes decorated with Cu<sub>2</sub>O nanoparticles also act as efficient photocathodes for hydrogen generation using solar radiation [88]. Indeed, there are a large number of possible metal and metal-oxide catalysts that can be used together with BDD electrodes for solar-driven photo-EWS [89], most of which have yet to be studied. This is an area where huge progress may be possible in the next few years.

### 3.6. Water purification

Detecting possible toxic compounds and ions in water sources is only the first part of the problem. Arguably the more difficult part involves subsequently cleaning up the water, *i.e.*, removing organic toxins, such as chemical agents [90] or bacteria/viruses [91]. So-called electrolytic destruction [92] involves using a series of electrodes to pass a current of many tens of amperes through the contaminated water. The high current breaks apart any dissolved or suspended molecules or particles; the organic components are converted into CO<sub>2</sub>, while any toxins are rendered harmless. However, such high currents sustained for long periods of time (hours, days, or even continuously) cause rapid degradation of most electrodes. These must then be regularly replaced, greatly increasing the operating costs. In this regard, BDD is more robust than most alternative electrode materials, enabling higher currents to be used for longer periods, thereby lengthening the time required between replacements [93].

In large-scale water purification, one of the most environmentally important challenges is to electrolytically destroy endocrine-disrupting chemicals (EDCs) that are found as contaminants in wastewater effluents [94]. EDCs are compounds that interfere with the function of the endocrine system in fish, birds, and mammals. Unfortunately, they are also commonly used in a wide range of industrial and agricultural products, including pesticides, some plastics, surfactants, and preservatives [95]. Reports show that many of these EDCs in small-scale water samples can be destroyed with very high

removal efficiencies using BDD anodes. However, scaling this up to enable the treatment of rivers or lakes is a difficult problem [94].

Commercial water-purification systems based on BDD-electrode technology are currently available from several companies, *e.g.*, *Proaqua* (Austria) [96] and *Weo* (France) [97]. At present, these BDD water-purification systems are suitable for household supplies, or perhaps a small factory, but not yet for larger-scale use. On a smaller scale, a company called *Enozo* [98] has recently miniaturised this technology to produce micro-ozone cells, which are being sold as a “green” replacement for bleach, alcohol or other cleaning fluids, in the form of household cleaning sprays.

### 3.7. Dye-sensitised solar cells (DSSCs)

In these devices, sunlight passes through a transparent electrode and excites electrons in the dye layer, which then flow into the conduction band of an adjacent *n*-type semiconductor (*e.g.*, TiO<sub>2</sub> or *n*-Si). The electrons then flow toward the transparent electrode where they are collected for powering a load or charging a battery. The electrons flowing through the external circuit are re-introduced into the cell *via* a counter electrode on the back, and flow into the electrolyte. The electrolyte then transports the electrons back to the dye layer completing the circuit.

Although other carbon-based materials, such as CNTs and graphene have been used as counter electrodes in DSSCs [99], there are very few reports describing the use of BDD for this purpose. In 2011, Vispute *et al.* [100] reported the successful use of CVD diamond as a DSSC counter electrode, however, this had very low efficiency due to the diamond being undoped. Oddly, the obvious improvement in conducting BDD has never been reported in the years since then.

### 3.8. Solvated electrons

Illuminating diamond with light at photon energies greater than the band gap of diamond (5.47 eV,  $\lambda < 225$  nm), excites electrons from the valence band into the conduction band. H-terminated diamond exhibits a negative electron affinity surface (see Section 7.1) which means that no potential barrier needs to be overcome for these excited electrons to escape the surface, and they can do so with several eV of kinetic energy. If, instead of air or a vacuum, water is present above the diamond surface, the high-energy emitted electrons may react with the water molecules to form “solvated electrons.” These are stable complexes where individual isolated electrons are surrounded by a cluster of polar water molecules [101]. Solvated electrons have an electrochemical potential of  $-4.6$  eV (*versus* a standard hydrogen electrode) which makes them extremely reactive reducing

agents that can drive chemical reactions that are impossible through conventional means.

In 2013, the group at the University of Madison-Wisconsin led by Robert Hamers first reported the spectroscopic detection of solvated electrons originating from electrons photo-emitted from diamond into water following irradiation with a pulsed 213 nm-laser [102]. The high-energy solvated electrons generated by irradiated diamond have subsequently been reported to facilitate several electrochemical reactions [103]. An example is the reaction between  $N_2$  gas and  $H_2$  gas to form  $NH_3$ , which usually requires very demanding high-temperature and high-pressure conditions due to both the high energy of the intermediates and the unwillingness of the reactants to adsorb on a solid catalyst or electrode. Solvated electrons avoid these limitations allowing the reaction to proceed at less extreme conditions [104]. This approach has successfully demonstrated the production of  $NH_3$  in both single-compartment and dual-compartment electrochemical cells [105] and improved further by using  $NH_2$ -terminated diamond [106], and by decorating the BDD electrodes with Ag nanoparticles [107]. Solvated electrons generated from diamond electrodes have also been used to reduce  $CO_2$  to CO with 95% efficiency [108].

Although solvated-electron chemistry is an extremely exciting development, in the decade since this process was first reported, surprisingly few reports of new reactions have appeared in the literature, possibly because other workers have found reproducing the exact conditions to be rather challenging. A few intriguing publications still appear occasionally [109], but mainstream adoption of this technology has been rather limited.

#### 4. Electronic devices

Compared to other wide-band-gap semiconductors, such as SiC or GaN, diamond has several advantages for device fabrication. These include its high hole and electron mobilities ( $>2000\text{ cm}^2\text{ V}^{-1}\text{ s}^{-1}$ ), high critical electric field ( $>10\text{ MV cm}^{-1}$ ), extremely high thermal conductivity ( $\sim 22\text{ W cm}^{-1}\text{ K}^{-1}$ ) and very wide band gap (5.47 eV) [110]. Consequently, diamond is considered to be an ideal semiconducting material for a large variety of applications in the medium-to-high-power regime. These are discussed in great detail in the recent excellent reviews by Donato *et al.* [111] and Araujo *et al.* [112], and in the book by Koizumi *et al.* [26]. However, many of these devices might currently be considered rather specialised because, rather than mainstream consumer electronics, they are focused on high-power, high-frequency and/or high-temperature applications. With improved efficiency in power electronics together with countries becoming more environmentally aware, such “niche” applications are starting to appear more important for everyday life. For example, in the UK there is a

loss of  $\sim 8\%$  of the generated energy by simply processing electricity along the chain from primary sources, such as power stations, solar farms, *etc.*, to end-users, like homes, shops and factories, houses [113], and these losses be considerably higher in larger countries with extensive power networks. The majority of these losses come from the use of inefficient Si-based power-conversion systems along the national grid at places like electricity sub-stations. Replacing these old Si devices with diamond-based power converters, that can switch higher power loads with fewer losses and at higher frequencies, could significantly reduce these energy losses—and on a national scale, this simple change could make a hugely positive environmental impact.

More generally, there are several problems that have hampered progress in diamond electronics since the early 1990s. Arguably, the most important issue is the continued lack of a suitable *n*-type dopant for diamond [114], without which many types of semiconductor devices are impossible. The second problem—the frustratingly slow progress in commercialising large-area SCD wafers—has also greatly hindered device development. For comparison, the standard wafer size used in SiC device fabrication is 150 mm (6 inches), and many SiC fabrication facilities are already moving to 200 mm (8 inch) wafers. Likewise, GaN-on-Si wafers can be bought relatively cheaply at all sizes up to 200 mm, and even gallium oxide, which is a relatively new semiconductor material, can be purchased as single-crystal wafers up to 100 mm (4 inch). Although significant progress has been made in recent years with increasing the size of SCD wafers, the diamond substrates that are currently commercially available in reasonable quantities are only 1 inch (25 mm) in diameter. This is not only significantly smaller than competing materials, but the diamond wafers are also substantially more expensive. Undoubtedly, over the next few years diamond-wafer sizes will increase while prices will fall. But the question is—as we saw earlier—whether the semiconductor industry will hang around waiting for diamond technology to catch up, or simply “make do” with the existing materials because they are “good enough” for most applications, and crucially, are available now.

##### 4.1. Schottky diodes (SDs)

These are probably the most studied type of diamond device [115] due to the lack of a suitable *n*-type dopant for diamond. SDs only require *p*-type diamond and so are a practical choice for researchers to prove to funding bodies that diamond has the potential to be used in useful, commercial devices.

A SD is formed by the junction of a semiconductor with a metal. This junction acts as a diode, in one direction (forward) it has low electrical resistance and therefore only a low forward voltage is needed to conduct

current. Conversely, the reverse direction has a high resistance that blocks current flowing backwards. If the semiconductor is  $p$ -type diamond, then the forward voltage is very low, while the reverse voltage is extremely high, which enables efficient operation of high-power systems operating at up to 20 A and at temperatures as high as 500 K, with little energy loss [116].

Because of its low serial resistance, a vertical structure is one of the most popular geometrical configurations used for diamond SDs. It is characterised by electrical current travelling vertically from a highly conductive substrate through several layers of different composition and conductivity, to a top electrode. Many different versions of vertical diodes have been reported, as shown in Figure 3. The difficulty with obtaining large-area heavily doped SCD substrates has led to the development of pseudo-vertical diamond SDs (Figure 3(b)), where layers of heavily doped  $p^+$  diamond are grown on top of a standard undoped SCD substrate. To improve the uniformity of the diamond-metal junction, as well as to reduce leakage currents which may result in premature breakdown of the device, different metals, such as W, Zr, Cu, and Pt, and surface treatments have been studied. For example, a pseudo-vertical diamond SD using Zr has been reported which operates at  $1000 \text{ A cm}^{-2}$  at 6 V with a high reverse breakdown field  $>7.7 \text{ MV cm}^{-1}$  [117]. Despite the poor performance of  $n$ -type diamond, some diodes using this material have still been reported, although the high resistance of the  $p$ - $n$  junction often limits their efficiency [118]. Nevertheless, various so-called PIN devices and Schottky PN diodes (see

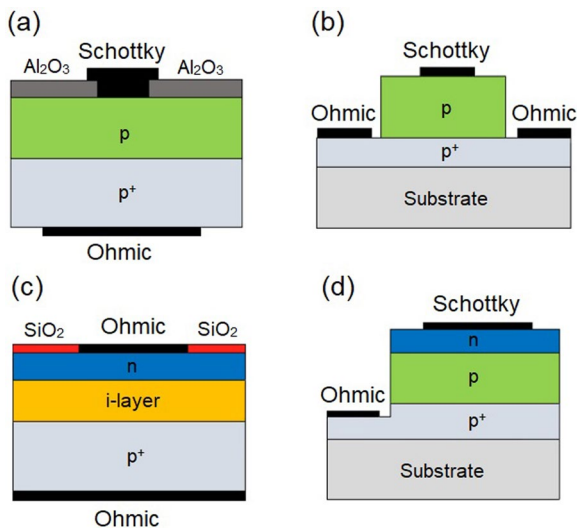


**Figure 3.** Different types of diamond diodes. Diamond layers are labelled: “ $p$ ” =  $p$ -doped, “ $n$ ” =  $n$ -doped, “ $p^+$ ” = heavily  $p$ -doped, “ $i$ -layer” = intrinsic undoped. (a) Vertical Schottky diode using only  $p$ -type diamond. (b) Pseudo-vertical Schottky diode which uses only  $p$ -type diamond but no back contact. (c) a PIN diode composed of an undoped intrinsic diamond layer sandwiched between a layer of  $p^+$ -type diamond and an  $n$ -type diamond layer on top, with ohmic contacts on either side. (d) Schottky PN diode. Figure reproduced from Ref. [111] and modified under the Creative Commons Attribution 3.0 licence.

Figures 3(c,d)) have been fabricated with promising electrical characteristics [111]. There are also diode structures which operate using electron emission from the diamond surface, and these are discussed in Section 7.5.

## 4.2. Field effect transistors (FETs)

These devices control the flow of current from one electrode (the source) to another (the drain) by applying a voltage to a third electrode (the gate). The gate voltage alters the conductivity of the material between the drain and source, allowing the FET to be used as a current amplifier (a small gate voltage controls a much larger source-drain current) or a digital on/off switch for binary electronics. The current through a FET involves either electrons or holes, but not both. As such, FETs can be fabricated using only  $p$ -type diamond. FET devices come in many different shapes and forms, but the ones which have been applied most to diamond are described in the next few sections.

### 4.2.1. Surface-channel FET devices

These devices usually employ a MOS (metal-oxide-semiconductor) structure for the gate electrode. Here, a highly conducting metallic gate electrode is electrically isolated from a semiconductor (in this case, doped diamond) substrate by a very thin oxide layer (see Figure 4). When a voltage is applied to the gate, carriers (electrons or holes) in the bulk are attracted towards the gate but become trapped and build up beneath the insulating oxide. With enough carriers present, a thin conducting channel is created temporarily, connecting the source to the drain, and allowing current to flow between them.

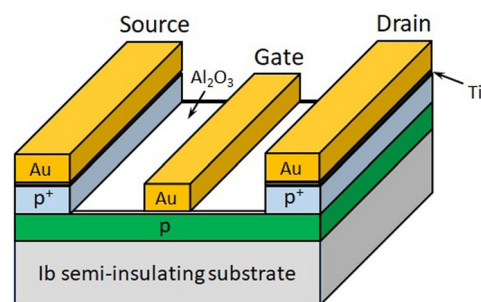


**Figure 4.** A typical design for a diamond lateral deep-depletion MOSFET-style device. A  $p$ -type BDD layer labelled “ $p$ ” is deposited homoepitaxially onto a standard type-1b diamond (usually HPHT) substrate. The source and drain electrodes are composed of heavily BDD labelled “ $p^+$ ”. Electrical contact to the BDD is improved by depositing thin capping layers of first, titanium (which when heated forms a carbide by reaction with the diamond), and second, of highly conducting metal, such as gold, which also prevents the Ti from oxidising in ambient air. These electrodes are patterned using standard photolithography and dry etching methods. The Au gate electrode is electrically isolated from the BDD layer by a thin gate oxide, in this case made from insulating  $\text{Al}_2\text{O}_3$ . Image reproduced and modified from Ref. [111] under the Creative Commons Attribution 3.0 licence.

When the gate voltage is switched off, the channel disappears, and the current flow stops.

Many variations of diamond-based MOSFET devices have been fabricated, with varying degrees of success. One problem with diamond FETs is that carbon (diamond) does not have a solid oxide, meaning the gate oxide has to be deposited in the form of a thin metal-oxide layer. The poor interface between these metal oxides and diamond is often highly defective, which disrupts the carrier mobility through the channel. Various diamond–metal-oxide interfaces have been studied [119], with  $\text{Al}_2\text{O}_3$  so far exhibiting the best performance [120]. The most efficient FET devices are CMOS (complementary MOS) which include both  $p$ - and  $n$ -type devices on the same wafer. Here, again, we run into the problem of  $n$ -type doping for diamond, and so most diamond FETs reported are  $p$ -channel devices.

These difficulties in making standard MOS devices have led to a range of new FET designs. One of these, called a finFET [121], has demonstrated reasonable device performance, but shows a rather high negative threshold voltage indicative of the presence of a high level of interface defects. The gate-oxide problem can be eliminated by using novel device designs which do not require a gate-oxide layer, such as Junction FETs (JFETs), metal-semiconductor FETs (MESFETs) and bipolar transistors. These devices are reviewed in detail in Ref. [111], and improvements in their performance are continually being made, albeit it at a rather slow pace. Unfortunately, competing materials, in particular SiC, have more than a decade's head start on diamond, and they may capture the market for high-power, high-temperature devices before superior diamond devices become commercially available. It may be that the prize is won by the material that delivers the solution *first*, not the one that works best.

For all the SD and FET devices mentioned in the sections above, the comprehensive analysis conducted by Donato *et al.* [111] has suggested that diamond may remain limited to devices with high junction temperatures ( $>450\text{ K}$ ), medium-high frequency ( $>20\text{ kHz}$ ), and high-voltage ( $>3\text{ kV}$ )—where they should outperform SiC and GaN commercial alternatives—for some time. Nevertheless, there are several more specialised diamond-based devices that may not suffer these limitations, as discussed in the following sections.

#### 4.2.2. $\delta$ -doped devices

So-called “delta doping” requires the epitaxial growth of a very thin ( $<2\text{ nm}$ ) heavily BDD subsurface layer with B concentration above the limit required for conductivity to become metallic. Due to its similarity to the abrupt “ $\delta$ -function” in mathematics, this highly conducting layer is called a “delta-doped layer” because it has atomically smooth and sharp interfaces with the undoped diamond layers immediately above and below it. Several research groups have reported attempts to make  $\delta$ -doped

FET devices [26,122], but controlling the concentration profile of the B dopant to near atomic-level precision is so difficult that results remain disappointing.

#### 4.2.3. 2-Dimensional hole gas (2DHG) FET devices

One promising design of diamond FET device is based on “surface transfer doping”—an unusual property of the diamond surface identified in 2004 [123,124]. Hydrogen-terminated diamond displays a surface dipole due to the electronegativity difference between the bulk carbon atoms and the surface H atoms. When this polar surface is exposed to ambient air, electron-accepting molecules adsorb onto the surface. Electrons from the bulk diamond then transfer to the adsorbates, which become negatively charged. Lacking electrons, the diamond forms a positively charged two-dimensional layer a few nm thick, located just below the surface, containing a high concentration of holes ( $10^{12}$ – $10^{13}\text{ cm}^{-2}$ ) [125]. Although constrained within this 2-dimensional layer, the highly mobile holes (mobility  $\sim 50$ – $120\text{ cm}^2\text{ V}^{-1}\text{ s}^{-1}$ ) possess many of the properties of a gas; thus the layer is termed a “2-dimensional hole-gas” (2DHG) [126]. Unfortunately, the electrical conductivity of the 2DHG layer can be altered or even destroyed by simply changing the atmosphere (pressure, humidity, temperature, *etc.*) above the surface, because this changes the nature and concentration of the adsorbates. One method to stabilise this fragile conductive layer is to cap the diamond surface with a protective layer of an electron-accepting oxide, such as  $\text{V}_2\text{O}_5$ ,  $\text{MoO}_3$ , or for optimal performance,  $\text{Al}_2\text{O}_3$  deposited by atomic-layer deposition (ALD) [127]. This capping layer hermetically seals the surface while also replacing the role of adsorbates in providing surface acceptors to generate and stabilise the 2DHG layer (see Figure 5). Research groups (*e.g.*, at Waseda University (Tokyo) [128] and Glasgow University [124]) have pioneered novel FET devices in which the source-drain current, moderated *via* a gate voltage, now travels through this 2DHG conductive layer, rather than through the semiconducting substrate.

#### 4.2.4. Accumulation-channel devices

In the last couple of years new variants on the 2DHG device have been developed where the device operation

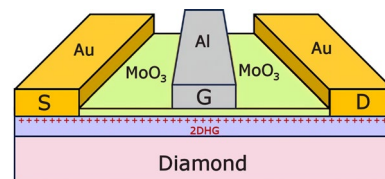


**Figure 5.** Schematic cross-sectional view of a diamond-based MOSFET device utilising the 2DHG conduction channel in H-terminated diamond protected by a  $\text{MoO}_3$  capping layer. S, G, and D refer to source, gate, and drain, respectively. For improved performance, often ALD-deposited  $\text{Al}_2\text{O}_3$  rather than  $\text{MoO}_3$  is used directly under the gate.

is dominated by field-effect carrier accumulation across the entire channel—more like that in a conventional Si MOSFET. Such a device architecture has been successfully implemented by replacing the C–H diamond termination with a layer of oxidised Si [129]. Due to the similar electronegativities of C and Si, the C–Si surface bonds generate only a small surface dipole compared to that of C–H bonds. Nevertheless, electrical measurements show that the source-drain channel is conducting, but has a conductivity  $\sim 3$  orders of magnitude lower than that seen with H termination, suggesting a comparably low-carrier-density 2DHG layer has probably been created. Therefore, to attract sufficient carriers into the channel, the *entire* source-drain region is gated (rather than just the region under the small gate electrode as in normal MOSFETs, like that shown in Figure 5). When a voltage is applied to this large gate, carriers can be attracted into the whole channel from the nearby ohmic-contact regions, and the device operates more like a typical FET.

Similarly, a Japanese group have recently reported fabricating *p*-channel FETs that use a hydrogenated diamond channel and an h-BN layer as a gate dielectric to reduce coulomb scattering and increase mobility [130]. These devices, again, operate as accumulation-channel FETs and require a gate voltage across the whole channel to generate the 2DHG. The devices exhibit very promising characteristics: a low sheet resistance ( $1.4\text{ k}\Omega$ ) and high on-current ( $200\text{ mA mm}^{-1}$ ) with a very high Hall mobility ( $680\text{ cm}^2\text{ V}^{-1}\text{ s}^{-1}$ ) at room temperature.

However, for both of these types of preliminary accumulation-channel architectures reported to date, the necessity to gate the whole channel may become a problem for high-power and high-frequency electronics due to the reduced breakdown voltages and the parasitic capacitances associated with the close proximity of the gate to the ohmic source-drain contacts.

Nevertheless, many of the 2DHG FETs mentioned in Section 4.2.3 and their accumulation-channel counterparts in this section exhibit excellent device performance [129], and offer huge promise for future development. The transfer-doping and accumulation-channel processes are intrinsically less thermally sensitive than standard impurity doping, and so could well be a better choice for electronics that need to operate across a wide temperature range. Furthermore, because they are fabricated directly onto an insulating diamond substrate, these devices should be considerably more radiation hard compared to standard Si-based devices, making them suitable for applications in space, nuclear power stations, or military equipment, as outlined in the next section.

#### 4.3. Radiation-hard devices

Most electronics based on Si, GaAs, GaN, or similar semiconductor materials, are unfortunately not

radiation-hard [131]. The radiation resistance of some devices, however, can be improved by using insulating substrates, such as silicon-on-sapphire (SoS) or silicon-on-insulator (SoI) wafers. In a variation of SoI technology, the insulator is an undoped insulating CVD diamond substrate, onto which the active semiconductor layer (*e.g.*, Si or GaN) is deposited. Such silicon-on-diamond (SoD) [132] or GaN-on-diamond (GoD) [133] technologies are currently being developed for thermal management in high-power devices (see Section 6). Studies suggest that SoD devices out-perform their SoI equivalents while being significantly more radiation hard [134]. The surface-transfer-doped FETs and accumulation-channel FETs described in Sections 4.2.3 and 4.2.4, respectively, are also inherently radiation-hard.

#### 4.4. SAW filters

Surface acoustic wave (SAW) filters remove unwanted frequencies from a circuit, and are particularly useful in removing noise from high-frequency communication signals, such as those found in televisions, mobile phones and radar. With the advent of 5G and 6G technology which operate at frequencies of 10s or 100s of GHz, the technical requirements for these filters will become challenging to meet. A SAW device converts signal voltages into acoustic waves at one end of the device using a piezoelectric material. These SAW waves then travel the length of the device at a speed determined by the material from which the device is constructed. The waves are then reconverted back into signal voltages at the other end using another piezoelectric, but with any higher-frequency noise components removed.

One approach to fabricate SAW devices that operate at these very high frequencies is to use a material for the SAW substrate that has an intrinsically high sound velocity. Diamond, due to its high Young's modulus, has the highest sound velocity of all materials ( $\sim 18\text{ km s}^{-1}$ ), and so is an ideal candidate for this substrate. But because diamond is not piezoelectric, it must be combined with a piezoelectric layer, such as a ZnO film, for the generation of the acoustic wave [135]. Another issue is that the smoothness of the substrate surface is a key requirement because any surface roughness leads to energy losses as the wave propagates. Hence, effective diamond surface polishing technology is crucial (Figure 6).

Since the mid-1990s, a range of practical SAW devices have been successfully fabricated using diamond films grown either on Si substrates or directly on SCD substrates, combined with ZnO, AlN, or AlScN as piezoelectric layers [136–138]). The characteristics of these devices are generally superior to those which use conventional SAW materials, with operational frequencies as high as 33 GHz being reported [138,139]. Indeed, due to its relative simplicity, the SAW filter was the first diamond electronic device to be commercially exploited,

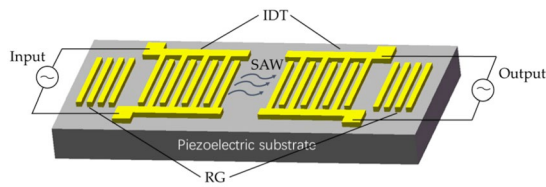


**Figure 6.** The basic structure of a two-port SAW resonator made from CVD diamond patterned into “fingers” to form two interdigitated transducers (IDTs), one of which forms the transmitter and the other the receiver. At either end of the device are a series of reflector grids (RG), while the whole device is fabricated on a piezoelectric layer, such as ZnO, deposited on a Si substrate. The input IDT converts the incoming electrical signal into acoustic waves. The nearby RG reflects the waves back onto the generating IDT creating a standing wave at a particular resonant frequency depending on the length and separation of the fingers. The acoustic wave then travels across the surface of the device (*i.e.*, as a surface acoustic wave, SAW) to the output IDT, causing it to resonate at the same frequency, while the underlying piezoelectric then reconverts this back into an electric output signal. Image reused from Ref. [14] under the Creative Common CC BY license.

mainly due to extensive development work by the Sumitomo company in Japan, which used diamond-based SAW filters in commercial mobile-phone equipment in the early 2000s. However, unresolved problems with combining the piezoelectric layer and diamond [14] delayed significant further progress for many years, such that competing materials which did not suffer these interface issues were able to capture the SAW market. As a result, interest and research into diamond SAW devices declined and there have been few further commercial products. Nevertheless, there are still a few sporadic papers published every year which keep the hope of commercial high-frequency diamond SAW filters alive.

#### 4.5. Micro electronic mechanical systems (MEMS)

These devices combine mechanical and electrical components and are fabricated on the micron-scale (MEMS) or nanoscale (NEMS) using semiconductor fabrication techniques. Common examples of these devices are accelerometers which can detect the sudden impact of a car crash, and then instantly discharge the safety airbags. They can also act as gravity sensors so that a mobile phone or handheld device knows which way is up and then can orient the display screen accordingly.

One of the most common designs for MEMS devices uses a cantilever made from a stiff material, which is fixed at one end but free to vibrate along its length—and looks a bit like a microscopic diving board. Piezoelectric circuitry attached to the fixed-end of the cantilever can induce it to vibrate at different frequencies, which depend upon the mechanical properties, especially the stiffness, of the cantilever material [140,141]. Diamond, having an extremely high stiffness, allows cantilevers to

vibrate at extremely high frequencies ( $>1$  GHz) [142], which therefore affords very high sensitivities to frequency change. These frequency changes depend upon the environment of the cantilever, and they can be monitored *via* a laser beam focused onto a reflective area on the top of cantilever [143]. Most diamond MEMS devices, to date, have been fabricated from PCD films grown on a Si substrate [144], with the Si being removed from around and under the diamond by wet etching, isotropic plasma etching, or other micromachining processes.

MEMS structures are not limited to cantilevers; a wide range of possible geometries and architectures can be used, and many diamond varieties are reviewed in Ref. [143]. Prototype diamond MEMS devices have been reported describing applications as diverse as transducers, actuators, and sensors, including RF applications, and in both gases and fluids [140]. Hybrid devices, where diamond and other electronic materials, such as SiC, GaN, or DLC are combined, have also been proposed [145], and these may enable a new class of hybrid-MEMS devices for extreme applications. Heavily boron-doped superconducting diamond resonators have also been reported operating at 10 MHz, which may readily be coupled to other superconducting circuits (see Section 4.6) [146]. Similarly, combining diamond MEMS with NV-centres opens the door to hybrid systems which can be used for precise quantum sensing and quantum information processing (Section 5) [147].

Another use for diamond MEMS technology is as an “electronic nose” (EN), which is a device that can detect and identify molecules for analysis purposes, or to “sniff” out illicit substances, such as drugs or explosives at ports and airports. EN devices must be inexpensive, portable, lightweight, and highly sensitive—but selective only to the molecules of interest. Many competing gas-sensor technologies are candidates for the next generation of EN [148], but CVD diamond ENs offer several advantages. They can sample smaller gas volumes, have reduced detection surfaces, and offer shorter detection times.

An example of a diamond-based EN developed by CEA (France) is shown in Figure 7 [149]. This device uses MEMS diamond cantilevers, the resonant frequency of which depends upon their dimensions, material composition, and crucially their mass. Because the cantilevers are made from diamond, their resonant frequency is very high (20–150 kHz), making them extremely sensitive to changes in mass. When gas molecules adsorb onto a cantilever, its total mass changes, which lowers the resonant frequency. This frequency change indicates the gas concentration. Selectivity for different gas molecules is achieved by covalently bonding a specific binding molecule (protein, antibody, inorganic reagent) to the diamond surface (see Section 7). The group reported successful trials of an 8-cantilever array sensor, each one

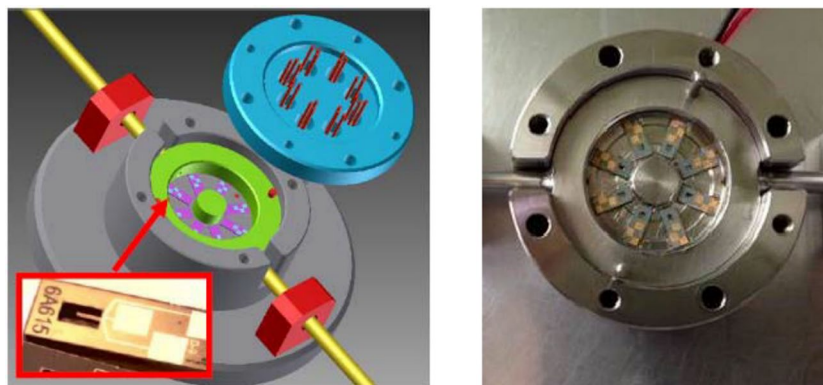


**Figure 7.** Left: Diagram of an EN gas sensor with 8 MEMS cantilevers. Right: Photograph of the sensor. Figure reproduced from Ref. [149] under CC BY 4.0 licence.

functionalised to detect a different molecule. Such systems are still in development, but scaling these up to detect perhaps 100 different molecules of interest simultaneously is the next step to commercialisation. The sensors could then be deployed at train stations, airports, and other critical buildings.

#### 4.6. Superconducting devices

With very heavy boron doping ( $[B] > 3 \times 10^{21} \text{ cm}^{-3}$ ), diamond transforms from a wide-band-gap semiconductor into a superconductor with a critical temperature  $T_c \sim 10 \text{ K}$  [150,151]. The superconducting behaviour of doped SCD appears to be consistent with that of conventional “low-temperature” Bardeen–Cooper–Schrieffer (BCS) superconductors, *i.e.*, involving coupled pairs of electrons called Cooper pairs [152]. However, in superconducting PCD films, the presence of multiple grain boundaries has been reported to make the material unexpectedly rich in exotic quantum phenomena. Reported oddities include an anomalous resistance peak before the superconducting transition [153], strong spatial modulation of the superconducting order parameter [154,155], and a superconducting anisotropy with opposite behaviour to that of any other superconducting thin films [156]. These bizarre quantum confinement phenomena suggest that granular nanodiamond could be used to fabricate novel superconducting quantum devices. Indeed, superconducting quantum interference devices (SQUIDs) have already been reported [157] which may act as sensitive magnetic-flux sensors or nanoscale motion detectors. Recently, Zhang *et al.* [158] demonstrated that the formation and trapping of Cooper pairs in nanoscale superconducting diamond-ring structures can produce an unconventional giant “magnetoresistance.” If these Cooper pairs trapped within such a nanoring can be released in a controlled manner, it could be feasible to integrate the rings as charged qubits into superconducting quantum circuits for logic operations.

#### 4.7. Laser written devices

These are very experimental novel diamond transistor devices that were first reported at the Hasselt diamond conference in March 2024 by groups from UCL and Oxford University. Using femtosecond laser pulses focused beneath the surface of SCDs, insulating, conducting, or semiconducting carbon tracks were written directly into the bulk diamond [159]. The conducting tracks can be used as micro- or nanoscale wires connecting electronic circuitry. However, the semiconducting tracks are more intriguing, as these can be gated using the conducting tracks as electrodes, suggesting the possibility of fabricating a future paradigm-changing all-carbon system for electronic devices. Further developments are eagerly awaited...

### 5. Quantum applications

Over the past few decades, several optically active atomic-scale defects have been identified within the diamond lattice, some of which have recently become the focus for a range of new and exciting diamond-based quantum technologies [160]. The most studied of these defects is the negatively charged nitrogen-vacancy centre (often just called the “NV-centre”) [22,28] although several other defects with similar properties have also been investigated, including  $\text{SiV}^-$  [161],  $\text{SiV}^0$  [162],  $\text{GeV}^-$  [163],  $\text{SnV}^-$  [164], and  $\text{PbV}^-$  [165], with many more candidate defects being discovered regularly [166,167] (Figure 8).

The electrons linked with these defects have some useful properties. First, the transparency of diamond allows the electrons to be accessed and manipulated using light. The electrons also possess a spin which is sensitive to external magnetic fields. Additionally, due to their extraordinary isolation by the surrounding diamond lattice from other nearby NV-centre spins, these spins possess long coherence times (the duration for which the spin remains stable and predictable). This isolation means that an NV-centre behaves like a single

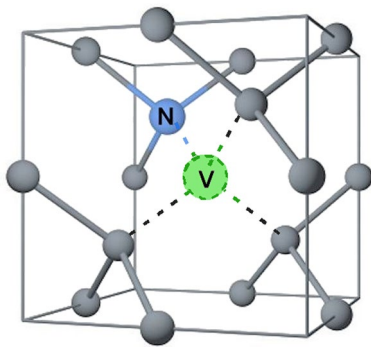


**Figure 8.** A schematic representation of the structure of the negative NV-Centre in diamond.

isolated pseudo-atom, *i.e.*, it can absorb or re-emit only *one* photon at a time. When a laser beam composed of billions of laser photons is used to probe the defect, only *one* of those photons will be absorbed at any one time, exciting *one* electron in the defect to a higher energy state, while all the other photons pass through the diamond unaffected. After a short delay, the excited electron will relax to a lower state, emitting only *one* photon again, but often of lower energy than the original laser photon. In the case of the NV-centre, the laser probe usually uses wavelengths in the green ( $\lambda = 532$  nm) while the emitted fluorescence is in the red ( $\lambda = 637$  nm) [168].

The spin of the electrons is measured using a process called optically detected magnetic resonance (ODMR), which can be viewed as a hybrid of photoluminescence (PL) spectroscopy and electron spin resonance (ESR) spectroscopy. An NV defect possesses an extraordinary set of energy levels—it does not matter what spin the initial ground-state electron has, because when the diamond is illuminated with green light the electron will absorb a green photon and then relax and re-emit a red photon—only to reabsorb another green photon and repeat the cycle. In this way, the electron cycles through all the allowed energy levels repeatedly as it is irradiated. Due to the rules of quantum selection combined with the relative lifetimes of the states involved, statistically the electron is ultimately more likely to end up in the ground state with spin  $m_s = 0$  than those with  $m_s = \pm 1$ . For multiple NV-centres cycled around this loop enough times, nearly all their electrons will eventually end up in this same ground state, which effectively “resets” the system, ensuring that for any subsequent experiment, the starting point is always the same.

The energy gap between the  $m_s = 0$  and  $m_s = \pm 1$  states occurs in the microwave region, so once reset, microwave radiation of the correct frequency (2.87 GHz) will excite the electron to the higher state, and in doing so, change the defect spin from 0 to  $\pm 1$ . In ODMR, the NV-centre is exposed to continuous microwave radiation whose frequency is varied in a controlled way, while simultaneously monitoring the red fluorescence signal from a continuous green probe laser. The spin state of the defect (“up” or “down”) can be inferred by simply

observing a decrease in red fluorescence intensity as a function of microwave frequency. For more details on the transitions and energy levels involved, please see the excellent review in Ref. [22].

The red fluorescence photon from an NV-centre will be emitted with spin properties determined by those of the original electron, which are known from the ODMR observation. If emitted near the diamond surface, these single photons can be focused using various microfabricated lenses and optics into a fibre-optic waveguide. Photons from different NV-centres can then be brought together inside a single waveguide and combined to create so-called quantum superpositions and entanglement [169] (see Figure 9). Such entangled photons form quantum bits (qubits) which are the basis of quantum communication and computing.

Furthermore, monitoring of the absorption by the NV of the applied microwaves as a function of microwave frequency enables an ESR spectrum to be obtained. When no magnetic field is present, there is only one ESR peak due to the single  $m_s = 0 \rightarrow m_s = \pm 1$  transition. But when a magnetic field is present, the Zeeman effect causes the two degenerate  $m_s$  levels to split, producing two peaks corresponding to transitions from  $m_s = 0 \rightarrow -1$  and  $m_s = 0 \rightarrow +1$ . The energy separation of the two peaks is proportional to the applied magnetic field, allowing this phenomenon to be used for magnetic sensing applications (see Section 5.3). The

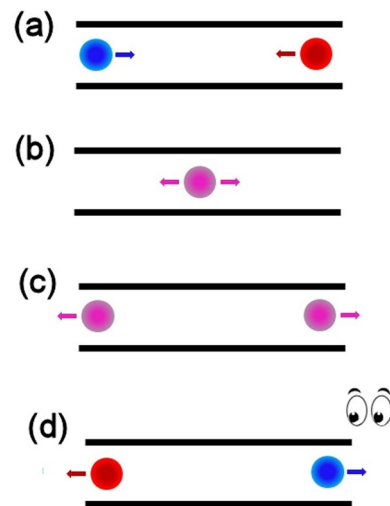


**Figure 9.** A simplistic representation of quantum entanglement of two photons. (a) Two photons emitted from different NV-centres, with opposite spins (depicted as red and blue), approach each other inside a fibre-optic waveguide. (b) When they meet, their wavefunctions entangle and they both attain the same superposition wavefunction—*i.e.*, the photons are now both red and blue simultaneously. (c) Upon separation, both photons remain entangled in the same shared quantum state, until (d) one of the photons is eventually observed, at which instant the superposition wavefunction collapses and the spin of that photon is fixed (in this case, blue). At that same instant, the spin of the other photon (red) becomes known, although it was never observed and might now be thousands of km from its partner.

splitting between the  $m_s$  sub-levels also depends on temperature, external electric fields, and lattice strain which enables the NV centre to be used as a sensor for these quantities also.

### 5.1. Quantum computing

In conventional binary computing, a “bit” represents either 0 or 1. If we call 1 spin-up, and 0 spin-down, then a qubit comprised of two entangled photons would exist in a state of both 0 and 1 simultaneously, persisting in this superposition until observation collapses the state of one of the pair (see Figure 9). However, when the spin of the observed photon is revealed, the spin of the other photon immediately becomes known, even though the latter has not been examined and may now be located at a very long distance from the first photon. Quantum theory states that there is actually *no* limit to this separation. The two photons might now be thousands of km apart—yet the communication between them remains instantaneous.

Quantum computing is so powerful because changing one of the states of *one* of the qubits instantly changes the states of *all* of its entangled partners. As such, for  $n$  qubits, the number of calculations that can be performed “instantly” scales as  $2^n$ . So, entangling only 20 qubits together enables the equivalent of over a million calculations to be performed in one go. Hence, a calculation requiring multiple steps, such as additions, multiplications, *etc.*, performed sequentially by a normal computer, can be done by a quantum computer in one *single* very fast step. Quantum computers, therefore, have the potential for extraordinary computing speeds, and coupled with the rapid progress in artificial intelligence, may become truly world-changing in the coming decades.

The qubits in today’s quantum computers are not yet created *via* diamond defects [170], and so they need to be liquid-helium cooled to temperatures  $\sim 10\text{--}20$  K for them to attain the sufficient coherence times needed for complex calculations. Diamond-based quantum computers should operate at room temperature, eliminating the need for cooling, and making them vastly cheaper and easier to operate. Think of the possibilities if a small quantum computer could be embedded within your desktop PC, your mobile phone, or your smartwatch!

The first demonstration of entanglement between an NV spin and a photon was reported in 2010 [171], and progress in the field of diamond quantum computing has been fairly rapid since then. Three years later, the photons from two separated NV-centres were entangled using lenses patterned into the diamond surface acting as amplifiers [172]. In the same year, the “node” separation (the distance between the entangled qubit photons) was extended to 3 m [173]. In 2015, the node separation was extended further to  $>1$  km [174]. Only a few years

later, a 10-qubit register was reported by a group at Delft University that could store quantum information for up to 75 s [175]. These long timescales are sufficient to perform controlled logical operations (AND, NOR, *etc.*) between different spin qubits [176]. Scale up further into multi-qubit quantum registers requires rapid and easy initialisation and manipulation of the diamond NV-centre spins, and this can now be performed with single-shot measurements [177].

Current research in this area is now following two approaches. The first aims to improve the hardware, *i.e.*, the quality of the diamond. The goal here is to reduce or eliminate unwanted defects, and to develop methods to control the positioning and density of NV (or other) centres. Maximising the photon extraction efficiency from individual NV-centres [178] is also crucial, and this can be achieved by fabricating photonic nanostructures (lenses, waveguides, *etc.*) near the NV-centres. The second approach involves developing new software that is needed to drive these quantum systems. Key to the success of quantum systems lies in code to detect and correct errors in qubit states. Examples of such codes have already been demonstrated in small qubit networks [179]. The crucial challenge for the future is how to scale up quantum networks from tens of qubits to possibly hundreds of qubits. Although such work is now rapidly proceeding, it may be many more years yet before we see a fully functioning diamond quantum computer [180].

### 5.2. Quantum cryptography

The control and entanglement of photon spins from an NV-centre may also enable perfectly secure electronic communications [181]. The information being sent is first encrypted using an entangled quantum key—generated by entangled photons from diamond NV-centres—that is known only to the sender and receiver. If the message were to be intercepted by a third party, the entanglement of the quantum key would break, and the attempted eavesdropping event would be exposed. Such unbreakable codes would enable secure communications which should, in theory, make copying or modifying confidential data impossible [160]. Data security is becoming increasingly important—and diamond-based quantum cryptography may play an important future role in examples such as PIN numbers sent over the internet, medical or other personal data stored on a company database, banking records, or even your internet browsing history!

### 5.3. Quantum sensing and magnetometry

The electronic spins in NV (and other) centres are sensitive to temperature, electric and magnetic fields, and lattice strain, and can be used as highly sensitive

room-temperature sensors. Most of the reported work concerns magnetometry, and describes the measurement of tiny magnetic fields at the nm scale, especially in the study of new semiconducting or superconducting materials (see Figure 10) [183].

In practical applications, quantum sensing employs a diamond sample with a high-density, thin layer of near-surface NV-centres. This sample is then placed or deposited onto the substrate to be tested. Subsequently, the substrate is illuminated with light of a suitable wavelength, typically green for exciting the NV-centres. Upon absorption of this light by the NV-centres, they emit red fluorescence, enabling tracking of NV-centre movement or measurement of a desired parameter (such as temperature or magnetic field) through the small wavelength shift of the fluorescence.

The NV-centres can also be incorporated into nanodiamond (ND) particles (see Section 15) or other nanostructures to achieve nm proximity to the site of interest. They can also be attached to the end of fibre-optics to

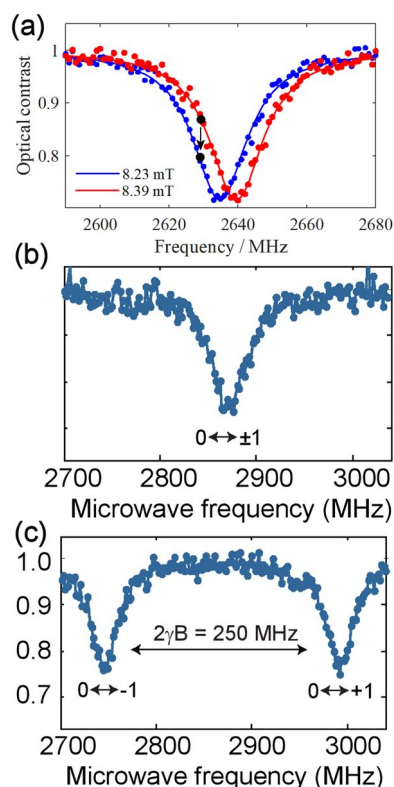


**Figure 10.** An example of magnetometry using NV-centres in diamond. (a) Continuous illumination of the sample with both laser light and microwave radiation allows detection of the magnetic field *via* the spectral line shift as the NV-centre is moved across the magnetic region. The frequency difference between the curves is 4.7 MHz, corresponding to a magnetic field difference between these two scanned regions of 0.16 mT. (b,c) Alternatively, if the laser illumination is held constant while the microwave frequency is scanned, the single ESR peak seen for zero magnetic field in (b) splits into two peaks with a magnetic field present due to the Zeeman effect (c), with the difference between the two peaks dependent upon the magnitude of the magnetic field. Images were taken from or replotted based on data from Ref. [182].

make magnetic endoscopes. For example, biological cells can ingest ND particles containing NV-centres enabling *in situ* sensing and tracking as the nanoparticles move around inside the cell [183,184] (see Figure 11). The local temperature inside a living cell has also been monitored by ingested NV-centres providing information about a cell's metabolism and transport pathways [185]. The first reports of NV-based magnetic sensing appeared in 2008 [186–188], and since then, this technique has been used to detect a range of other physical quantities, such as electric fields, charge, voltage, current, orientation, strain, temperature, and pressure. A summary of different sensor types with their related sensitivities is given in Nebel's detailed review paper [28].

Diamond quantum technology in all its variations is causing a great deal of excitement in the scientific and commercial world. There are a growing number of companies interested in this topic, including large companies, such as *Lockheed Martin*, *Bosch*, and *Thales*, as well as many start-ups, such as *Quantum Diamond Technologies* [189], *NVision* [190], and *Qnami* [191]. In parallel with the development of high-purity substrates to contain the NV-centres (or other suitable fluorescent defects), quantum technology could well become one of the key applications for diamond technology in the coming decades.

## 6. Thermal management

Diamond has the highest room-temperature thermal conductivity of any known material ( $\sim 2200 \text{ W m}^{-1} \text{ K}^{-1}$  for high-quality SCD), which together with its low coefficient of thermal expansion (CTE) and remarkable electronic and optical properties, makes it ideal for thermal management [192,193]. Indeed, diamond heat spreaders were one of the first diamond products to be commercialised in the 1990s, and nowadays there are dozens of companies worldwide that supply “thermal grade” diamond as commercial products; they can even be purchased from the online retail store *Alibaba!* [194].

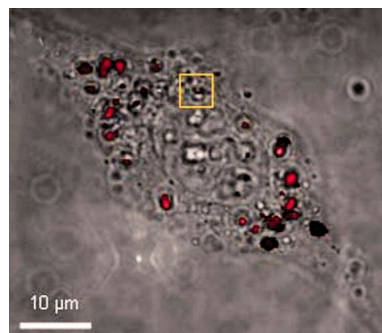


**Figure 11.** Red fluorescence showing the positions of single 35 nm NDs in a HeLa cell. Most of the uptaken NDs are seen to distribute in the cytoplasm. Image taken from Ref. [184] with permission. Copyright (2007) National Academy of Sciences, USA.

Heat spreaders are particularly relevant for high-power electronic devices, laser diodes, nanophotonic circuits, radar amplifiers, and high-electron-mobility transistors (HEMTs), where the intense heat generated locally by the device can be dissipated rapidly by attaching it directly to a diamond heat spreader which then conducts the heat to a remote heat sink, radiator or even a microfluidics assembly. In doing so, not only is the device temperature greatly reduced allowing it to be operated at even high powers and therefore speeds, but its lifetime, linearity, and stability can be hugely increased, while also enabling a reduction in size and cost savings. A good example of this is for GaN devices which are currently used in power electronics, radio frequency (RF) components, and the transmitter base stations for 5G mobile-phone networks. Such commercial GaN devices typically run at power densities  $\sim 5\text{--}10\text{ W mm}^{-1}$  (equivalent to a staggering  $10\text{ GW m}^{-2}$ ), but as much as 50% of the electrical power is dissipated as waste heat [195,196]. Unsurprisingly, there are major efforts worldwide to develop a hybrid GaN-diamond technology (Figure 12), either by depositing CVD diamond onto GaN (with or without a SiC or AlN barrier layer), or the opposite, depositing GaN onto diamond, or simply by glueing GaN wafers and diamond wafers together—face-to-face—in a process called wafer bonding. An excellent review of the progress in this area can be found in Ref. [195].

## 7. Applications of functionalised diamond surfaces

Because of the predominantly hydrogen atmosphere present during CVD, as-grown diamond necessarily has a hydrogenated surface, *i.e.*, all the surface carbon atoms are terminated with H. This gives rise to a surface dipole which makes the surface hydrophobic but allows airborne molecules to adsorb onto the surface and exchange electrons with the bulk, creating the 2DHG layer mentioned in Section 4.2.3. The H-terminated surface also

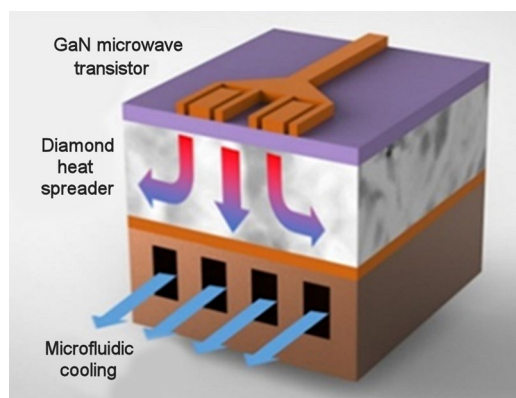


**Figure 12.** Proposed GaN-on-diamond HEMT with heat extraction at the back of the assembly. (Copyright University of Bristol 2017).

exhibits negative electron affinity which is the basis for several applications involving electron emission (see Sections 3.8 and 7.1).

These C–H surface bonds can be readily modified using standard chemical reagents [103]. Indeed, simply leaving the as-grown diamond in ambient air for a few days or weeks changes the surface conductivity [197], presumably by oxidising some of the C–H bonds to C–OH bonds. Oxidising the diamond surface can also be done deliberately—the four most common methods are hot acid treatment, ozone treatment usually generated from a UV lamp, O<sub>2</sub> plasma exposure, or an O<sub>2</sub> cracking system under UHV. These different methods produce different types of oxygen termination (see Figure 13) on the surface (*e.g.*, ketone C=O, ether bridges C–O–C, hydroxides C–OH, or more complex structures, such as carboxylic acid groups or lactones) in different proportions [199]. Oxidising the diamond termination in this way changes the polar nature of the surface from hydrophobic to hydrophilic, and this is useful for fabricating electrochemical electrodes with different activities (see Section 3), or surfaces which respectively inhibit or support biological cell growth (see Section 11).

Similarly, the surface H atoms can also be chemically replaced by other elements or groups, such as N, NH<sub>3</sub>, S, and halogens [200]. These more-reactive surface groups can be further exploited to covalently attach larger molecules, such as fluorophores, light-harvesting dyes, DNA strands, antibodies, proteins, or polymers. The most common functionalisation strategies involve attaching aryl-diazonium salts [201] or short-chained terminal alkenes [202] which act as linker molecules, onto which the larger molecules will be attached. In the case of alkenes, the double bond is activated by UV light, and bonds to the diamond by displacing a surface H, while at the other end of the molecule is a reactive species, such as a carboxylic acid or amine that is chemically prevented from reaction by protecting groups. Similarly, the aryl-diazonium salts with *para*-substituted reactive species (also chemically protected) can be activated electrochemically to attack and bond to the diamond surface. Once grafted onto the surface, the protecting groups are chemically removed from the untethered end, revealing the reactive end-group ready for reaction with the larger molecule of choice [203].

O-terminated diamond is also often employed for further functionalisation *via* silanisation or esterification reactions, while N- or NH<sub>2</sub>-terminated diamond can be amidised [204]. Such chemically modified diamond surfaces afford a variety of different applications, such as biochemical or electrochemical sensors (Section 3), the creation of solvated electrons to drive electrochemical reactions (Section 3.8), as an artificial nose (Section 4.5), and as antimicrobial surfaces (Section 11.5). An excellent comprehensive review on diamond functionalised surfaces is given by Raymakers *et al.* [103].

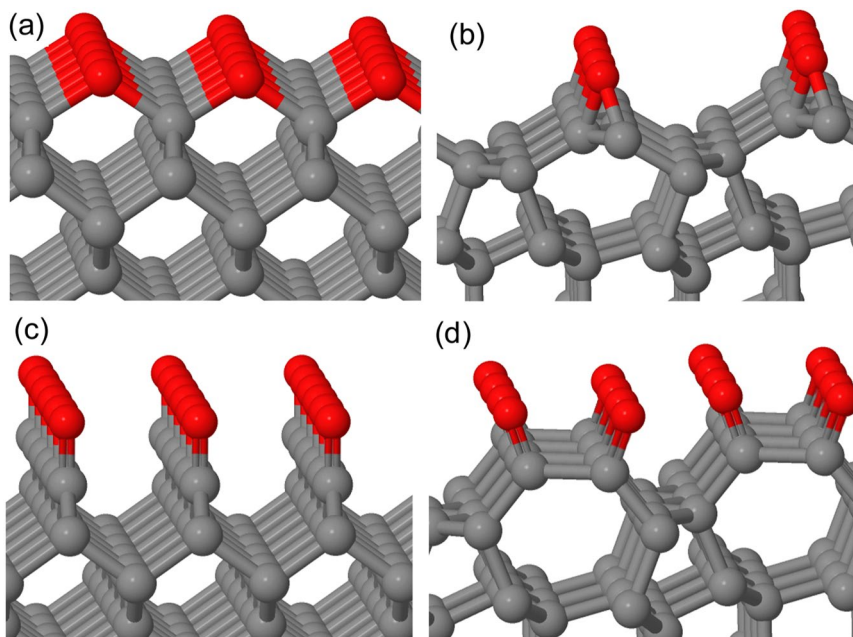


**Figure 13.** Simulations of the (a,b) ether O-terminated (100) and (111) diamond surfaces, respectively, and (c,d) the ketone O-terminated (100) and (111) diamond surfaces, respectively. C and O atoms are shown in grey and red, respectively. Image modified from Ref. [198].

### 7.1. Electron emission from diamond surfaces

Many advanced technological applications exploit the controlled emission of electrons from a surface for their operation. These include, for example, emissive flat-panel displays, spacecraft ion engines, high-power microwave amplifiers, X-ray sources, electron microscopy, and electron-beam lithography techniques [205]. For an electron to be emitted from a surface, it must possess sufficient energy to overcome the potential barrier situated at the interface between the surface and the external medium, which is usually a vacuum, but could be air or water. This potential barrier—the work function,  $\phi$ —is defined as the energy difference between the Fermi level (the electrochemical potential of electrons inside the material) and that of the vacuum level. For wide-band-gap semiconductor materials operating at normal temperatures, the conduction band (CB) is usually empty of electrons while the valence band (VB) is partially or fully occupied. The two bands are separated by an energy band gap of a few eV (e.g., 1.1 eV for Si and 5.47 eV for diamond). This means  $\phi$  for most metals and semiconductors is also typically several eV. Hence, either UV photons or temperatures  $>1500$  K are required to provide sufficient energy to emit electrons located at the Fermi energy in the VB directly into the vacuum or to excite them into the CB to be subsequently emitted from there.

However, for some semiconductors and insulators, such as diamond, an alternative emission pathway is possible if the conduction band minimum (CBM) lies higher in energy than the vacuum level. This uncommon situation is known as negative electron affinity (NEA).

Here, any electrons located in the CB experience no emission barrier to escape the surface. As such, bulk electrons residing in the VB (or in mid-band-gap states as a result of *p*- or *n*-type doping), only need to be excited into the CB for emission to take place. Consequently, materials with NEA require far less photon or thermal energy for electron emission, and so are promising candidates for next-generation electron-emission applications [205].

Diamond possesses an NEA surface when it is terminated with certain electropositive chemical species [206]. As mentioned above, the most common species found on the surface of natural and CVD diamond is hydrogen. The small difference in electronegativity between carbon and hydrogen creates a surface dipole, with the positive charge outermost, lowering the emission barrier and establishing the NEA. As a consequence, electrons are, to some extent, repelled from the negatively charged bulk and attracted toward the positive surface, from where they are emitted into vacuum, while the NEA ensures there is little or no barrier for emission.

As-deposited CVD diamond is fully H terminated and possesses an NEA measured as  $-1.3$  eV for the (100) surface and  $-1.27$  eV for the (111) surface [207,208]. Diamond with other types of termination or with a bare surface that has lost its terminating groups can be re-hydrogenated by  $H_2$ -plasma treatment in a microwave CVD (MWCVD) reactor [209]. This hydrogenated NEA diamond surface is an excellent candidate for many applications requiring efficient sources of electrons, as discussed in the subsections below.

## 7.2. Cold-cathode electron emitters

In the case of field emission, a positive potential is applied between the diamond film surface and a nearby electrode at room temperature (hence the other name for this process, cold-cathode emission) causing electrons to emit from the surface and travel to the electrode, resulting in an emission current. The NEA surface of diamond (see Section 7.1) means that compared to many competing materials (W, LaB<sub>6</sub>), higher emission-current densities can be achieved with lower applied voltages. Diamond has other advantages—it has excellent mechanical and chemical stability, including high hardness, high thermal conductivity, and compatibility with Si fabrication processes, plus its surface can be chemically functionalised to tailor the emission properties (Section 7) [210]. As such, diamond has been considered a potential candidate for a range of vacuum microelectronic devices [211], such as high-power switches, electron sources for microwave tubes, large-area electron guns for high-definition television, high speed, high-power amplifiers, and even integrated circuits [212]. In the years from 2000 to 2010, extensive work in this area using diamond and other forms of carbon emitter (DLC, carbon nanotubes, and ND), reported field-emission current densities of up to 1 mA cm<sup>-2</sup> for applied electric fields of <5 V μm<sup>-1</sup> [213], which are sufficient for use in flat-panel displays [214,215] and X-ray [216] and microwave generators [217]. Improvements to the emission current while reducing the emission threshold voltages were reported by the use of nanostructured diamond “Spindt tips” [218] or diamond-coated teepee structures [219], by depositing a thin metallic layer on the diamond surface [210], or by using ultrananocrystalline diamond (UNCD) with a high density of grain boundaries [220] (Figure 14).

The latter report—that field emission occurred readily from flat UNCD films—suggested that the commonly

held mechanism for field emission based upon Fowler-Nordheim theory—was insufficient to explain electron emission in PCD. The theory suggests that the applied electric field concentrates and amplifies around sharp tips and edges. Thus, nanostructured needles and cones exhibit increased emission current compared to flat emitters for the same applied bias. However, this geometrical enhancement was insufficient to explain the extremely large current increases being reported for some diamond films, and could not explain the enhanced emission from *flat* UNCD films. The electron emission seemed to be correlated with the number and density of grain boundaries containing *sp*<sup>2</sup> carbon [222]. Also, SCD with no grain boundaries exhibited little, if any, field emission.

To explain this, Cui *et al.* [223] devised a mechanism in which the threshold for field emission is lowered due to a local reduction of the electron affinity of the diamond surface surrounding nanoscale graphitic surface structures, such as defects or grain boundaries. The electron emission takes place from this graphitic region, although the emission barrier is controlled by the surrounding diamond lattice. Direct evidence for this mechanism was provided in 2015 when tunnelling AFM was used to observe the emission coming *only* from the grain boundaries of microcrystalline diamond (MCD) films [224], with the grain boundaries “lighting up” in the AFM images due to the emitted electrons while the bulk crystallites remained dark.

These findings mean that the surface topology and grain boundaries are more important for field emission from diamond than the presence, or otherwise, of an NEA surface. However, an NEA surface is still preferable to a PEA surface to ensure the overall work function is as low as possible.

Since about the mid-2010’s, interest in diamond field-emission devices, and in particular flat-panel displays, has dropped off significantly. Although, in theory,

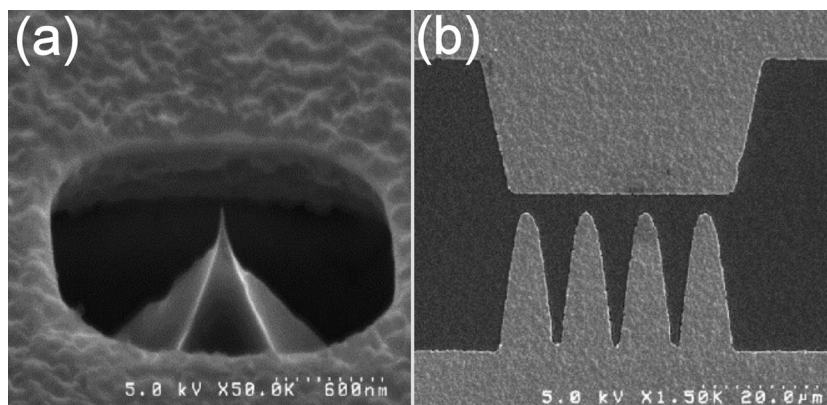


**Figure 14.** Example field emission devices made from diamond. (a) SEM image of a vertical diamond field emission triode. The fabricated diamond emitter has a very sharp tip (~5 nm) surrounded by a self-aligned silicon gate. The diamond cathode is electrically insulated from the silicon gate by a 2-μm-thick SiO<sub>2</sub> layer. (b) SEM image of a lateral diamond field emission diode with four diamond “fingers” configured as a field emission cathode and a diamond anode located laterally 2 μm from the diamond fingertips. Images reproduced from Ref. [221] with permission.

diamond field-emission displays should afford several benefits compared to conventional displays, such as high brightness, large viewing angle, and fast response, the competing technologies (LCD, LED, and recently OLED) won the race to commercialisation. Emissive diamond (and CNT) displays, despite their potential advantages, simply lagged too far behind the market to make further development worthwhile, and many commercial manufacturers, such as *Samsung* and *Sony*, abandoned field emission in favour of other display technologies [15]. This is, perhaps, a sobering lesson for other fledgling diamond applications—sometimes it's not the *best* product that wins, but the first product to get to market that is good enough for the job [225]!

### 7.3. Thermionic energy generation

Diamond has been proposed as a candidate for energy generation using a thermionic energy converter (TEC) [226,227]. In a TEC (Figure 15), electrons emitted from a hot cathode (the emitter) travel across a high-vacuum gap and are captured by a cooler anode (the collector). The difference in work function between the anode and cathode creates a potential difference between the electrodes. Connecting the two electrodes completes the circuit, and permits electrons to flow from the collector back to the emitter, driving an electric current through a load. Thus, heat can be converted directly into electricity within a solid-state device that has no moving parts. Ideally, the heating of the emitter would be obtained in the form of infrared light from the sun, which would be collected using a solar-tracking array and focused onto the back of the emitter. A solar TEC, such as this might provide an alternative to standard photovoltaic (PV) solar cells for renewable energy generation [228].

The efficiency of a basic TEC device can be improved by using either light or additional electrons to enhance the electron-emission process. Such variations include

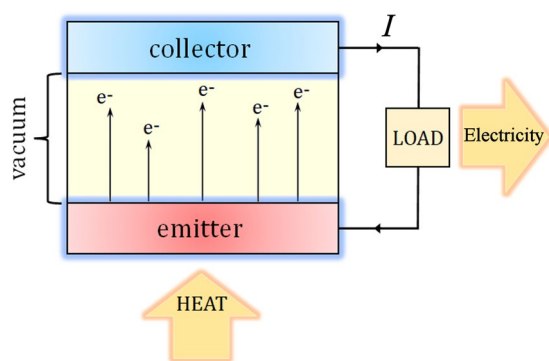


**Figure 15.** Simplified schematic diagram of a thermionic emission converter. Electrons are emitted from a heated emitter and travel across a vacuum gap to strike a cooler collector. Connecting the two electrodes allows a current,  $I$ , to flow back to the emitter through a load. Thus, heat is converted into electricity. Redrawn based upon a diagram in Ref. [206].

photon-enhanced thermionic emission (PETE)—where photon absorption and thermal energy both contribute towards energising electrons into the conduction band [229]—and using electrons from radioactive  $\beta$ -decay to assist the thermionic process in a similar process to beta-voltaic devices (see Section 14).

TECs could be coupled with existing heating systems for domestic electric-power co-generation and waste-heat scavenging [230]. Small, portable TEC devices have also been suggested as a method of reducing the heat signature of military vehicles, making them harder to detect by IR thermometry or to target with heat-seeking weapons.

Thermionic emission begins for hydrogenated diamond at only  $\sim 500^\circ\text{C}$ , and by  $\sim 900^\circ\text{C}$  the emission current density often exceeds  $1\text{ mA cm}^{-2}$  [206], with the highest value reported to date being  $210\text{ mA cm}^{-2}$  for N-doped diamond on Mo at 1500 K [231]. This emission threshold temperature compares to values of over  $1500^\circ\text{C}$  that are typically required for thermionic emission from metals or semiconductors [206], and which often support current densities much less than  $1\text{ mA cm}^{-2}$ . Unfortunately, the relatively low adsorption energy of  $\sim -4\text{ eV}$  for H onto diamond means that these surfaces remain stable to only  $\sim 600\text{--}800^\circ\text{C}$ , after which the H atoms start to desorb leaving a bare surface without an NEA leading to a significant decrease in emission current. The hydrogenated surface also partially oxidises in air or water over a period of days or weeks, with a resulting loss in NEA, and it can also undergo surface transfer doping with airborne adsorbates (Section 4.2.3), which impair or block electron emission. A great deal of effort has been expended, therefore, to find a suitable diamond surface termination that exhibits similar or improved NEA properties to hydrogen-terminated diamond but with greater stability at higher temperatures under thermionic emission conditions and/or under ambient conditions in air [206].

Most work on alternative termination species has involved depositing monolayers or sub-monolayers of electropositive metals (M), such as Li, Mg, Na, Ti, Al, and Sc, directly onto the diamond surface [206]. Relatively few metal adsorbates have been studied experimentally to date, but several of those have shown promising thermionic characteristics. However, although many of these metals may establish a useful NEA surface when adsorbed onto diamond at room temperature, due to weak M–C bonding, at elevated temperatures they often desorb or the surface reconstructs into a non-NEA form. Additionally, many of these metals oxidise easily, so on exposure to air, the M–C bonds break in favour of new M–O bonds, and the NEA surface is again destroyed.

One approach to solve these issues is to pre-oxidise the diamond surface before metal deposition. While it may appear counterintuitive to surface terminate with electronegative O, provided a sufficiently electropositive metal is bonded on top of the oxygen layer, the overall

M–O–C sandwich can produce a *net* NEA surface. A number of such sandwich structures have been investigated both experimentally and theoretically [206], and a few general observations have been made, which apply to both M–C and M–O–C surface structures. Results suggest that small metal adsorbates ( $\text{Li}^+$ ,  $\text{Na}^+$ ) are preferable to larger ones because they lie closer to the diamond surface and thus have high adsorption energies with increased temperature stability. Metals with high electropositivity, or which ionise easily to form highly charged ions ( $\text{Mg}^{2+}$ ,  $\text{Al}^{3+}$ ,  $\text{Ti}^{4+}$ ,  $\text{Sc}^{3+}$ ), and which form strong, stable bonds with both C and O, are also good candidates for further investigation. Indeed, Sc-terminated diamond has recently been reported [232] to have the highest NEA for a metal adsorbed onto bare diamond measured to date ( $-1.45$  and  $-1.13$  eV on diamond (100) and (111) surfaces, respectively), as well as being thermally stable up to  $900^\circ\text{C}$  (Figure 16). Si [233] and Ge [234] terminations have also been investigated experimentally and theoretically, and look very promising. Boron termination on bare diamond has been

predicted theoretically to be thermally stable and exhibit a reasonable NEA [235], however, no experimental work has yet been reported for this system.

The related termination approach with N instead of O, *i.e.*, M–N–C structures, has so far only been reported for Ti [236] and Sc [237], but calculations show that these, too, should exhibit NEA with high-temperature stability. The most promising candidates so far studied include LiO [238], MgO [239], and ScO [240], although thermionic emission data under realistic operating conditions and lifetime tests have yet to be reported.

#### 7.4. Secondary electron emission

Electronically, light is usually detected by focusing photons onto a photocathode, which then emits electrons, that are subsequently collected on an electrode and measured in the form of an electrical current. At low light intensity, the small number of emitted electrons have to be amplified to obtain a usable signal. This multiplication is usually achieved by devices, such as photomultiplier tubes or microchannel plates [241]. These use high voltages to accelerate the slow emitted electrons to high velocities, which then strike surfaces that have been chosen due to their high ( $>1$ ) secondary-electron emission yield (SEY). For these surfaces, the high-energy primary-electron impacts liberate multiple secondary electrons depending on the SEY of the surface. These secondaries are then accelerated deeper into the device to strike another surface, which, in turn, emits even more electrons. Most electron-multiplication devices require many such amplification stages, determined by the SEY of each surface and the gain required. For example, a dynode device comprised of five amplification stages, each with a SEY of 10, will amplify the signal  $10^5$  times.

Secondary electron emission is generally interpreted as a three-step process, in which the excitation of the emitted electrons in the bulk, their transport to the solid surface, and their escape into the vacuum, are described by three different processes [242]. For an efficient emitting surface, each primary electron can liberate multiple secondary electrons, and providing these can be accelerated to sufficiently high energy, they can excite other electrons by means of a cascade generation process. At each collision the electrons lose energy, until ultimately, they thermalise at the bottom of the CB. The emission of these low-energy electrons now depends only on their ability to overcome the energy barrier present at the surface.

Diamond exhibits excellent secondary-electron emission characteristics, with SEY values higher than metals and many insulator materials [243,244]. Indeed, SEY values as high as 80 (*i.e.*, 80 electrons emitted for every primary electron that strikes a surface) at 3 keV are reported for pristine SCD [245,246] and  $\sim 10$  for

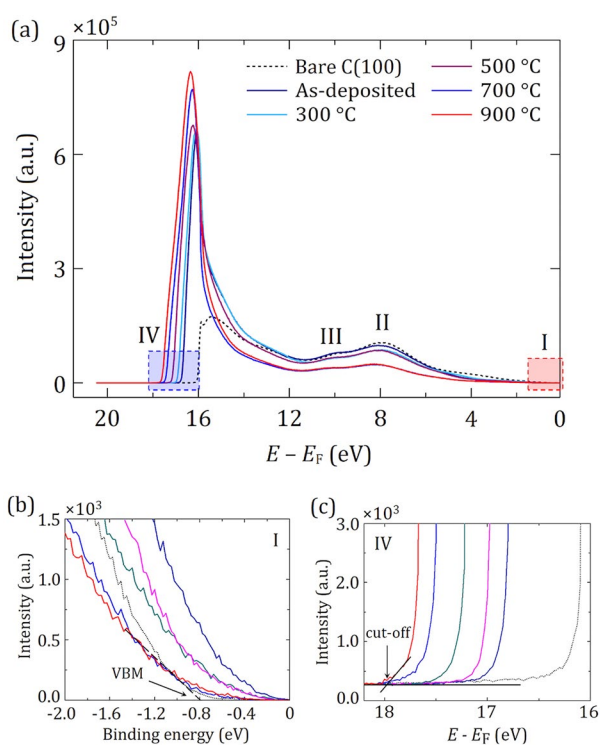


**Figure 16.** (a) The UPS spectra of Sc on the bare SCD (100) surface observed at different sample preparation stages: the bare unhydrogenated surface, immediately after Sc deposition, and following annealing at four different temperatures. The steeply rising curves around 17–18 eV are indicative of electron emission from the conduction band, and the cut-off energies can be used to calculate the electron affinity. Regions labelled I and IV provide information about valence-band and conduction-band electrons, respectively, while regions II and III come from bulk electrons. Extrapolations to determine the position of the valence band maximum (VBM) and cut-off energy relative to the Fermi level are shown in (b) for region I, and (c) for region IV, respectively. Figures reprinted under CC BY 3.0 licence from Ref. [232] (published by the Royal Society of Chemistry).

polycrystalline CVD films [247]. High SEYs can usually be obtained from hydrogen-terminated electrically conducting BDD films [248]. This is attributed to the combination of efficient electron transport from the bulk (where the secondary electrons are generated) to the surface, resulting in a large mean escape depth (around a few tens of nm for a primary energy of  $\sim 1$  keV), together with an NEA surface which removes the potential barrier for emission (see Section 7.1).

The applications for diamond-based electron amplification devices are numerous and diverse [249]. Photomultiplier tubes and microchannel plates are ubiquitous in many fields of science, especially in advanced spectroscopic techniques and mass spectrometry. They are also used for medical imaging in PET scanners and for the detection of ionised particles and neutrinos. Diamond-based electron multipliers, such as those shown in Figure 17 have been investigated for use in night-vision goggles [251], and as a converter of back-scattered electrons into secondary electrons in scanning electron microscopy [243].

However, despite this promise, very few such diamond dynode devices have been commercialised to date. The problem may be that the emission of electrons through the hydrogenated diamond surface, especially at high currents, causes gradual desorption of the H, removing the NEA vital for high SEY. However, following recent reports of the more thermally robust diamond NEA surfaces using metal adsorbates and/or metal-oxygen adsorbates (see Section 7.3), interest in diamond secondary-electron applications has reawakened [249]. This may be a field to watch in the coming years.

### 7.5. Diamond PN/PIN diode-type electron emitters

Recently, the Schottky diode designs discussed in Section 4.1 have been modified to fabricate devices that operate *via* electron emission from an NEA diamond

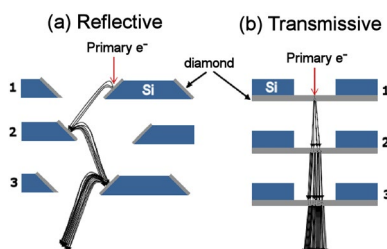


**Figure 17.** Two geometries typically used for secondary electron multiplication dynode devices, except here using thin-film diamond as the dynode material. Three multiplication stages are shown for each, with each stage having a higher positive bias compared to the previous stage. (a) “Venetian blind”-style reflective device. (b) A transmissive device involving thin diamond membranes. Image taken from Ref. [250] under the Creative Commons 3.0 licence.

surface [252]. The NEA surfaces so far have all been H-terminated, but nevertheless have begun to show a great deal of promise for applications, such as high-voltage switching or as electron sources. These devices operate at room temperature and operate *via* a mechanism which involves the creation of excitons (electron-hole pairs) by supplying sufficient energy (in the form of UV photons or high voltage) to electrons residing in the valence band (VB) that they emit directly into vacuum without first thermalising in the conduction band (CB). The loss of an electron leaves a positive hole in the VB, which can be neutralised by an electron injected from an external circuit.

These devices require an NEA diamond surface to eliminate the energy barrier for electron emission, however, to achieve high emission currents they also need to minimise the overall energy required to create the excitons. One way to achieve this is to use *n*-type diamond, where the donor level sits just below the CB minimum (CBM). Unfortunately, *n*-type diamond can cause strong upward band-bending which inhibits electron emission [253]. An alternative is to use *p*-type diamond which creates downward band-bending favourable for emission, however, with the acceptor level being far from the CB, this means there are few electrons at the CBM. The solution is to combine both *p*-type and *n*-type diamond into a 2-layer device, as shown in Figure 18(a). Here, electrons are injected from the *n*-type layer into the *p*-type layer, while holes travel in the opposite direction. The electrons injected into the *p*-layer are effectively in an “excited” state, from which they can then be emitted more easily by the application of a suitable voltage or a photon of the correct frequency.

The first such diamond PN junction was successfully fabricated in 2001 and demonstrated clear diode characteristics and electron emission [254]. Moreover, 235 nm UV light was generated, which was attributed to the phonon-assisted recombination of free excitons, consistent with the proposed exciton-emission mechanism. Over the next few years, improvements in crystalline quality and *n*-doping efficiency using phosphorus helped increase the emission efficiency to 1.9% [255].

An improvement over these simple PN diodes incorporates an undoped (intrinsic) diamond layer between the *p*-type and *n*-type layers, to make a PIN diode device. This is because intrinsic diamond can support a much higher density of free exciton states than the doped layers, which enables a higher current through the device leading to higher electron emission. As well as electrons, the recombination of the excitons in PIN devices causes emission of deep-UV photons, which has been used to fabricate deep-UV LEDs [256]. A further improvement on the design added a heavily *n*-doped layer between the *n*-doped layer and the metal contact to reduce the contact resistance (Figure 18(b)) [257].

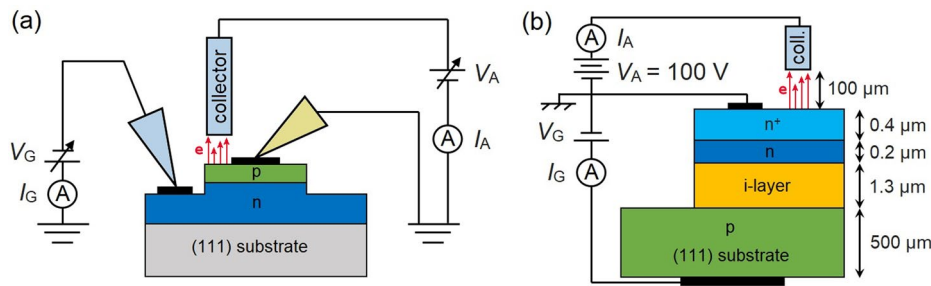


**Figure 18.** (a) Typical design for a PN diode emission device. The  $p$ -type diamond layer is patterned using dry etching to form a protruding “mesa” structure from which the electrons are emitted into vacuum to be captured by a nearby collector electrode. The  $p$ -layer sits directly on top of an  $n$ -type layer, which itself sits on an undoped single-crystal diamond substrate. Electrons are returned to the  $n$ -layer via an electrical contact on the surface. A removable contact on the  $p$ -type surface is used to measure the conduction properties through the diode device in the absence of electron emission. (b) Schematic diagram of the design of a PIN diode with a heavily doped  $n^+$  top layer. Both redrawn from Ref. [252].

These early PN/PIN diode devices used (111) diamond because this orientation is easier to  $n$ -dope with phosphorus. However, recent advances in the  $P$ -doping efficiency of the more common, cheaper, and higher quality (100) orientated diamond, may allow significant improvements in the emission current from these devices in the near future. This may lead to a range of new applications, including proposed compact high-voltage power-switches [258] for use in intelligent power grids running off sporadic “green” energy sources, such as wind and solar power. At present, such devices have been demonstrated at 10 kV [259] with a room-temperature power-transmission efficiency of 73% at 9.8 kV. But, in theory, with further improvements in diamond quality, it should be possible to increase the voltage to 100 kV or more. NEA surfaces that use termination schemes that are more robust and more thermally stable than H, such as metals or metal oxides (see Section 7.1) may also improve device performance and longevity. Thus, PN/PIN electron-emission diodes might soon be found in telecommunications, radar, and analysis instruments, such as X-ray scanners and in free electron lasers.

## 8. Diamond composites

Addition of diamond to a material to form a composite can improve its properties, in particular physical properties, such as strength, brittleness, wear behaviour, or thermal conductivity. The diamond is usually added in the form of particles with sizes ranging from a few  $\mu\text{m}$  to tens of  $\mu\text{m}$ , while the matrix material can be metals, alloys, oxides, carbides, nitrides,  $sp^2$  carbon, and organic polymers, all of which are reviewed in Ref. [260]. The majority of these diamond composites are used for mechanical applications, such as cutting, grinding, or polishing (Section 2), but they are beginning to find uses for applications, such as biosensors [261], energy storage [262], supercapacitors [263], and photoelectrochemistry [264].

Composites can also be fabricated by embedding diamond-coated fibres, which are extremely rigid, into

a suitable metal or plastic matrix. Embedding short diamond fibres in random orientations increased the overall stiffness of the material in three dimensions. But if the embedded fibres are long and aligned, the stiffness of the composite is hugely increased—but only in the direction perpendicular to the fibres—leading to a composite with tuneable anisotropic stiffness properties [265]. Such diamond-fibre-reinforced metal-matrix composites may be useful for aerospace applications where strong, stiff but lightweight materials are essential. Furthermore, diamond’s huge thermal conductivity means that if the matrix material is plastic, such as epoxy, then embedding long, aligned diamond fibres enables the fabrication of heat-conducting composites which are electrically insulating [266]. These could be useful to remove heat from localised sources, such as electronic devices without the risks and problems associated with water-cooling.

## 9. Optics

Diamond is unique among materials due to its wide spectral transparency [267]. Depending on its level of purity, diamond can be transparent from its fundamental cut-off at  $\sim 225$  nm through to the far infrared (with the exception of a multi-phonon absorption band in the wavelength range of 2.5–6.7  $\mu\text{m}$ ), as well as through much of the X-ray region. Diamond’s very high thermal conductivity and small thermal-expansion coefficient allow it to dissipate huge, localised sources of heat (e.g., from a laser spot or beamline) to a nearby heat sink without significantly distorting its shape, making it an ideal material for windows, lenses, beam-splitters, and other optics [268,269].

Three game-changing advances over the past 20 years have driven the use of diamond for optics. The first is the ability to deposit CVD diamond at high rates to produce freestanding mm-thick diamond plates, ideal for bulk optics. Thick SCDs—although primarily for the gemstone market—can be polished and shaped to make excellent bulk optical components [270]. Even PCD can

now be manufactured with sufficiently high purity and transparency for use as freestanding windows with diameters  $\sim 150$  mm and excellent transmissivity [271] (see Figure 19). Smaller versions of these, typically 10–50 mm diameter, have now become the preferred window material for high-power multi-kW CO<sub>2</sub> laser systems, replacing the previous ZnSe windows which had problems with thermal lensing leading to poor beam quality and laser focus. In contrast, because diamond windows have high thermal conductivity, low  $dn/dT$  (i.e., the refractive index does not change much with temperature), and excellent IR transparency, the thermal-lensing effect is significantly reduced. As such, diamond windows can handle much higher power levels without any deteriorating effect on the laser beam. Interference effects between the front and back surfaces of windows can be minimised by fabricating them with wedge angles close to 1° [273].

The second advance is the development of low-temperature growth over large areas using novel plasma methods, such as linear antenna plasma deposition (LAPD) [274], distributed antenna array microwave (DAAM) deposition [275], or surface wave plasma (SWP) deposition [276]. These have made it possible to deposit a protective nanocrystalline diamond (NCD) layer onto delicate IR window materials, such as ZnS, and ZnSe, as well as more conventional optical materials, such as quartz and glass [277].

The final advance is the development of techniques to process diamond to obtain optically smooth surfaces with roughness  $< 1$  nm by polishing using a slurry made from conventional diamond grit, or RIE etching, and chemical-mechanical polishing [278].

The higher powers and larger wavelength ranges now accessible to lasers that use diamond windows are enabling new technologies. High-power CO<sub>2</sub> lasers operating in the IR (10.6  $\mu\text{m}$ ) are used in industry for welding, hardening, or remelting metals, and can cut all

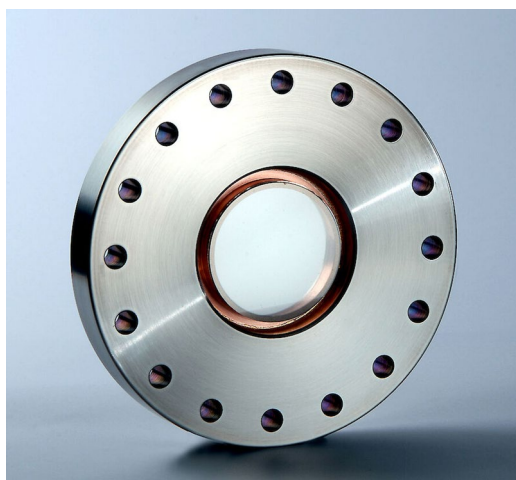


**Figure 19.** An example of a CVD diamond window embedded in a UHV conflat vacuum flange. Photo: used with permission from *Diamond Materials* [272].

types and thicknesses of metal and other materials: mild steel, stainless steel, aluminium, as well as plastic, tile, marble, and stone. Because diamond windows are transparent to microwaves, they are beginning to find use in gyrotrons in fusion reactors (see Section 13.2), in radar, or in planned directed-energy applications, especially military weapons where high-powered (100 MW) microwave laser beams may be used to incapacitate personnel or knock-out electronics [279]. High-power UV lasers using diamond windows are also at the forefront of extreme ultraviolet lithography (EUVL) (13.5 nm) for semiconductor fabrication [280].

Other diamond optics are becoming essential in a diverse range of advanced X-ray devices, such as X-ray monochromators, beam splitters, high-reflectance back-scattering mirrors, lenses, phase plates, diffraction gratings, bent-crystal spectrographs, and for the generation of fully coherent hard X-rays by seeded free-electron lasers—see the detailed review of these in Ref. [269].

### 9.1. Anti-reflective coatings (ARCs)

ARCs are used in many optical products in daily life, such as on spectacle lenses, on the screens of smartphones or tablets, on the dashboards of cars, and on the control panels of house-management systems. DLC is commonly employed as a combined wear-resistant layer and ARC on many types of optics [281]. Unfortunately, using a CVD diamond layer instead of DLC in this way is problematic due to the fact that most optical materials (glass, plastics) do not survive the high-temperature CVD process. Nevertheless, using a low-temperature CVD process along with surface layers of low-refractive silicon dioxide or other oxides, promising results have been reported with diamond ARC layers on quartz and glass substrates [282]. IR optics which use Si as the optical material are easier to coat with a CVD diamond ARC, and reports show that diamond-coated Si optics have been successfully used to monitor processes in the high-temperature, highly corrosive environment of steelworks [283]. Rather than use films of diamond on optics, bulk SCDs can act as attenuated total reflection (ATR) crystals, enhancing the accuracy and precision of chemical analysis [284].

### 9.2. Missile domes

Heat-seeking missiles use IR sensors to lock on to their targets. However, the IR-sensitive materials used (ZnS, ZnSe) are fragile and prone to damage—especially if the missile were to fly at high speed (up to Mach 5) through rain or sandy dust clouds. Such devices need to be protected by a window that (a) is IR-transparent, (b) can survive high-velocity impacts from sand particles or water droplets, (c) can cope with aerodynamic heating—the large temperature increases resulting from friction

with the fast-moving air, and (d) is dome shaped for aerodynamical efficiency. PCD domes were developed for this application by the UK and US air forces in the late 1990s. There remains a lot of secrecy surrounding the final outcome of this work and whether or not the domes were even adopted by the military, but the lack of recent publications in this area suggests that the cost of the diamond domes proved uneconomic compared with competing materials, such as sapphire. Nevertheless, their development instigated several advances in CVD technology, including how to deposit and then polish diamond on macroscopic 3D substrates [285], which led directly to the development by *Element Six* of CVD diamond tweeters for high-end music systems [286].

### 9.3. Raman lasers

Raman lasers use an optical pump laser to excite high-frequency lattice vibrations (phonons) in a suitable transparent crystal, such as potassium gadolinium tungstate (KGW),  $YVO_4$ , or  $Ba(NO_3)_2$ . These phonons absorb some of the laser energy and then re-emit the remaining energy as a lower-energy (longer-wavelength) laser beam. Their utility lies in the fact that they can convert commonly available laser wavelengths into unusual laser wavelengths, such as yellow light (see Figure 20), which are difficult to achieve by conventional laser or optical systems, but which have important applications in chemical analysis and medical treatment. However, the absorbed pump-laser energy causes the target crystal to heat up significantly, distorting the outgoing laser beam—a problem which limits most conventional Raman lasers to low powers.

The advent of large (multi-mm-sized) high-purity optical-quality CVD diamond crystals enables many of the limitations of current Raman laser systems to be overcome [288]. Diamond's very high thermal conductivity eliminates many of the excessive heating problems, meaning Raman lasers with much higher output power levels can be achieved. Diamond also has a higher Raman gain coefficient (which governs what fraction of the pump-laser power is converted into the frequency-shifted laser light), than any of its competing materials,

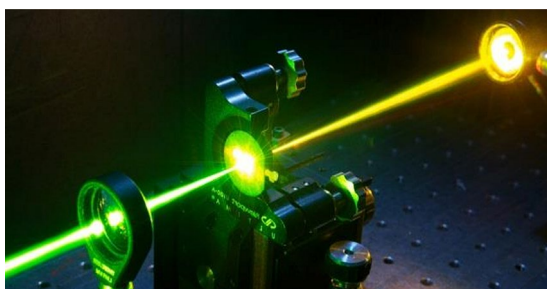


**Figure 20.** Conversion of green laser light to yellow/orange using a monolithic diamond Raman resonator. Image taken from Ref. [287] with permission.

making the process very efficient. In the last few years, researchers at Macquarie University [289] and Strathclyde University [290], amongst others, have reported a range of different diamond-based Raman laser variations, including continuous wave, Q-switched, and ultrafast lasers, with wavelengths from the deep-UV to the mid-IR. The power limits of diamond Raman lasers are still being pushed, with kW lasers now being developed. As larger and higher-purity diamond components become available, the possible uses for such high-power diamond Raman lasers will doubtless increase.

## 10. Radiation detectors and other applications for synchrotrons and particle beams

The extreme power densities and heat fluxes associated with synchrotron radiation, especially when highly focused, make conventional optics challenging. CVD diamond is radiation hard and compatible with ultra-high vacuum, and is highly transparent from the ultraviolet through to the infrared, as well through the X-ray region. As such, it is often the only material that can be used in such challenging conditions.

### 10.1. H-atom beam generation

Diamond's robustness, even in the form of thin, large-area, freestanding foils, makes it resistant to damage and distortion when placed into high-energy ion beams. Nanocrystalline diamond foils (<1  $\mu\text{m}$  thick,  $10 \times 16$  mm) supported on one edge, have been used to strip electrons from  $H^-$ -ion beams to produce H-atom beams [291]. Remarkably, these very thin but large-area diamond foils can withstand the energy of a 1.0 GeV ion beam. To prevent distortion, the foils are patterned with U-shaped corrugations to enhance their mechanical strength and prevent them curling up under thermal or mechanical stress. Such diamond foils may allow future synchrotrons to create and utilise H-atom beams with unprecedented energy and flux.

### 10.2. CVD Diamond fluorescent screens

Perfect diamond does not show any visible fluorescence. However, when CVD diamond is struck by high-intensity light, the nitrogen and vacancy-related defects present in the lattice create fluorescence in many visible colours, ranging from blue-violet and green down to red-orange. Thus, CVD diamond fluorescent screens can be used to track the position of "invisible" synchrotron beams, and have proven to be a powerful tool for the monitoring of synchrotron radiation. Indeed, the brightness of the fluorescence is sufficient to monitor white undulator beams as well as monochromatic beams [292].

### 10.3. X-ray lenses

Diamond displays several outstanding properties that make it desirable for X-ray optics and instrumentation, especially for high-brilliance third- and fourth-generation X-ray sources. In these high intensity X-ray beams, many competing materials (such as Si) simply do not function or remain stable. Due to its low atomic number ( $Z=6$ ), diamond is much more transparent to X-rays than silicon ( $Z=14$ ), because absorption scales as  $\sim Z^3$ . With less energy absorbed, diamond X-ray optics heat up to a lesser extent, and with their high thermal conductivity and low CTE, these optics are very efficient and stable. For X-rays lenses, the important metric is a short focal length, and diamond achieves this due to its relatively large decrement of the refractive index, meaning less material is required to produce a short focal-length optic—and less material means fewer absorbance losses. Alianelli *et al.* [293] demonstrated an X-ray planar compound refractive lens (CRL) fabricated *via* CVD growth of a conformal NCD layer onto an etched Si template. The Si substrate was removed to produce a freestanding diamond CRL, as shown in Figure 21. Testing on a high-power X-ray synchrotron beam yielded a line focus of sub-micron width. Further improvements in this technology may enable nm-scale focusing of high-power X-ray beams. Such unprecedented improvements in resolution for X-ray scattering studies should permit the molecular structure of proteins and other biomolecules to be determined to astonishing precision.

### 10.4. Particle and radiation detectors

So long as the particle energies involved are greater than the band gap of diamond (5.47 eV), diamond radiation detectors can be designed to detect and analyse most forms of ionising and non-ionising radiation, including neutrons [294], protons [295], alpha [296], beta [297], and gamma [298] radiation, as well as UV [299] and X-rays [300] (see the comprehensive reviews in Refs. [301,302]). Compared to competing materials and technologies, diamond has several distinct advantages in

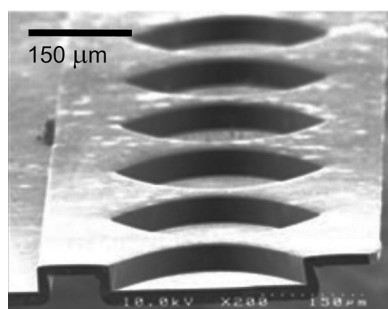


**Figure 21.** An X-ray linear CRL fabricated using freestanding NCD deposited conformally into a prepatterned Si mould. Photo reproduced with permission from Ref. [293] (Copyright AIP 2010).

relation to detecting and measuring radiation levels [303]. Diamond-based detectors are very robust and therefore seldom require repair or replacement. They generally have a very fast response ( $<100$  ps) due to their high mobility of free charges ( $\sim 4500$  cm<sup>2</sup> V<sup>-1</sup> s<sup>-1</sup> for electrons, 3800 cm<sup>2</sup> V<sup>-1</sup> s<sup>-1</sup> for holes [304]) and they can be operated at room temperature with no need for cooling. They have a resistivity several orders of magnitude greater than Si-based detectors, with extremely low leakage currents, which makes them highly sensitive. Unlike Si detectors, diamond detectors do not require *p*-type or *n*-type junctions to connect the detector to the control electronics. Because such junctions are often a point of failure, diamond detectors are more robust, allowing them to be used in extreme environmental conditions, *e.g.*, high humidity, high temperature, and highly corrosive environments.

These features, combined with diamond's intrinsic properties, give diamond detectors perhaps their most important advantage over other materials—they are resistant to the extremely high radiation levels at which most other detectors stop functioning. Indeed, the main Atlas detector used on the Large Hadron Collider at CERN is made from diamond, as no other material could survive the huge radiation levels (proton fluences of  $1 \times 10^{15}$  cm<sup>-2</sup> and instantaneous rates of at least  $1 \times 10^9$  cm<sup>-2</sup> s<sup>-1</sup> [305]) in the beam. The intense beams of X-rays from synchrotron sources at ESRF (Grenoble) and the Diamond Light Source (Harwell, UK) are monitored using diamond detectors and have been focused using diamond compound refractive lenses (see Section 10.3), while the Joint European Torus (JET) nuclear fusion facility at Culham (UK) uses diamond detectors for UV and neutron detection. The next-generation fusion energy source, ITER, will use diamond detectors for several applications, including as part of their neutral-particle analyser [306].

Details on the design and operation of the different diamond detectors used for various types of radiation can be found in Refs. [301,302]. In brief, most diamond detectors work on the same principle as photovoltaic devices or ionisation chambers (see Figure 22). An incoming high-energy particle or photon strikes the diamond and travels through the bulk, losing energy *via* collisions with the carbon nuclei or bulk electrons. As it travels through the diamond, the particle leaves behind it a trail of electron-hole pairs. A potential difference applied across the diamond causes these charges to separate, with electrons drifting towards a positive electrode and the holes drifting in the opposite direction towards a negative electrode. This movement of charge creates a measurable current, the magnitude of which is related to the energy and number of incoming particles.

The diamond research group at CEA Saclay in France have developed several different diamond-based radiation detectors, the operation and applications of which

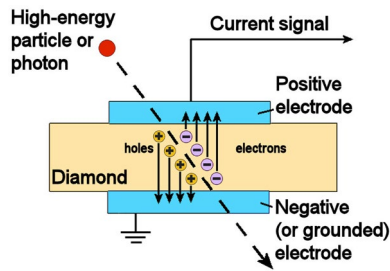


**Figure 22.** Schematic diagram showing the operating principles of a diamond radiation detector.

are described in detail in Ref. [307]. There are now several companies worldwide that produce such detectors commercially, including *PTW-Freiburg* (Germany), *St. Gobain/Norton Diamond Film* (Northboro, MA, USA), and *Element Six, Ltd* (Harwell, UK).

### 10.5. Dosimeters

Diamond can also be used as a radiation dosimeter, to detect and monitor the total dosage absorbed by humans exposed to radiation [308,309]. Most dosimeters are designed for medical and therapeutic use, for example, in X-rays and computerised axial tomography (CAT) scans, but these often only work at low radiation levels. Moreover, many existing technologies have limitations: Si dosimeters suffer from radiation damage and low lifetime, whereas ionisation chambers have low spatial resolution and low sensitivity.

Dosimeters that utilise diamond overcome some of these problems. Diamond has a low atomic number ( $Z=6$ ) compared to the mean value for soft tissue of  $Z\sim 6.5-7.5$ . Thus, diamond is described as being “tissue equivalent.” This means diamond dosimeters have fewer calibration errors or offsets than, say, Si ( $Z=14$ ) detectors, and do not over-estimate the dosage at lower energies [310]. However natural diamond dosimeters are expensive. Therefore, multiple research groups worldwide are actively developing dosimeters that instead use cheaper CVD diamond. Examples include the EU project MAESTRO (Methods & Advanced Equipment for Simulation & Treatment in Radiation Oncology) [311] and two projects funded by the Italian National Institute of Nuclear Physics called CANDIDO and CONRAD, on natural and synthetic diamond-based dosimeters for clinical radiotherapy [312].

## 11. Biomedical applications

Diamond is emerging as one of the major new biomaterials of the twenty-first century that could reshape the way medical treatment is performed, especially when invasive procedures are required, as explained in detail in these reviews [25,313]. The two main properties of diamond that make it a highly desirable candidate for biomedical applications are that it is bioinert, meaning

that there is minimal immune response when diamond is implanted into the body and that its electrical conductivity can be controlled from insulating to near-metallic enabling electrical signals to be sent to or received from cells, such as neurons.

### 11.1. Coatings for artificial joints

DLC coatings for metal and ceramic replacement hip-joints have been around for over 20 years, providing high wear resistance for the mechanical ball-and-socket joints and increased lifetimes. However, these coatings have become less favoured due to reports of the films delaminating after a few years and generating damaging particulates [314]. Similar worries prevented the adoption of CVD diamond coatings in artificial joints, which initially had poor adhesion onto the most commonly used implant material, Ti. However, some modern hip implants now use silicon nitride rather than Ti, and these are much more amenable to diamond CVD, with the diamond forming smooth adherent coatings. Extremely low wear rates for NCD-coated nitride hip-joints have been reported [315], but it is unclear whether these will become the mainstream solution for joint prostheses. A recent review on diamond for medical devices can be found in Ref. [316].

### 11.2. Culturing cells on diamond

Another approach for using diamond medicinally is as a bioinert culture-plate upon which to grow biological cells, including stem cells, cardiac muscle cells, various types of neurons, osteoblasts, fibroblasts, macrophages, and epithelial cells [25,317]. These cells are then available as *in vitro* test subjects for determining the efficacy of new drug treatments, or for studying the toxic effects of chemical or neurological agents—without the cost and controversy of using *in vivo* tests or animal experiments. Cells cultured on diamond plates can survive for many months, unlike those on traditional glass or plastic substrates which typically die after a few weeks. This means that long-term testing is possible, as are inheritance tests that require multiple generations of cells.

Studies at University College London [318] and the University of Bristol [319] have demonstrated that human stem cells thrive on diamond culture-plates and that they can later be transformed into other cell types (kidney, liver, and especially neurons) using suitable chemical treatments. When BDD is used as the plate, then the cells growing on its surface can be electrically interrogated or stimulated *via* this conducting substrate. The substrate can also be patterned or treated such that areas of the surface are amenable to cell growth, while other areas are not. In this way, cells, such as neurons, can be persuaded to grow only in certain areas, allowing two-dimensional neural networks to be fabricated (see

Figure 23) [320]. These “brains-on-a-plate” act as models that mimic to some degree the behaviour of a real 3D brain, allowing neuroscientists to study how different types of stimuli propagate through the neural network. Such studies may pave the way for future development of organic computers.

### 11.3. Bone and cartilage scaffolds

Coating traditional joint and bone implants with crystalline diamond can increase biocompatibility and cell adhesion, as well as reducing adverse reactivity, inflammation, erosion, and release of metal nanoparticles into the bloodstream. The diamond implant acts as a scaffold around and upon which new bone growth occurs [321]. The challenge is to optimise the CVD process on standard implant alloys, for which, as mentioned earlier, diamond deposition is usually unfavourable. Despite significant progress being made recently for deposition on Ti, Co-Cr, and even steel substrates (see the review by Catledge *et al.* [322]), it is likely that such scaffolding technology will first appear in dental implants [323]. Cartilage, too, can utilise diamond as a scaffold for growth or regrowth [324], suggesting future scenarios where body parts, such as the ears, nose, trachea, or even larynx, could be repaired or even regrown in the laboratory.

### 11.4. Neural implants, bionic organs, and brain-computer interfaces

Diamond is rapidly becoming the material of choice for bioimplants [325,326] because it does not provoke an immune response when implanted inside the body. As such, diamond-based implants produce minimal inflammation or scarring, and can therefore survive and function for years—or even decades—within the body, with no need for the cost and trauma of surgical replacement. Diamond is not chemically attacked by the body’s fluids. Thus, it can be used to protect non-biologically inert components (such as Si microprocessor circuitry) within

hermetically sealed diamond “boxes.” An example of this is the “bionic eye” project from Melbourne University [327–329], which uses an artificial retina chip sealed inside a protective diamond shell, implanted into the eye, to provide some degree of sight for patients with a malfunctioning retina.

Electrically conducting BDD can be used as an active biosensor, allowing electrical signals to be transferred to and from cells. This is especially useful for neurons situated in the brain, the central nervous system, or in the periphery, such as arms and legs [319]. Recently, there have been two major EU-funded research consortia (DREAMS [330] and NEUROCARE [331]) to study diamond-based implants that interface with living human neurons. The aim was to find treatments for neurological disorders, such as Alzheimer’s, Parkinson’s, stroke, epilepsy, paralysis due to trauma, and many others. An example biosensor is an artificial retina, reported by a collaboration between several French research groups, that uses a conducting diamond film grown onto a flexible polyimide substrate that can wrap around the back of the eyeball and transfer signals from the retina to the optic nerve [332]. Similarly, diamond sensors were implanted into the auditory cortex of a live guinea pig, allowing neuronal sound-dependent stimulations to be recorded [333] as the first step towards a “bionic ear.” Other examples currently being researched are diamond sensors embedded into the spinal cord of paraplegic patients, which pick up signals from the brain and transfer them wirelessly to an external computer. Interpretation of these signals using special software may allow robotic legs to be moved at will by the patient. Such treatments for paralysis have already been demonstrated using multiple external sensors placed on the scalp [334], but with an internal diamond implant, the sensor would be portable and remain *in situ* for perhaps 30 years.

Such two-way communication also opens up other possibilities, such as direct brain-computer interfaces (BCIs) [334]. In this case, the diamond sensors permanently implanted into the brain would pick up the neural

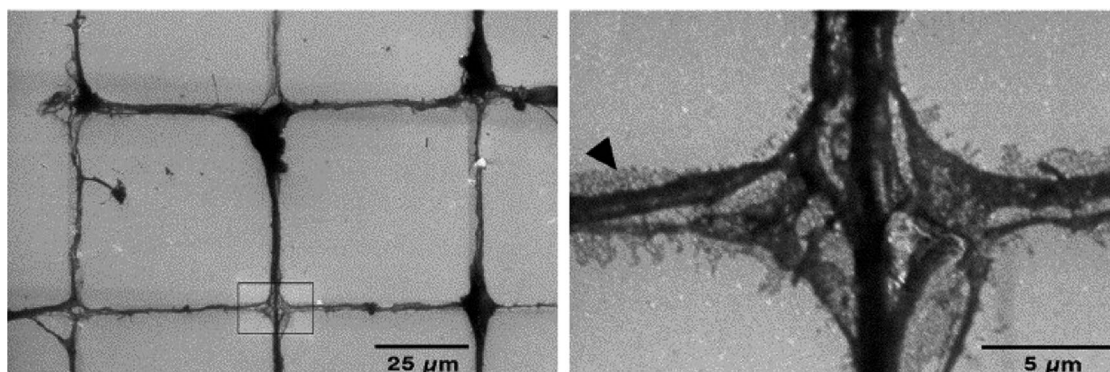


**Figure 23.** Ordered growth of neurons on a laminin-coated hydrophilic diamond substrate. The right-hand image shows a detailed higher magnification image of the part of the left-hand image indicated by the rectangle. Multiple neurites cross this intersection, possibly originating from several neurons. Images reproduced from Ref. [320] with permission.

impulses and transfer them wirelessly to an external computer. With suitable software to interpret the signals (a difficult problem in itself), it may, in time, be possible to develop thought-controlled equipment (TVs, cars, drones, *etc.*). Although this may seem rather far away, the implications of BCI technology for medical applications, military applications, and society as a whole, are huge—as any science-fiction author would attest!

### 11.5. Antibacterial coatings

Medical experts are currently warning about an antibiotic crisis due to the increasing number of strains of bacteria that are evolving resistance to antibiotics. As well as developing new types of antibiotics, another strategy is to develop antimicrobial coatings that kill bacteria mechanically rather than chemically. It would prove much more difficult for bacteria to evolve resistance against such surfaces, which would then function as a preventative, rather than a cure. One possible answer has been suggested following the study by Ivanova *et al.* [335] of the microstructure of the wings of dragonflies and cicadas, which are covered with micropillars a few 100 nm tall. Biologists believe these micropillars act as a protective mechanical antimicrobial surface. A surface with properties similar to these was fabricated using so-called black silicon—a synthetic nanostructured material that contains high-aspect-ratio nanopikes on its surface produced through plasma etching. Ivanova *et al.* found that black Si acts as an effective bactericidal surface for both Gram-negative and Gram-positive bacteria. However, the nanostructured Si surface is fragile and is easily damaged or scratched. A solution to this may be to coat the needles with a conformal layer of diamond, 50–100 nm thick, making the nanostructures far more robust and less likely to become damaged. As well as having excellent electrochemical properties (see Section 3.3), the diamond-coated spikey surface (called “black diamond”), was also found to kill bacteria efficiently and effectively [45,336] (see Figure 24). When the surfaces of the black-diamond needles were fluorinated by exposure to an SF<sub>6</sub> plasma, they became superhydrophobic, further increasing their antimicrobial

properties, as well as hindering the growth of biofilm [337,338].

Realistically, for real world applications, microbial-resistant surfaces will never be coated with exotic materials, such as black diamond. Instead, similar nanostructured surfaces could be fabricated from more conventional materials like stainless steel, Ti, polytetrafluoroethylene (PTFE), or medical-grade rubber. Nevertheless, the general findings from studies, such as those on black diamond will provide important information for the development of next-generation antibacterial surfaces made from more practical materials. Several other strategies for using diamond in antibacterial coatings are reviewed in Ref. [339].

### 12. Diamond anvil cells (DACs)

In a DAC, a sample placed between the flat, parallel faces of two opposed SCD stones (the anvils) is subjected to extreme pressure (up to 600 GPa) when a force pushes the two anvils together [340,341]. The transparency of the diamond anvils in the visible, IR, and X-ray regions has enabled a variety of optical and X-ray techniques to be used to study materials *in situ* under these extreme high-pressure conditions. Moreover, heating the sample to temperatures as high as 6000 K is possible using a focused laser passed through the transparent diamond. Static compression studies using DACs have explored a wide range of phenomena in materials at pressures of up to ~200 GPa and temperatures from near 0 K to several thousand K.

The advent of lab-grown CVD SCD anvil cells, which can be significantly larger and cheaper than natural stones, has enabled experiments to be performed at even higher pressures and temperatures, and with larger volume samples [342]. Such studies are proving invaluable for geologists to understand the environment deep within the Earth. CVD diamond anvils can now be grown with bespoke properties that have been optimised for a particular application, for example, X-ray or neutron scattering. Furthermore, sensors and electrical circuits can be fabricated onto the anvil surface and then overgrown with a layer of CVD diamond to embed the

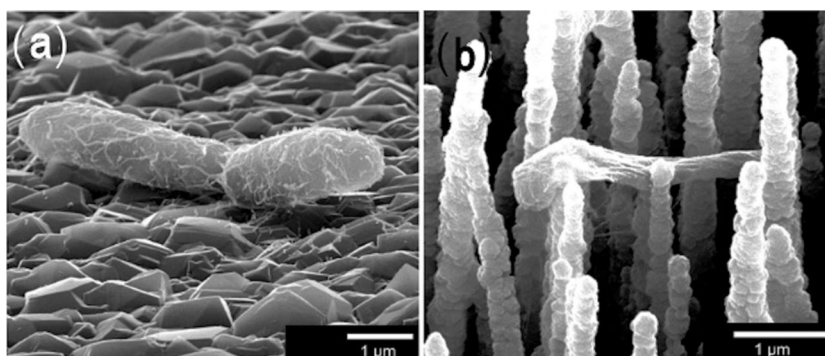


**Figure 24.** SEM images of *E. coli* bacteria, showing (a) healthy, turgid bacterial cells on MCD control samples, but (b) deformed and flaccid dead bacteria on a spikey black diamond surface. Figures reproduced from Ref. [337] under the CC BY 4.0 licence.

electronics inside the anvil. This process creates “smart” anvils [343] enabling electrical and thermal transport measurements [344], or localised heating [345], to be performed while the sample is under extreme pressure.

### 13. Nuclear fusion applications

The sun’s energy source, nuclear fusion, is seen as a potentially important option to provide cheap, clean energy here on Earth. However, the conditions required for nuclear fusion are extreme—to say the least! Diamond, with its own extreme properties, is often the material of choice for fusion power generation *via* the two most promising methods: laser compression of hollow spheres containing nuclear fuel (ICF—Section 13.1) or by plasmas in tokamak reactors (Sections 13.2 and 13.3).

#### 13.1. Diamond spheres for inertial confinement fusion (ICF)

One of the methods used to create nuclear fusion in the lab is ICF, in which the nuclear fuel (a mixture of deuterium and tritium, abbreviated as DT) is encapsulated inside a thin-walled, mm-sized, hollow sphere (called an ablator target) made of a low-atomic-number element, such as carbon. Extremely powerful lasers are focused onto this target from all sides simultaneously, causing it to collapse and compress to extremely high pressures and temperatures—sufficient to initiate nuclear fusion in the fuel (see Figure 25).

As you might imagine, fabrication of these hollow spherical ablator targets is tricky, and the material used is key. CVD diamond has several advantages over other possible materials (*e.g.*, Be and plastic). First, its high

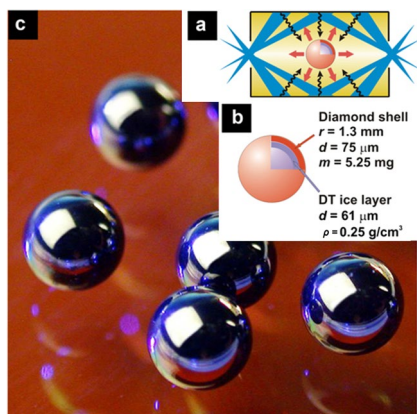


**Figure 25.** Diagrams of the ICF process at the US National Ignition Facility (NIF). (a) The hollow diamond ablator containing the DT fuel sits in the centre of a small cylinder, whereupon the incident UV laser light is focused onto the inside wall of the cylinder where it is converted to soft X-rays which compress the ablator target. (b) Optimised diamond ablator design consisting of a 2.6 mm diameter hollow diamond capsule with a wall thickness of 75  $\mu\text{m}$  surrounding the 61  $\mu\text{m}$  thick DT ice fuel layer. (c) Photographs of the nanocrystalline diamond targets. Images taken from Ref. [346] with permission.

atomic density means that diamond can adsorb 10–20% more energy than competing materials. Also, its extremely high yield strength enables handling of the filled targets—in which the gas mixture has a pressure of  $\sim 1000 \text{ atm}$  at room temperature, without them bursting. Finally, CVD diamond can be mass-produced relatively inexpensively, and in an environmentally friendly manner (depending on the method of electricity generation used to power the CVD reactors).

The main problem is how to fabricate diamond ablator shells that are defect-free and nearly perfectly spherical. This has been achieved by a group based at the Fraunhofer Institute in Freiburg, who used solid silicon spheres as substrates for diamond CVD, with the Si spheres being continually rotated during the deposition process. The diamond-coated Si sphere is then polished, and a 5  $\mu\text{m}$  hole is laser-cut into it, enabling the Si core to be dissolved away using a wet etch process [346]. The resulting hollow diamond spheres are currently under test at the National Ignition Facility (NIF) based at Lawrence Livermore National Labs in the USA. In December 2022, the NIF researchers reported they had achieved more fusion power output than was required to run the lasers—demonstrating net fusion power generation by the ICF method for the first time [347]. Similar technologies using spherical CVD diamond ablaters are also being developed in Japan [348] and China [349].

#### 13.2. Gyrotron windows

The most well-known method used to study nuclear fusion is a high-power plasma located in a doughnut-shaped reactor called a tokamak. Heating the plasmas within tokamak reactors to temperatures of  $\sim 150$  million K required for nuclear fusion is achieved using a gyrotron—a microwave generator employing cyclotron resonance coupling between microwave fields and a beam of electrons. They are notable because they can generate enormous power levels (tens of megawatts) at microwave frequencies [350]. The ITER fusion reactor, part of the European “Fusion for Energy” project [351], is planning to use 56 such gyrotrons located some 100 m away from the tokamak to avoid perturbations from its magnetic field. The high-power microwaves from the gyrotrons will travel through waveguides to the ITER plasma chamber. Because both the gyrotrons and the tokamak chamber are under vacuum, the only way to get the microwave power out of the waveguides and into the chamber is through a microwave-transparent CVD diamond window [352]. Each of the 56 windows will be about 80 mm in diameter and 1.1 mm thick, and be capable of transmitting up to 2 MW of microwave power for durations of up to 3000 s. They must also be extremely pure, as any defects might absorb microwave energy and cause catastrophic local heating of the window, possibly

triggering it to shatter. Even more powerful gyrotrons, requiring even thicker and larger diamond windows, are being developed for other high-power plasma applications [353].

### 13.3. Reactor coatings

The “plasma-facing” inside walls of a tokamak fusion reactor must withstand extreme conditions, such as tremendously high temperatures, the surfaces being bombarded by high fluxes of charged and neutral species, rapid changes of pressure, and plasma transients (arcing) [354]. Not only must the surface coatings of the wall and any components in this environment protect them from damage, but any particulates or atoms from the coating that are etched or sputtered into the plasma must not contaminate the fusion process. Atoms with high atomic numbers are particularly problematic with regard to plasma contamination, which makes coatings made from commonly used wear-resistant materials, such as tungsten ( $Z=74$ ), undesirable (although W is still often used, albeit reluctantly, due to its *very* low erosion rate). As such, graphite or carbon-fibre composite (CFC) coatings are preferred for this purpose due to their resistance to high temperatures and their low atomic number ( $Z=6$ ), meaning any C atoms that evaporate into the gas phase do not significantly perturb the plasma. However, graphitic carbon etches relatively rapidly when exposed to high fluxes of H isotopes, which decreases the lifetime of the coating. Moreover, the etched carbon atoms can then be redeposited elsewhere in the reactor, causing a problem with tritium absorption. Tritium and deuterium are the main reactants in the fusion reaction, but graphitic carbon can absorb and retain significant amounts of these H isotopes, depleting them from the gas phase, and thereby limiting the fusion process.

One possible solution to this is to use CVD diamond as a protective coating for plasma-facing components. Diamond has all the advantages of being made from carbon, without the high erosion rate of graphite in H atmospheres. Moreover, its dense crystalline structure means diamond does not absorb tritium or deuterium to the same extent as graphitic carbons. Several groups have studied PCD coatings for this purpose, and the results look promising [355]. However—using ITER (see Figure 26) as an example—its internal surface area is  $\sim 600\text{ m}^2$  and will be protected by 440 “blanket” modules made from beryllium ( $Z=4$ , expensive and toxic) or tungsten ( $Z=74$ , potentially contaminating). Replacing such large-surface-area modules with equivalent CVD-diamond-coated versions would be too costly using current technology, especially if the modules need to be replaced regularly due to erosion. As such, it is more likely that diamond may be used in specific areas of the reactor with particularly high thermal load, such as the

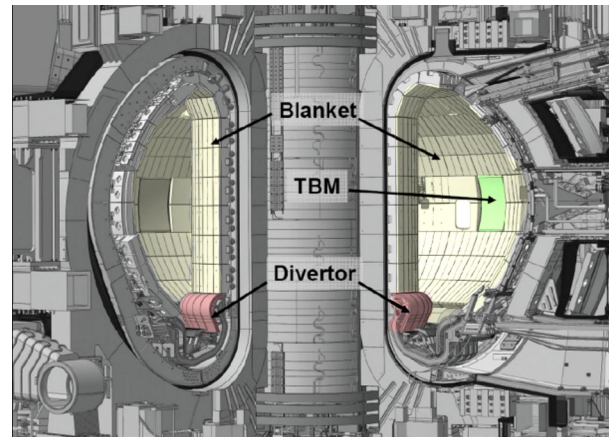


**Figure 26.** Cut-away representation of the ITER tokamak fusion reactor. The blanket module (yellow) is composed of a large number of tiles which provides the main thermal and nuclear shielding of the vacuum vessel and components. The test blanket modules (TBM, green) are replaceable panels used to test the performance of new plasma facing materials. The divertor (red) is located at the bottom of the plasma chamber; it exhausts the major part of the plasma thermal power and minimises the helium and impurity content in the plasma. It must tolerate high heat loads while at the same time providing neutron shielding for the chamber and magnet coils in its vicinity. Diagram coloured and reproduced with permission from Ref. [356].

divertor. ITER is still many years away from completion, however, and the final design and choice of blanket-coating material are yet to be finalised.

### 13.4. Microplasma arrays

These are plasma sources with sub-millimetre dimensions which maintain stable, high-density nonthermal discharges in diverse working gases at pressures exceeding 1 atm [357]. Applications include ignition triggers for fusion plasmas, as well as high-efficiency sources of vacuum-UV excimer radiation, the remediation of environmental pollutants and destruction of biological pathogens, mass spectrometer ionisation sources, process chemistry, large-area visible or UV lighting, and ion-thrusters for spacecraft. However, severe demands are placed on the electrodes by the high gas temperatures and ion energies produced under high-power, high-pressure d.c. operation, limiting the achievable power density and device lifetime. Most microplasma devices have employed electrodes manufactured either from Si or refractory metals, such as Mo. Diamond is a promising candidate for microplasma applications due to its low sputter yield and superlative thermal conductivity [358]. Moreover, monolithic all-diamond devices are possible where the insulating layers are made from undoped diamond and the conducting electrodes from BDD. Prototype monolithic diamond hollow-cathode devices with cavity diameters on the order of  $100\text{ }\mu\text{m}$  have been reported that operate at nearly 10 atm [359].

## 14. “Everlasting” nuclear batteries

Diamond has been proposed as a material with which to fabricate nuclear electrical batteries with extremely long lifetimes. A nuclear battery turns radioactivity into electricity, and they were developed due to their long battery life, mainly for powering spacecraft as they travel to distant planets over periods of many years. Many different types exist, depending upon the design and type of radioactivity involved.

One type of nuclear battery that is currently gaining a lot of interest [360] is based on diamond composed of radioactive  $^{14}\text{C}$ , which is a beta emitter with a half-life of  $\sim 8000$  years (see Figure 27). Because this type of device generates electrical power from beta radiation, they are also known as betavoltaic batteries. The raw material for the  $^{14}\text{C}$  diamond layer is radioactive graphite which is a waste product from many nuclear power stations. This graphite contains  $^{14}\text{C}$ , and when burnt in a  $\text{H}_2$  atmosphere this is converted into  $^{14}\text{CH}_4$  which can then be separated from any  $^{12}\text{CH}_4$ . The isotopically pure  $^{14}\text{CH}_4$  is then used in the gas mixture in a CVD reactor to deposit a thin layer of  $^{14}\text{C}$  diamond onto a conducting substrate. The substrate is placed under vacuum, and a metal “collector” electrode is positioned  $\sim 100\ \mu\text{m}$  away, facing the diamond layer. The  $^{14}\text{C}$  layer emits high-energy beta electrons which travel across the vacuum gap to strike the collector. Connecting the two electrodes allows current,  $I$ , to flow back to the emitter, driving an external load, in a similar fashion to thermionic energy generation (Section 7.3).

Such betavoltaic devices could produce electrical power almost indefinitely (thousands of years!) and can be made into small, portable, sealed solid-state packages, with no moving parts which require zero maintenance. The output power would be perhaps only a few  $\mu\text{W}$  per device, but if required, hundreds or thousands of devices could be daisy-chained together in series to produce higher powers. Because the battery is always on, it could continuously trickle-charge a capacitor ready for intermittent high-power use, e.g., a transmitter on a spacecraft that sends all its data back to Earth in a short high-frequency burst once a day. Other uses include places where changing a battery is difficult, costly, or impossible, for example, military applications (e.g., remote surveillance), aerospace applications (e.g., sensors inside jet engines), or medical applications

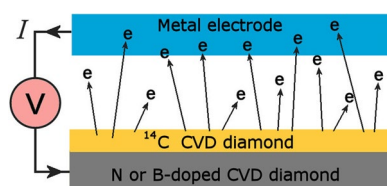


**Figure 27.** Schematic diagram of a concept for a diamond-based betavoltaic battery.

(perpetual heart pacemakers). Commercial applications are numerous, too, such as batteries for domestic use (watches, calculators, mobile-phone chargers, *etc.*), although possibly the largest application would be for powering “smart” devices for the “Internet of Things” [361]. A great many household devices, from kettles to fridges, may soon be connected to the internet, and these will require a small but continual supply of power—just enough to power the wifi connection. It would be impractical for all these appliances to be mains-powered, whilst normal batteries would need changing regularly, but a betavoltaic battery could supply the small power levels required indefinitely.

Other designs based on layers of alternating  $p$ - or  $n$ -doped diamond sandwiched between  $^{14}\text{C}$  diamond emitting layers [362], that utilise  $^{63}\text{Ni}$  or tritium as the radioactive sources [363], or which combine beta radiation and thermionic emission [364], have also been proposed. Such devices are possibly on the verge of commercialisation [365], so it may not be too long before we see our first “everlasting” battery in the shops.

## 15. Applications of 0D, 1D, and 2D diamond nanostructures

As well as diamond in the form of single-crystal gemstones or thin films, diamond can be fabricated at the nanoscale in the form of zero-dimensional particles, one-dimensional fibres or needles, or two-dimensional sheets [366]. Generally, there are two main approaches that are used to make these materials: bottom-up deposition and top-down etching. For deposition, the overall shape of the resultant diamond nanostructure is determined by that of the substrate. The same criteria apply to these types of deposition as for macroscopic CVD, namely the substrate material must be stable enough to withstand the CVD conditions, there needs to be a high-quality interface with the diamond for good adhesion, and the CTE of the substrate must be low to prevent stress formation and delamination. An extra consideration is that uniform deposition of diamond on all sides of the substrate may be necessary.

Conversely, top-down processing involves first depositing a thick planar CVD diamond film and then etching this into the required structures using  $\text{O}_2$ -based plasmas [367] and nanoscale masks, or with catalytically active metal nanoparticles [368,369].

However, only a few applications have been reported for most of these novel nanostructures to date, so the reader is referred to the comprehensive review of this subject by Li *et al.* [366].

### 15.1. Nanodiamond

Diamond particles in the range  $\mu\text{m}$  to  $\text{mm}$ , usually obtained from the debris of processing natural and

lab-grown diamond into gemstones, find several lucrative applications in cutting, grinding, and polishing (see Section 2). But nanodiamond (ND) particles with sizes 2–10 nm (see Figure 28(a)) are arguably of more scientific interest [371,372]. The most common method of production for NDs is *via* detonation of an explosive mixture (such as TNT and hexogen) in an inert atmosphere or in water/ice, inside a steel chamber [373]. The shockwave produced by this detonation propagates through the reaction mixture at supersonic speeds. The prevailing pressure and temperature within the transient shockwave can be  $p \sim 10\text{--}20$  GPa and  $T \sim 2000\text{--}4000$  K, under which conditions diamond is the thermodynamically favoured phase of carbon. However, at all other times, the pressure and temperature conditions favour other forms of carbon. As the high-pressure, high-temperature shockwave passes through the reaction mixture, the carbon atoms in the explosive begin to crystallise into diamond. But within a few  $\mu\text{s}$ , the shockwave passes by, the ambient conditions revert to much lower  $p$  and  $T$ , and the remaining unreacted carbon atoms solidify as amorphous or graphitic carbon material. Thus, the explosion produces a mixture of diamond nanoparticles (whose size is determined by the speed of the shockwave), soot, and other  $sp^2$  carbon material.

The powdery mixture of products from the detonation is cleaned with various acids and reagents to remove unwanted metallic impurities and soot, and the diamond component extracted. The resulting material, often called “detonation nanodiamond” (DND) is commercially available from many suppliers worldwide as a powder or as a suspension in water. It is currently produced at a rate of several tons per year and sold for as little as \$100/kg! Unfortunately, due to its fabrication process, the DND particles tend to fuse into aggregates  $\sim 100$  nm in size (see Figure 28(b)), and therefore the as-supplied material requires de-aggregation before subsequent processing. This can be achieved in many ways, including ball milling, pulverisation, high-power sonication, acid treatments, controlled heating in  $\text{O}_2$  or  $\text{H}_2$ , or combinations of these methods [374]. The resulting DND particles are best described as having a diamond core surrounded by a (partially) graphitic or fullerene-like

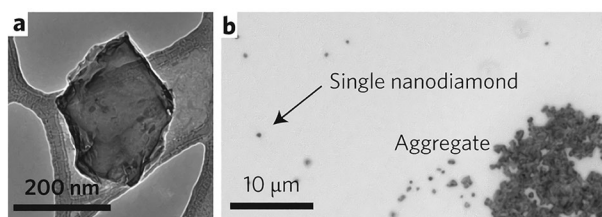


**Figure 28.** (a) TEM Image of a single nanodiamond on a hollow electron microscopy carbon film. (b) Brightfield optical microscopy image of nanodiamonds in water, drop cast onto a glass coverslip. Images reproduced with permission from Ref. [370].

shell—and are sometimes described as “bucky-diamonds” [375].

Following the various cleaning processes applied after detonation synthesis, the surfaces of DND particles are usually terminated with oxygen-containing groups, such as carboxyl, hydroxyl, or bridging-ether groups. DND particles are therefore usually hydrophilic, which helps their stability when in aqueous suspensions. This oxygenated surface can be modified by standard chemical methods, replacing the O-groups with H (producing a mildly hydrophobic surface), with F (which is superhydrophobic), or with  $\text{NH}_2$ . Both O-terminated and  $\text{NH}_2$ -terminated ND are of particular interest because they enable the subsequent binding of a large variety of functional molecules, such as bioactive compounds (proteins, enzymes, antibodies, DNA), catalysts, drug molecules, or polymer building-blocks by amide bond formation or other standard chemical procedures [376].

ND particles containing fluorescent NV-centres exhibit bright luminescence, which, combined with a readily modifiable surface and biocompatibility, make them extremely promising for biomedical applications [377], and, in particular, for use as a biomarker to “tag” biomolecules of interest as they travel around within living organisms [378] (see Section 5.3). Chemically functionalized NDs have also been used as delivery vehicles in targeted drug therapy [379]. These so-called “magic bullets” are treatments that affect only the afflicted part of the body, such as an organ or a tumour [380]. Although these sorts of treatments are still under development, results so far look impressive and promising, and may provide a novel means of tackling diseases, such as cancer in the near future.

## 15.2. CVD diamond seeding

The discovery and commercial production of DND is perhaps the most important advance relevant to diamond film nucleation in the last 20 years [371]. DND is now commonly used to seed non-diamond substrates, reducing the induction period at the start of CVD before diamond growth starts. Their small size allows a near-monolayer coverage of close-packed DND particles to be deposited onto a surface, which not only protects delicate substrate materials (such as GaN, see Section 6) from etching in the CVD atmosphere but enables thin, conformal diamond layers to coalesce rapidly into continuous coatings, even on highly textured 3D structures (see Section 11.5).

The fabrication, processing, and characterisation of ND and its wide variety of applications is a huge subject which is beyond the scope of this review, so readers are invited to consult the various books on the subject [381,382].

## 16. Conclusions

The upsurge in the market for lab-grown diamond jewellery over the last decade has seen huge increases in the number of gemstones produced, along with improvements in their size, quality, and throughput. These developments in the gem industry have fed into the scientific sector in terms of ultra-pure SCD substrates with increasingly larger wafer sizes for electronic and quantum applications, and at ever lower costs. This, in turn, gave rise to a renaissance in CVD technology from about the year 2010 onwards, where the number of applications for CVD diamond expanded enormously. The discovery that the NV-centre in diamond could act as a single-photon source opened up an entirely new research field of diamond-based quantum applications, and offered the exciting prospect that a room-temperature diamond quantum computer might be possible “in the near future.” BDD electrodes also began to become commercialised, with several companies selling these electrodes for electrochemical assays or water purification. These same electrodes can be used to generate solvated electrons which can drive many high-energy chemical reactions in solution without the need for high temperatures. Following 30 years of development, diamond electronic devices have built upon their steady progress—helped by the advances in several exciting new approaches which are now re-energising this field. For example, delta-doped devices, although somewhat controversial, are intriguing—if the fabrication difficulties can be overcome—while 2DHG FETs are emerging as viable candidates for radiation-hard high-power high-temperature operation. Alongside these, there is a huge number of possible diverse applications for CVD diamond that are also beginning to make an impact in medicine, the nuclear industry, optics, aerospace, *etc.*, many of which are close to market or already being commercialised.

After all the hype surrounding CVD diamond in the 1990s, followed by the crash in the early 2000s when several technological set-backs made it seem like the “wonder material” might not be so wondrous after all, diamond has bounced back in the 2020s with a truly remarkable number and diverse range of applications. After that somewhat shaky start, it may be that CVD diamond is finally living up to its promise of being the ultimate engineering material.

## Acknowledgments

The authors wish to thank Professor David Moran from Glasgow University for useful discussions concerning the intricacies of 2DHG devices, and Professor Christian Degen of Zurich ETS for access to the raw magnetic-sensing data to enable us to replot the spectra in Figure 10. We also wish to thank Professor Christoph Wild for permission to use the image of a diamond window.

## Disclosure statement

No potential conflict of interest was reported by the author(s).

## Funding

RZ wishes to acknowledge the funding scheme of the Government of the Republic of Kazakhstan under the Bolashak International program.

## Notes on contributors

**Dr Ramiz Zulkharnay** received his BSc and MSc in Chemistry from the Eurasian National University (Kazakhstan) in 2012 and 2014, respectively. He obtained his PhD from the University of Bristol (UK) in 2023 and is currently working as a Postdoctoral Research Associate at the same university. His research focuses on the synthesis, design and fabrication of diamond-based energy devices. With a background in the surface functionalisation of diamond for thermionic applications, he has published several papers in high-impact journals and presented his work at international conferences.

**Professor Paul May** graduated from Bristol University in 1985 with a BSc degree in Chemistry, and then worked at GEC Hirst Research Centre in Wembley studying the fabrication of microchips and looking into the properties of the (then) new high temperature superconducting ceramics. In 1988, he returned to Bristol University to do a PhD in the area of plasma etching of semiconductors. After graduating in 1991, he co-founded the CVD diamond group at Bristol with colleague Prof Mike Ashfold FRS. He later won a *Ramsay Memorial Fellowship*, followed by a *Royal Society University Research Fellowship*, which allowed him to expand the Bristol diamond activities into a self-contained research group within the department. Paul became a full-time lecturer in 1997, and was made a Professor in Aug 2009. Paul's research area focuses upon CVD diamond, but nevertheless remains very diverse, being partway between Chemistry, Physics, Materials and Engineering plus some Biology and Medical applications. Over the years, he has studied the fundamental chemistry of diamond growth via experiment and computer modelling, doping of diamond, X-ray lenses, bioimplants, antimicrobial coatings, microplasma generation, large-surface-area BDD electrochemical electrodes, and most recently, metal adsorption onto diamond for NEA and thermionic emission applications. He has published nearly 300 scientific papers in peer-reviewed Journals, along with several book chapters. He won the Royal Society of Chemistry's prize for Higher Education teaching in 2002. He is also the editor of well-known websites such as the 'Molecule of the Month', and the (infamous) 'Molecules with Silly or Unusual Names', and is a the co-author of the popular science book 'Molecules which Amaze Us'.

## ORCID

Ramiz Zulkharnay  <http://orcid.org/0000-0002-7420-399X>

Paul W. May  <http://orcid.org/0000-0002-5190-7847>

## References

- [1] Field JE. The properties of natural and synthetic diamond. London: Academic Press; 1992.

- [2] May PW. Diamond thin films: a 21st century material. *Phil Trans R Soc Lond A*. 2000;358(1766):473–495.
- [3] May PW, Zulkharnay R. Diamond thin films: a 21st century material. Part 2: a new hope. *Phil Trans R Soc Lond A*. 2024.
- [4] D’Haenens-Johansson UFS, Butler JE, Katrusha AN. Synthesis of diamonds and their identification. *Rev Miner Geochem*. 2022;88(1):689–753.
- [5] Diamond Tools Market. Global market insights, Report ID: GMI5798; 2023. Available from: <https://www.gminsights.com/industry-analysis/diamond-tools-market>
- [6] Gaukroger MP, Martineau PM, Crowder MJ, *et al*. X-ray topography studies of dislocations in single crystal CVD diamond. *Diam Relat Mater*. 2008;17(3):262–269.
- [7] Sumiya H, Tamasaku K. Large defect-free synthetic type IIa diamond crystals synthesized via high pressure and high temperature. *Jpn J Appl Phys*. 2012;51(9R):090102.
- [8] Angus JC. Diamond synthesis by chemical vapor deposition: the early years. *Diam Relat Mater*. 2014;49:77–86.
- [9] McDonald JA. Diamonds hit the big time. III-Vs *Rev*. 1993;6(4):34–37.
- [10] Butler JE, Windischmann H. Developments in CVD-diamond synthesis during the past decade. *MRS Bull*. 1998;23(9):22–27.
- [11] Kohn E, Ebert W. Electronic devices on CVD diamond. In: Dischler B, Wild C, editors. *Low-pressure synthetic diamond*. Springer series in materials processing. Berlin; Heidelberg: Springer; 1998.
- [12] Wang S-F, Hsu Y-F, Pu J-C, *et al*. Determination of acoustic wave velocities and elastic properties for diamond and other hard materials. *Mater Chem Phys*. 2004;85(2–3):432–437.
- [13] Nakahata H, Higaki K, Hachigo A, *et al*. High frequency surface acoustic wave filter using ZnO/diamond/Si structure. *Jpn J Appl Phys*. 1994;33(1R):324.
- [14] Lei L, Dong B, Hu Y, *et al*. High-frequency surface acoustic wave resonator with diamond/AlN/IDT/AlN/diamond multilayer structure. *Sensors*. 2022;22(17):6479.
- [15] Laszczyk KU. Field emission cathodes to form an electron beam prepared from carbon nanotube suspensions. *Micromachines*. 2020;11(3):260.
- [16] Roy RK, Lee KR. Biomedical applications of diamond-like carbon coatings: a review. *J Biomed Mater Res*. 2007;83B(1):72–84.
- [17] Wright NG, Horsfall AB, Vassilevski K. Prospects for SiC electronics and sensors. *Mater Today*. 2008;11(1–2):16–21.
- [18] Flack TJ, Pushpakaran BN, Bayne SB. GaN technology for power electronic applications: a review. *J Elec Mater*. 2016;45(6):2673–2682.
- [19] Shivani DK, Ghosh A, Kumar M. A strategic review on gallium oxide based power electronics: recent progress and future prospects. *Mater Today Comm*. 2022;33:104244.
- [20] Novoselov K, Fal’ko V, Colombo L, *et al*. A roadmap for graphene. *Nature*. 2012;490(7419):192–200.
- [21] Barkan T. Graphene: the hype versus commercial reality. *Nat Nanotechnol*. 2019;14(10):904–906.
- [22] Jelezko F, Wrachtrup J. Single defect centres in diamond: a review. *Phys Status Solidi A*. 2006;203(13):3207–3225.
- [23] Einaga Y, Foord JS, Swain GM. Diamond electrodes: diversity and maturity. *MRS Bull*. 2014;39(6):525–532.
- [24] Eaton-Magana S, Shigley JE. Observations on CVD-grown synthetic diamonds: a review. *G&G*. 2016;52:222–245.
- [25] Nistor PA, May PW. Diamond thin films: giving biomedical applications a new shine. *J R Soc Interface*. 2017;14(134):20170382.
- [26] Koizumi S, Umezawa H, Pernot J, *et al*. Power electronics device applications of diamond semiconductors. Sawston, Cambridge, UK: Woodhead Publishing; 2018.
- [27] Macpherson JV. A practical guide to using boron doped diamond in electrochemical research. *Phys Chem Chem Phys*. 2015;17(5):2935–2949.
- [28] Nebel CE. Chapter four – Nitrogen-vacancy doped CVD diamond for quantum applications: a review. *Semicond Semimetals*. 2020;103:73–136.
- [29] Zheng Y, Li C, Liu J, *et al*. Chemical vapor deposited diamond with versatile grades: from gemstone to quantum electronics. *Front Mater Sci*. 2022;16(1):220590.
- [30] Simic D, Deljanin B. Laboratory grown diamonds: information guide to HPHT-grown and CVD grown diamonds. 3rd ed. Vancouver, Canada: Gemmological Research Industries Inc; 2020.
- [31] Gicquel A, Hassouni K, Silva F, *et al*. CVD diamond films: from growth to applications. *Curr Appl Phys*. 2001;1(6):479–496.
- [32] Li G, Rahim MZ, Pan W, *et al*. The manufacturing and the application of polycrystalline diamond tools: a comprehensive review. *J Manuf Proc*. 2020;56:400–416.
- [33] Konstanty J. Sintered diamond tools: trends, challenges and prospects. *Powder Metall*. 2013;56(3):184–188.
- [34] Zhan G, Xu J, He D. Applications of polycrystalline diamond (PCD) materials in oil and gas industry. In: Zhan G, editor. *Chapter in applications and use of diamond*. London, UK: IntechOpen; 2023.
- [35] Gat R. CVD diamond for everyone. *Cutting Tool Engineering*; 1995. Available from: <https://www.ctemag.com/news/articles/cvd-diamond-everyone>
- [36] Sein H, Ahmed W, Jackson M, *et al*. Performance and characterisation of CVD diamond coated, sintered diamond and WC–Co cutting tools for dental and micro-machining applications. *Thin Solid Films*. 2004;447–448:455–461.
- [37] Lin Q, Chen S, Shen B, *et al*. CVD diamond coated drawing dies: a review. *Mater Manuf Proc*. 2021;36(4):381–408.
- [38] Liu X, Zhang H, Lin G, *et al*. Advances in deposition of diamond films on cemented carbide and progress of diamond coated cutting tools. *Vacuum*. 2023;217:112562.
- [39] Diamond Coatings Market. Diamond coatings market analysis by CVD and PVD in metal, ceramics, composites and others from 2023 to 2033. Available from: <https://www.factmr.com/report/diamond-coatings-market>
- [40] Ricci D, Braga PC, editors. *Atomic force microscopy: biomedical methods and applications*. In: *Methods in molecular biology*. Totowa (NJ): Humana Press Inc; 2004. p. 25.
- [41] Agrawal R, Moldovan N, Espinosa HD. An energy-based model to predict wear in nanocrystalline diamond atomic force microscopy tips. *J Appl Phys*. 2009;106(6):064311.
- [42] Kranz C. Diamond as advanced material for scanning probe microscopy tips. *Electroanalysis*. 2016;28(1):35–45.
- [43] Hrdličková V, Matvieiev O, Navrátil T, *et al*. Recent advances in modified boron-doped diamond electrodes: a review. *Electrochim Acta*. 2023;456:142435.
- [44] Einaga Y. Diamond electrodes for electrochemical analysis. *J Appl Electrochem*. 2010;40(10):1807–1816.

- [45] May PW, Clegg M, Silva TA, *et al.* Diamond-coated 'black silicon' as a promising material for high-surface-area electrochemical electrodes and antibacterial surfaces. *J Mater Chem B*. 2016;4(34):5737–5746.
- [46] Yu Y, Wu L, Zhi J. Diamond nanowires: fabrication, structure, properties, and applications. *Angew Chem Int Ed*. 2014;53(52):14326–14351.
- [47] Varga M, Stehlik S, Kaman O, *et al.* Templated diamond growth on porous carbon foam decorated with polyvinyl alcohol-nanodiamond composite. *Carbon*. 2017;119:124–132.
- [48] Petrák V, Vlčková Živcová Z, Krýsová H, *et al.* Fabrication of porous boron-doped diamond on SiO<sub>2</sub> fiber templates. *Carbon*. 2017;114:457–464.
- [49] Kiran R, Scorsone E, de Sanoit J, *et al.* Boron doped diamond electrodes for direct measurement in biological fluids: an *in situ* regeneration approach. *J Electrochem Soc*. 2013;160(1):H67–H73.
- [50] Element Six, Ltd. (UK). Available from: <https://www.e6.com/>
- [51] Condias. Available from: <https://www.condias.de/>
- [52] Sumitomo Chemical. Available from: <https://www.sumitomo-chem.co.jp/sciocs/english/products/diamond.html/>
- [53] Boromond. Available from: <https://www.boromond.com/>
- [54] sp3 Diamond Technologies. Available from: <https://sp3-cvd.com/coating>
- [55] Amazon. Available from: <https://www.amazon.co.uk/electrode-diamond-evolution-chlorine-treatment/dp/B0BRRY8RRL/>
- [56] Manivannan A, Seehra MS, Tryk DA, *et al.* Electrochemical detection of ionic mercury at boron-doped diamond electrodes. *Anal Lett*. 2002;35(2):355–368.
- [57] Zazoua A, Khedimallah N, Jaffrezic-Renault N. Electrochemical determination of cadmium, lead, and nickel using a polyphenol-polyvinyl chloride-boron-doped diamond electrode. *Anal Lett*. 2018;51(3):336–347.
- [58] Ivandini TA, Sato R, Makide Y, *et al.* Electrochemical detection of arsenic(III) using iridium-implanted boron-doped diamond electrodes. *Anal Chem*. 2006;78(18):6291–6298.
- [59] Berek J, Fischer J, Navrátil T, *et al.* Nontraditional electrode materials in environmental analysis of biologically active organic compounds. *Electroanal*. 2007;19(19–20):2003–2014.
- [60] Brocenschi RF, Rocha-Filho RC, Duran B, *et al.* The analysis of estrogenic compounds by flow injection analysis with amperometric detection using a boron-doped diamond electrode. *Talanta*. 2014;126:12–19.
- [61] Wang J, Chen G, Chatrathi MP, *et al.* Microchip capillary electrophoresis coupled with a boron-doped diamond electrode-based electrochemical detector. *Anal Chem*. 2003;75(4):935–939.
- [62] Rivera-Utrilla J, Sánchez-Polo M, Ferro-García MÁ, *et al.* Pharmaceuticals as emerging contaminants and their removal from water. A review. *Chemosphere*. 2013;93(7):1268–1287.
- [63] Park J, Quaiserová-Mocko V, Patel BA, *et al.* Diamond microelectrodes for *in vitro* electroanalytical measurements: current status and remaining challenges. *Analyst*. 2008;133(1):17–24.
- [64] Park J, Galligan JJ, Fink GD, *et al.* *In vitro* continuous amperometry with a diamond microelectrode coupled with video microscopy for simultaneously monitoring endogenous norepinephrine and its effect on the contractile response of a rat mesenteric artery. *Anal Chem*. 2006;78(19):6756–6764.
- [65] Patel BA, Bian X, Quaiserová-Mocko V, *et al.* *In vitro* continuous amperometric monitoring of 5-hydroxytryptamine release from enterochromaffin cells of the guinea pig ileum. *Analyst*. 2007;132(1):41–47.
- [66] Fan B, Rusinek CA, Thompson CH, *et al.* Flexible, diamond-based microelectrodes fabricated using the diamond growth side for neural sensing. *Microsyst Nanoeng*. 2020;6(1):42.
- [67] Yang N, Foord JS, Jiang X. Diamond electrochemistry at the nanoscale: a review. *Carbon*. 2016;99:90–110.
- [68] Kondo T. Recent electroanalytical applications of boron-doped diamond electrodes. *Curr Opin Electrochem*. 2022;32:100891.
- [69] Song MJ, Kim JH, Lee SK, *et al.* Fabrication of Pt nanoparticles-decorated CVD diamond electrode for biosensor applications. *Anal Sci*. 2011;27(10):985–989.
- [70] Shahrokhian S, Ranjbar S, Ghalkhani M. Modification of the electrode surface by Ag nanoparticles decorated nano diamond-graphite for voltammetric determination of ceftizoxime. *Electroanalysis*. 2016;28(3):469–476.
- [71] Song MJ, Lee SK, Lee JY, *et al.* Electrochemical sensor based on Au nanoparticles decorated boron-doped diamond electrode using ferrocene-tagged aptamer for proton detection. *J Electroanal Chem*. 2012;677–680:139–144.
- [72] Li H, Qin J, Li M, *et al.* Gold-nanoparticle-decorated boron-doped graphene/BDD electrode for tumor marker sensor. *Sens Actuators B*. 2020;302:127209.
- [73] McLaughlin MH, Pakpour-Tabrizi AC, Jackman RB. A detailed EIS study of boron doped diamond electrodes decorated with gold nanoparticles for high sensitivity mercury detection. *Sci Rep*. 2021;11(1):9505.
- [74] Subramanian P, Motorina A, Yeap WS, *et al.* An impedimetric immunosensor based on diamond nanowires decorated with nickel nanoparticles. *Analyst*. 2014;139(7):1726–1731.
- [75] Marton M, Michniak P, Behul M, *et al.* Bismuth modified boron doped diamond electrode for simultaneous determination of Zn, Cd and Pb ions by square wave anodic stripping voltammetry: influence of boron concentration and surface morphology. *Vacuum*. 2019;167:182–188.
- [76] Yang N, Gao F, Nebel CE. Diamond decorated with copper nanoparticles for electrochemical reduction of carbon dioxide. *Anal Chem*. 2013;85(12):5764–5769.
- [77] Verlato E, Barison S, Einaga Y, *et al.* CO<sub>2</sub> reduction to formic acid at low overpotential on BDD electrodes modified with nanostructured CeO<sub>2</sub>. *J Mater Chem A*. 2019;7(30):17896–17905.
- [78] Jiwanti PK, Einaga Y. Further study of CO<sub>2</sub> electrochemical reduction on palladium modified BDD electrode: influence of electrolyte. *Chem Asian J*. 2020;15(6):910–914.
- [79] Jiwanti PK, Ichzan AM, Dewandaru RKP, *et al.* Improving the CO<sub>2</sub> electrochemical reduction to formic acid using iridium-oxide-modified boron-doped diamond electrodes. *Diam Relat Mater*. 2020;106:107874.
- [80] Jiwanti PK, Natsui K, Nakata K, *et al.* The electrochemical production of C<sub>2</sub>/C<sub>3</sub> species from carbon dioxide on copper-modified boron-doped diamond electrodes. *Electrochim Acta*. 2018;266:414–419.
- [81] He Y, Lin H, Guo Z, *et al.* Recent developments and advances in boron-doped diamond electrodes for electro-

- chemical oxidation of organic pollutants. *Sep Purif Technol.* 2019;212:802–821.
- [82] Bossel U, Eliasson B. Energy and the hydrogen economy, AFDC Report; 2003. Available from: [https://afdc.energy.gov/files/pdfs/hyd\\_economy\\_bossel\\_eliasson.pdf](https://afdc.energy.gov/files/pdfs/hyd_economy_bossel_eliasson.pdf)
- [83] Brillas E, Martínez-Huitle CA. Synthetic diamond films: preparation, electrochemistry, characterization, and applications. New York (NY): Wiley; 2011.
- [84] Geiger S, Kasian O, Mingers AM, *et al.* Catalyst stability benchmarking for the oxygen evolution reaction: the importance of backing electrode material and dissolution in accelerated aging studies. *ChemSusChem.* 2017;10(21):4140–4143.
- [85] Al-Abdallat Y, Jumah I, Jumah R, *et al.* Catalytic electrochemical water splitting using boron doped diamond (BDD) electrodes as a promising energy resource and storage solution. *Energies.* 2020;13(20):5265.
- [86] Ashcheulov P, Taylor A, Mortet V, *et al.* Nanocrystalline boron-doped diamond as a corrosion-resistant anode for water oxidation via Si photoelectrodes. *ACS Appl Mater Interfaces.* 2018;10(35):29552–29564.
- [87] Behúl M, Vojs M, Marton M, *et al.* Nanostructured boron doped diamond enhancing the photoelectrochemical performance of TiO<sub>2</sub>/BDD heterojunction anodes. *Vacuum.* 2020;171:109006.
- [88] Mavrokefalos CK, Hasan M, Rohan JF, *et al.* Electrochemically deposited Cu<sub>2</sub>O cubic particles on boron doped diamond substrate as efficient photocathode for solar hydrogen generation. *Appl Surf Sci.* 2017;408:125–134.
- [89] Qiu Y, Pan Z, Chen H, *et al.* Current progress in developing metal oxide nanoarrays-based photoanodes for photoelectrochemical water splitting. *Sci Bull.* 2019;64(18):1348–1380.
- [90] Clematis D, Panizza M. Application of boron-doped diamond electrodes for electrochemical oxidation of real wastewaters. *Curr Opin Electrochem.* 2021;30:100844.
- [91] Martínez-Huitle CA, Brillas E. A critical review over the electrochemical disinfection of bacteria in synthetic and real wastewaters using a boron-doped diamond anode. *Curr Opin Solid State Mater Sci.* 2021;25(4):100926.
- [92] Brosler P, Vi. Girão A, Silva RF, *et al.* In-house vs. commercial boron-doped diamond electrodes for electrochemical degradation of water pollutants: a critical review. *Front Mater.* 2023;10:1–27.
- [93] Li D, Qu J. The progress of catalytic technologies in water purification: a review. *J Environ Sci.* 2009;21(6):713–719.
- [94] De Luna Y, Bensalah N. Review on the electrochemical oxidation of endocrine-disrupting chemicals using BDD anodes. *Curr Opin Electrochem.* 2022;32:100900.
- [95] La Merrill MA, Vandenberg LN, Smith MT, *et al.* Consensus on the key characteristics of endocrine-disrupting chemicals as a basis for hazard identification. *Nat Rev Endocrinol.* 2020;16(1):45–57.
- [96] Proaqua. Available from: <https://www.proaqua.at/en/>
- [97] Weo. Available from: <https://we-o.com/weo-the-bottle/>
- [98] Enozo. Available from: <https://enozo.com/>
- [99] Wu J, Lan Z, Lin J, *et al.* Counter electrodes in dye-sensitized solar cells. *Chem Soc Rev.* 2017;46(19):5975–6023.
- [100] Vispute RD, Vats A, Venkatesan V, *et al.* Electrical conducting diamond thin-films: an alternative counter electrode material for dye sensitized solar cells. *MRS Proc.* 2011;1282:1404.
- [101] Nebel CA. A source of energetic electrons. *Nature Mater.* 2013;12(9):780–781.
- [102] Hamers RJ, Bandy JA, Zhu D, *et al.* Photoemission from diamond films and substrates into water: dynamics of solvated electrons and implications for diamond photoelectrochemistry. *Faraday Discuss.* 2014;172:397–411.
- [103] Raymakers J, Haenen K, Maes W. Diamond surface functionalization: from gemstone to photoelectrochemical applications. *J Mater Chem C.* 2019;7(33):10134–10165.
- [104] Christianson JR, Zhu D, Hamers RJ, *et al.* Mechanism of N<sub>2</sub> reduction to NH<sub>3</sub> by aqueous solvated electrons. *J Phys Chem B.* 2014;118(1):195–203.
- [105] Zhu D, Zhang L, Ruther RE, *et al.* Photo-illuminated diamond as a solid-state source of solvated electrons in water for nitrogen reduction. *Nat Mater.* 2013;12(9):836–841.
- [106] Zhu D, Bandy JA, Li S, *et al.* Amino-terminated diamond surfaces: photoelectron emission and photocatalytic properties. *Surf Sci.* 2016;650:295–301.
- [107] Li S, Bandy JA, Hamers RJ. Enhanced photocatalytic activity of diamond thin films using embedded Ag nanoparticles. *ACS Appl Mater Interfaces.* 2018;10(6):5395–5403.
- [108] Zhang L, Zhu D, Nathanson GM, *et al.* Selective photoelectrochemical reduction of aqueous CO<sub>2</sub> to CO by solvated electrons. *Angew Chem Int Ed.* 2014;53(37):9746–9750.
- [109] Bachman BF, Zhu D, Bandy J, *et al.* Detection of aqueous solvated electrons produced by photoemission from solids using transient absorption measurements. *ACS Meas Sci Au.* 2022;2(1):46–56.
- [110] Sussmann R, editor. CVD diamond for electronic devices and sensors. Chichester: Wiley; 2009.
- [111] Donato N, Rouger N, Pernot J, *et al.* Diamond power devices: state of the art, modelling, figures of merit and future perspective. *J Phys D Appl Phys.* 2020;53(9):093001.
- [112] Araujo D, Suzuki M, Lloret F, *et al.* Diamond for electronics: materials, processing and devices. *Materials.* 2021;14(22):7081.
- [113] Electricity lost in transmission in the United Kingdom (UK) in selected years from 1970 to 2021. Statista Research Department; 2023 [cited 2024 Mar 7]. Available from: <https://www.statista.com/statistics/550583/electricity-losses-in-transmission-uk/>
- [114] Pinault M-A, Barjon J, Kociniowski T, *et al.* The *n*-type doping of diamond: present status and pending questions. *Physica B.* 2007;401–402:51–56.
- [115] Gurbuz Y, Esame O, Tekin I, *et al.* Diamond semiconductor technology for RF device applications. *Solid-State Electron.* 2005;49(7):1055–1070.
- [116] Bormashov VS, Terentiev SA, Buga SG, *et al.* Thin large area vertical Schottky barrier diamond diodes with low on-resistance made by ion-beam assisted lift-off technique. *Diam Relat Mater.* 2017;75:78–84.
- [117] Traoré A, Muret P, Fiori A, *et al.* Zr/oxidized diamond interface for high power Schottky diodes. *Appl Phys Lett.* 2014;104(5):052105.
- [118] Saremi M, Hathwar R, Dutta M, *et al.* Analysis of the reverse IV characteristics of diamond-based PIN diodes. *Appl Phys Lett.* 2017;111(4):043507.
- [119] Liu J, Koide Y. An overview of high-*k* oxides on hydrogenated-diamond for metal-oxide-semiconductor capacitors and field-effect transistors. *Sensors.* 2018;18(6):1813.

- [120] Pham T, Maréchal A, Muret P, *et al.* Comprehensive electrical analysis of metal/ $\text{Al}_2\text{O}_3$ /O-terminated diamond capacitance. *J Appl Phys.* 2018;123(16):161523.
- [121] Matsumoto T, Kato H, Oyama K, *et al.* Inversion channel diamond metal-oxide-semiconductor field-effect transistor with normally off characteristics. *Sci Rep.* 2016;6(1):31585.
- [122] Butler JE, *et al.* Nanometric diamond delta doping with boron. *Phys Status Solidi RRL.* 2017;11:1600329.
- [123] Strobel P, Riedel M, Ristein J, *et al.* Surface transfer doping of diamond. *Nature.* 2004;430(6998):439–441.
- [124] Crawford KG, Maini I, Macdonald DA, *et al.* Surface transfer doping of diamond: a review. *Prog Surf Sci.* 2021;96(1):100613.
- [125] Kawarada H. Diamond p-FETs using two-dimensional hole gas for high frequency and high voltage complementary circuits. *J Phys D Appl Phys.* 2023;56(5):053001.
- [126] Nebel CE. Surface-conducting diamond. *Science.* 2007;318(5855):1391–1392.
- [127] Ren Z, Zhang J, Zhang J, *et al.* Polycrystalline diamond MOSFET with  $\text{MoO}_3$  gate dielectric and passivation layer. *IEEE Electron Device Lett.* 2017;38(9):1302–1304.
- [128] Kawarada H, Yamada T, Xu D, *et al.* Durability-enhanced two-dimensional hole gas of C-H diamond surface for complementary power inverter applications. *Sci Rep.* 2017;7(1):42368.
- [129] Fei W, Bi T, Iwataki M, *et al.* Oxidized Si terminated diamond and its MOSFET operation with  $\text{SiO}_2$  gate insulator. *Appl. Phys. Lett.* 2020;116(21):212103.
- [130] Sasama Y, Kageura T, Imura M, *et al.* High-mobility p-channel wide-bandgap transistors based on hydrogen-terminated diamond/hexagonal boron nitride heterostructures. *Nat Electron.* 2021;5(1):37–44.
- [131] Messenger GC. Radiation hardening. In: Access science. New York: McGraw-Hill Education; 2014.
- [132] Mazellier JP, Faynot O, Cristoloveanu S, *et al.* Integration of diamond in fully-depleted silicon-on-insulator technology as buried insulator: a theoretical analysis. *Diamond Relat. Mater.* 2008;17(7–10):1248–1251.
- [133] Francis D, Faili F, Babić D, *et al.* Formation and characterization of 4-inch GaN-on-diamond substrates. *Diam Relat Mater.* 2010;19(2–3):229–233.
- [134] Aleksov A, Gobien JM, Li X, *et al.* Silicon-on-diamond – an engineered substrate for electronic applications. *Diam Relat Mater.* 2006;15(2–3):248–253.
- [135] Si S. CVD diamond for surface acoustic wave filters. In: Dischler B, Wild C, editors. Low-pressure synthetic diamond. Springer series in materials processing. Berlin; Heidelberg: Springer. 1998.
- [136] Nakahata H, Fujii S, Higaki K, *et al.* Diamond-based surface acoustic wave devices. *Semicond Sci Technol.* 2003;18(3):S96–S104.
- [137] Luo JT, Zeng F, Pan F, *et al.* Filtering performance improvement in V-doped ZnO/diamond surface acoustic wave filters. *Appl Surf Sci.* 2010;256(10):3081–3085.
- [138] Wang L, Chen S, Zhang J, *et al.* High performance 33.7 GHz surface acoustic wave nanotransducers based on AlScN/diamond/Si layered structures. *Appl Phys Lett.* 2018;113(9):093503.
- [139] Fujii S. High-frequency surface acoustic wave filter based on diamond thin film. *Phys Status Solidi A.* 2011;208(5):1072–1077.
- [140] Luo JK, Fu YQ, Le HR, *et al.* Diamond and diamond-like carbon MEMS. *J Micromech Microeng.* 2007;17(7):S147–S163.
- [141] Liao M. Progress in semiconductor diamond photodetectors and MEMS sensors. *Funct Diam.* 2021;1(1):29–46.
- [142] Gaidarzhy A, Imboden M, Mohanty P, *et al.* High quality factor gigahertz frequencies in nanomechanical diamond resonators. *Appl Phys Lett.* 2007;91(20):203503.
- [143] Kusterer J, Kohn E. CVD diamond MEMS. In: Sussman R, editor. CVD diamond for electronic device and sensors. Chichester: Wiley; 2009. Ch. 18, p. 469.
- [144] Auciello O, Aslam DM. Review on advances in microcrystalline, nanocrystalline and ultrananocrystalline diamond films-based micro/nano-electromechanical systems technologies. *J Mater Sci.* 2021;56(12):7171–7230.
- [145] Lee K-W. 3-D hetero-integration technologies for multi-functional convergence systems. *J Microelectron Packag Soc.* 2015;22(2):11–19.
- [146] Bautze T, Mandal S, Williams OA, *et al.* Superconducting nano-mechanical diamond resonators. *Carbon.* 2014;72:100–105.
- [147] Sun H, Zhang Z, Liu Y, *et al.* Diamond MEMS: from classical to quantum. *Adv Quantum Technol.* 2023; 6:2300189.
- [148] Wilson AD, Baietto M. Applications and advances in electronic-nose technologies. *Sensors.* 2009;9(7):5099–5148.
- [149] Possas-Abreu M, Ghassemi F, Rousseau L, *et al.* Development of diamond and silicon MEMS sensor arrays with integrated readout for vapor detection. *Sensors.* 2017;17(6):1163.
- [150] Ekimov EA, Sidorov VA, Bauer ED, *et al.* Superconductivity in diamond. *Nature.* 2004;428(6982): 542–545.
- [151] Takano Y, Nagao M, Sakaguchi I, *et al.* Superconductivity in diamond thin films well above liquid helium temperature. *Appl Phys Lett.* 2004;85(14):2851–2853.
- [152] Bustarret E. Superconducting diamond: an introduction. *Phys Status Solidi A.* 2008;205(5):997–1008.
- [153] Zhang G, Zeleznik M, Vanacken J, *et al.* Metal–bosonic insulator–superconductor transition in boron-doped granular diamond. *Phys Rev Lett.* 2013;110(7):077001.
- [154] Zhang G, Turner S, Ekimov EA, *et al.* Global and local superconductivity in boron-doped granular diamond. *Adv Mater.* 2014;26(13):2034–2040.
- [155] Zhang G, Samuely T, Kačmarčík J, *et al.* Bosonic anomalies in boron-doped polycrystalline diamond. *Phys Rev Appl.* 2016;6(6):064011.
- [156] Zhang G, Kačmarčík J, Wang Z, *et al.* Anomalous anisotropy in superconducting nanodiamond films induced by crystallite geometry. *Phys Rev Appl.* 2019;12(6):064042.
- [157] Mandal S, Bautze T, Williams OA, *et al.* The diamond superconducting quantum interference device. *ACS Nano.* 2011;5(9):7144–7148.
- [158] Zhang G, Zulkharnay R, Ke X, *et al.* Unconventional giant “magnetoresistance” in bosonic semiconducting diamond nanorings. *Adv Mater.* 2023;35(22):e2211129.
- [159] Salter PS, Villar MP, Lloret F, *et al.* Laser engineering nanocarbon phases within diamond for science and electronics. *ACS Nano.* 2024;18(4):2861–2871.
- [160] Praver S, Aharonovich I, editors. Quantum information processing with diamond: principles and applications. Woodhead; Cambridge: Elsevier; 2014.
- [161] Neu E, Steinmetz D, Riedrich-Möller J, *et al.* Single photon emission from silicon-vacancy colour centres in chemical vapour deposition nano-diamonds on iridium. *New J Phys.* 2011;13(2):025012.

- [162] Becker JN, Neu E. The silicon vacancy center in diamond. *Semicond Semimetals*. 2020;103:201–235.
- [163] Nguyen M, Nikolay N, Bradac C, *et al.* Photodynamics and quantum efficiency of germanium vacancy color centers in diamond. *Adv Photon*. 2019;1(6):1.
- [164] Görlitz J, Herrmann D, Fuchs P, *et al.* Coherence of a charge stabilised tin-vacancy spin in diamond. *NPJ Quantum Inf*. 2022;8(1):45.
- [165] Trusheim ME, Wan NH, Chen KC, *et al.* Lead-related quantum emitters in diamond. *Phys Rev B*. 2019;99(7):075430.
- [166] Rodgers LVH, Hughes LB, Xie M, *et al.* Materials challenges for quantum technologies based on color centers in diamond. *MRS Bull*. 2021;46(7):623–633.
- [167] Thiering G, Gali A. Chapter one – color centers in diamond for quantum applications. *Semicond Semimetals*. 2020;103:1–36.
- [168] Jeske J, Lau DWM, Vidal X, *et al.* Stimulated emission from nitrogen-vacancy centres in diamond. *Nat Commun*. 2017;8(1):14000.
- [169] Patel RN, Schröder T, Wan N, *et al.* Efficient photon coupling from a diamond nitrogen vacancy center by integration with silica fiber. *Light Sci Appl*. 2016;5(2):e16032.
- [170] Arute F, Arya K, Babbush R, *et al.* Quantum supremacy using a programmable superconducting processor. *Nature*. 2019;574(7779):505–510.
- [171] Togan E, Chu Y, Trifonov AS, *et al.* Quantum entanglement between an optical photon and a solid-state spin qubit. *Nature*. 2010;466(7307):730–734.
- [172] Liu S, Yu R, Li J, *et al.* Creation of quantum entanglement with two separate diamond nitrogen vacancy centers coupled to a photonic molecule. *J Appl Phys*. 2013;114(24):244306.
- [173] Bernien H, Hensen B, Pfaff W, *et al.* Heralded entanglement between solid-state qubits separated by three metres. *Nature*. 2013;497(7447):86–90.
- [174] Hensen B, Bernien H, Dréau AE, *et al.* Loophole-free Bell inequality violation using electron spins separated by 1.3 kilometres. *Nature*. 2015;526(7575):682–686.
- [175] Bradley CE, Randall J, Abobeih MH, *et al.* A ten-qubit solid-state spin register with quantum memory up to one minute. *Phys Rev X*. 2019;9(3):031045.
- [176] van der Sar T, Wang ZH, Blok MS, *et al.* Decoherence-protected quantum gates for a hybrid solid-state spin register. *Nature*. 2012;484(7392):82–86.
- [177] Neumann P, Beck J, Steiner M, *et al.* Single-shot readout of a single nuclear spin. *Science*. 2010;329(5991):542–544.
- [178] Liu K, Zhang S, Ralchenko V, *et al.* Tailoring of typical color centers in diamond for photonics. *Adv Mater*. 2021;33(6):e2000891.
- [179] Nakazato T, Reyes R, Imaike N, *et al.* Quantum error correction of spin quantum memories in diamond under a zero magnetic field. *Commun Phys*. 2022;5(1):102.
- [180] Pezzagna S, Meijer J. Quantum computer based on color centers in diamond. *Appl Phys Rev*. 2021;8(1):011308.
- [181] Beveratos A, Brouri R, Gacoin T, *et al.* Single photon quantum cryptography. *Phys Rev Lett*. 2002;89(18):187901.
- [182] Loretz MG. Diamond-based nanoscale nuclear magnetic resonance [DSc thesis]. Zurich: ETH Zurich (Physics); 2015. Available from: <https://www.research-collection.ethz.ch/handle/20.500.11850/107684>
- [183] Schirhagl R, Chang K, Loretz M, *et al.* Nitrogen-vacancy centers in diamond: nanoscale sensors for physics and biology. *Annu Rev Phys Chem*. 2014;65(1):83–105.
- [184] Fu C-C, Lee H-Y, Chen K, *et al.* Characterization and application of single fluorescent nanodiamonds as cellular biomarkers. *Proc Natl Acad Sci USA*. 2007;104(3):727–732.
- [185] Kucsko G, Maurer PC, Yao NY, *et al.* Nanometer scale thermometry in a living cell. *Nature*. 2013;500(7460):54–58.
- [186] Balasubramanian G, Chan IY, Kolesov R, *et al.* Nanoscale imaging magnetometry with diamond spins under ambient conditions. *Nature*. 2008;455(7213):648–651.
- [187] Degen CL. Scanning magnetic field microscope with a diamond single-spin sensor. *Appl Phys Lett*. 2008;92(24):243111.
- [188] Taylor JM, Cappellaro P, Childress L, *et al.* High-sensitivity diamond magnetometer with nanoscale resolution. *Nat Phys*. 2008;4(10):810–816.
- [189] QDTI. Available from: <https://qdti.com/>
- [190] NVision. Available from: <https://www.nvision-imaging.com/>
- [191] Qnami. Available from: <https://qnami.ch/>
- [192] Zhang C, Vispute RD, Fu K, *et al.* A review of thermal properties of CVD diamond films. *J Mater Sci*. 2023;58(8):3485–3507.
- [193] Chandran B, Gordon MH, Schmidt WF. Comparison of CVD diamond to other substrate materials for thermal management. *InterSociety Conference on Thermal Phenomena in Electronic Systems, I-THERM V*; Orlando, FL, USA; 1996. p. 226–232.
- [194] Alibaba (search for ‘diamond heat spreader’) [cited 2024 Feb 4]. Available from: <https://www.alibaba.com/showroom/cvd-diamond-heat-spreader.html>
- [195] Francis D, Kuball M. GaN-on-diamond materials and device technology: a review. In: Tadjer MJ, Anderson TJ, editors. *Thermal management of gallium nitride electronics*. Sawston, Cambridge, UK: Woodhead Publishing; 2022. Ch. 14, p. 295–331.
- [196] Sang L. Diamond as the heat spreader for the thermal dissipation of GaN-based electronic devices. *Funct Diam*. 2021;1(1):174–188.
- [197] Geis MW, Fedynyshyn TH, Plaut ME, *et al.* Chemical and semiconducting properties of NO<sub>2</sub>-activated H-terminated diamond. *Diam Relat Mater*. 2018;84:86–94.
- [198] James MC. Aluminium and oxygen termination of diamond for thermionic applications [PhD thesis]. Bristol: University of Bristol; 2020. Available from: <https://www.chm.bris.ac.uk/pt/diamond/michael-james-thesis/Michael-James-thesis.pdf>
- [199] Zulkharnay R, Zulpukarova G, May PW. Oxygen-terminated diamond: insights into the correlation between surface oxygen configurations and work function values. *Appl Surf Sci*. 2024;658:159776.
- [200] Szunerits S, Nebel CE, Hamers RJ. Surface functionalization and biological applications of CVD diamond. *MRS Bull*. 2014;39(6):517–524.
- [201] Zhong Y-L, Loh KP, Midya A, *et al.* Suzuki coupling of aryl organics on diamond. *Chem Mater*. 2008;20(9):3137–3144.
- [202] Nebel CE, Shin D, Takeuchi D, *et al.* Alkene/diamond liquid/solid interface characterization using internal photoemission spectroscopy. *Langmuir*. 2006;22(13):5645–5653.
- [203] Zhong YL, Loh KP. The chemistry of C-H bond activation on diamond. *Chemistry*. 2010;5(7):1532–1540.

- [204] Szunerits S, Boukherroub R. Different strategies for functionalization of diamond surfaces. *J Solid State Electrochem.* 2007;12(10):1205–1218.
- [205] Trucchi D, Melosh N. Electron-emission materials: advances, applications, and models. *MRS Bull.* 2017;42(07):488–492.
- [206] James MC, Fogarty F, Zulkharnay R, *et al.* A review of surface functionalisation of diamond for thermionic emission applications. *Carbon.* 2020;171:532–550.
- [207] Maier F, Ristein J, Ley L. Electron affinity of plasma-hydrogenated and chemically oxidized diamond (100) surfaces. *Phys Rev B.* 2001;64(16):165411.
- [208] Cui JB, Ristein J, Ley L. Electron affinity of the bare and hydrogen covered single crystal diamond (111) surface. *Phys Rev Lett.* 1998;81(2):429–432.
- [209] Kimura K, Nakajima K, Yamanaka S, *et al.* Hydrogen analysis of CVD homoepitaxial diamond films by high-resolution elastic recoil detection. *Nucl Instr Methods Phys Res B.* 2002;190(1–4):689–692.
- [210] May PW, Stone JC, Ashfold MNR, *et al.* The effect of diamond surface termination species upon field emission properties. *Diam Relat Mater.* 1998;7(2–5):671–676.
- [211] Davidson JL, Kang WP, Subramanian K, *et al.* Forms and behaviour of vacuum emission electronic devices comprising diamond or other carbon cold cathode emitters. *Phil Trans R Soc A.* 2008;366(1863):281–293.
- [212] Subramanian K, Kang WP, Davidson JL, *et al.* A review of recent results on diamond vacuum lateral field emission device operation in radiation environments. *Microelec Eng.* 2011;88(9):2924–2929.
- [213] Zou R, Hu J, Song Y, *et al.* Carbon nanotubes as field emitter. *J Nanosci Nanotech.* 2010;10(12):7876–7896.
- [214] Terranova ML, Orlanducci S, Rossi M, *et al.* Nanodiamonds for field emission: state of the art. *Nanoscale.* 2015;7(12):5094–5114.
- [215] Jaskie JE. Diamond-based field-emission displays. *MRS Bull.* 1996;21(3):59–64.
- [216] Sugie H, Tanemura M, Filip V, *et al.* Carbon nanotubes as electron source in an X-ray tube. *Appl Phys Lett.* 2001;78(17):2578–2580.
- [217] Milne WI, Teo KBK, Minoux E, *et al.* Aligned carbon nanotubes/fibers for applications in vacuum microwave amplifiers. *J Vac Sci Technol B.* 2006;24(1):345–348.
- [218] Geis MW, Twichell JC, Lyszczarz TM. Diamond emitters fabrication and theory. *J Vac Sci Technol B.* 1996;14(3):2060–2067.
- [219] Zou Y, May PW, Vieira SMC, *et al.* Field emission from diamond-coated multiwalled carbon nanotube ‘teepee’ structures. *J Appl Phys.* 2012;112:044903.
- [220] Krauss AR, Auciello O, Ding MQ, *et al.* Electron field emission for ultrananocrystalline diamond films. *J Appl Phys.* 2001;89(5):2958–2967.
- [221] Kang WP, Davidson JL, Wisitsora-At A, *et al.* Diamond vacuum field emission devices. *Diam Relat Mater.* 2004;13(11–12):1944–1948.
- [222] Pradhan D, Lin IN. Grain-size-dependent diamond-nondiamond composite films: characterization and field-emission properties. *ACS Appl Mater Interfaces.* 2009;1(7):1444–1450.
- [223] Cui JB, Ristein J, Ley L. Low-threshold electron emission from diamond. *Phys Rev B.* 1999;60(23):16135–16142.
- [224] Harniman RL, Fox OJL, Janssen W, *et al.* Direct observation of electron emission from grain boundaries in CVD diamond by PeakForce-controlled tunnelling atomic force microscopy. *Carbon.* 2015;94:386–395.
- [225] Logie J. Betamax vs VHS: the story of the first format war; 2020 [cited 2024 Feb 4]. Available from: <https://medium.com/swlh/vhs-vs-beta-the-story-of-the-original-format-war-a5fd84668748>
- [226] Khalid KAA, Leong TJ, Mohamed K. Review on thermionic energy converters. *IEEE Trans Electron Devices.* 2016;63(6):2231–2241.
- [227] Rahman E, Nojeh A. Semiconductor thermionics for next generation solar cells: photon enhanced or pure thermionic? *Nat Commun.* 2021;12(1):4622.
- [228] Kataoka M, Zhu C, Koeck FAM, *et al.* Thermionic electron emission from nitrogen-doped homoepitaxial diamond. *Diam Relat Mater.* 2010;19(2–3):110–113.
- [229] Elfimchev S, Chandran M, Akhvlediani R, *et al.* Trap-assisted photon-enhanced thermionic emission from polycrystalline diamond films. *Phys Status Solidi.* 2015;212:2583–2588.
- [230] Kribus A, Segev G. Solar energy conversion with photon enhanced thermionic emission. *J Opt.* 2016;18(7):073001.
- [231] Koeck FAM, Nemanich RJ. Emission characterization from nitrogen-doped diamond with respect to energy conversion. *Diam Relat Mater.* 2006;15(2–3):217–220.
- [232] Zulkharnay R, May PW. Experimental evidence for large negative electron affinity from scandium-terminated diamond. *J Mater Chem A.* 2023; 11(25):13432–13445.
- [233] Schenk A, Tadich A, Sear M, *et al.* Formation of a silicon terminated (100) diamond surface. *Appl Phys Lett.* 2015;106(19):191603.
- [234] Sear MJ, Schenk AK, Tadich A, *et al.* Germanium terminated (100) diamond. *J Phys Condens Matter.* 2017;29:145002.
- [235] Shen W, Pan Y, Shen S, *et al.* Electron affinity of boron-terminated diamond (001) surfaces: a density functional theory study. *J Mater Chem C.* 2019;7(31):9756–9765.
- [236] Fogarty F, Fox NA, May PW. Experimental studies of electron affinity and work function from titanium on oxidised diamond (100) surfaces. *Funct Diam.* 2022;2(1):103–111.
- [237] Zulkharnay R, Allan NL, May PW. *Ab initio* study of negative electron affinity on the scandium-terminated diamond (100) surface for electron emission devices. *Carbon.* 2022;196:176–185.
- [238] O’Donnell KM, Edmonds MT, Ristein J, *et al.* Diamond surfaces with air-stable negative electron affinity and giant electron yield enhancement. *Adv Funct Mater.* 2013;23(45):5608–5614.
- [239] O’Donnell KM, Edmonds MT, Tadich A, *et al.* Extremely high negative electron affinity of diamond via magnesium adsorption. *Phys Rev B.* 2015;92(3):035303.
- [240] Zulkharnay R, Fox NA, May PW. Enhanced Electron Emission Performance and Air-Surface Stability in ScO-terminated Diamond for Thermionic Energy Converters. *Small.* 2024. doi: 10.1002/sml.202405408
- [241] Wiza JL. Microchannel plate detectors. *Nucl Instr Methods.* 1979;162:587–601.
- [242] Werner WSM. Photon and electron induced electron emission from solid surfaces. In: *Slow heavy-particle induced electron emission from solid surfaces*, Springer tracts in modern physics. Berlin; Heidelberg: Springer; 2007. p. 225.
- [243] Ascarelli P, Cappelli E, Pinzari F, *et al.* Secondary electron emission from diamond: physical modeling and application to scanning electron microscopy. *J Appl Phys.* 2001;89(1):689–696.

- [244] Cazaux J. Some considerations on the secondary electron emission,  $\delta$ , from e-irradiated insulators. *J Appl Phys.* 1999;85(2):1137–1147.
- [245] Shih A, Yater J, Pehrsson P, *et al.* Secondary electron emission from diamond surfaces. *J Appl Phys.* 1997;82(4):1860–1867.
- [246] Yater JE, Shih A, Abrams R. Electron transport and emission properties of diamond. *J Vac Sci Technol A.* 1998;16(3):913–918.
- [247] Lapington JS, Taillandier V, Cann BL, *et al.* Erratum: investigation of the secondary electron emission characteristics of alternative dynode materials for imaging photomultipliers. *J Inst.* 2012;7(4):E04002.
- [248] Lapington JS, May PW, Fox NA, *et al.* Investigation of the secondary emission characteristics of CVD diamond films for electron amplification. *Nucl Instrum Methods A.* 2009;610(1):253–257.
- [249] Yater JE. Secondary electron emission and vacuum electronics. *J Appl Phys.* 2023;133(5):050901.
- [250] Vaz R, May PW, Fox NA, *et al.* Measurement of the secondary electron emission from CVD diamond films using phosphor screen detectors. *J Inst.* 2015;10(03):P03004.
- [251] Welch JO. Nanodiamonds: from biology to engineering [Doctoral thesis]. London: University College London; 2014. Especially Ch3.3 & Ch7. Available from: <https://discovery.ucl.ac.uk/1431008/1/Joseph%20Orin%20Welch%20Thesis%20corrections%2029%20may.pdf>
- [252] Takeuchi D, Koizumi S. Diamond PN/PIN diode type electron emitter with negative electron affinity and its potential for the high voltage vacuum power switch. In: Yang N, editor. Chapter 8 in novel aspects of diamond – from growth to applications. Cham, Switzerland: Springer; 2015.
- [253] Takeuchi D, Ogura M, Ri S-G, *et al.* Electron emission suppression from hydrogen-terminated n-type diamond. *Diam Relat Mater.* 2008;17(6):986–988.
- [254] Koizumi S, Watanabe K, Hasegawa M, *et al.* Ultraviolet emission from a diamond pn junction. *Science.* 2001;292(5523):1899–1901.
- [255] Koizumi S, Kono S. Proceedings of 16th Int Display Workshops; 2009. p. 1479.
- [256] Makino T, Yoshino K, Sakai N, *et al.* Enhancement in emission efficiency of diamond deep-ultraviolet light emitting diode. *Appl Phys Lett.* 2011;99(6):061110–1–061110-3.
- [257] Takeuchi D, Makino T, Kato H, *et al.* Electron emission from CVD diamond p-i-n junctions with negative electron affinity during room temperature operation. *Diam Relat Mater.* 2011;20(7):917–921.
- [258] Ono T, Sakai T, Sakuma N, *et al.* Field emitter triode for power switching—a new power device candidate. Proceedings of ISPSD'98; 1998. p. 151–154.
- [259] Takeucni D, Koizumi S, Makino T, *et al.* A 10kV vacuum switch with negative electron affinity of diamond p-i-n electron emitter. IEDM2012 (International Electron Devices Meeting), Technical Digest; San Francisco, CA, USA; 2012; Vol. 7. p. 167–170 (7.6.1–7.6.4).
- [260] Jian Z, Xu J, Yang N, *et al.* A perspective on diamond composites and their electrochemical applications. *Curr Opin Electrochem.* 2021;30:100835.
- [261] Zhai Z, Leng B, Yang N, *et al.* Rational construction of 3D-networked carbon nanowalls/diamond supporting CuO architecture for high-performance electrochemical biosensors. *Small.* 2019;15(48):e1901527.
- [262] Zhang C, Huang N, Zhai Z, *et al.* Bifunctional oxygen electrocatalyst of Co<sub>4</sub>N and nitrogen-doped carbon nanowalls/diamond for high-performance flexible zinc–air batteries. *Adv Energy Mater.* 2023;13:2301749.
- [263] Chen B, Zhai Z, Huang N, *et al.* Highly localized charges of confined electrical double-layers inside 0.7-nm layered channels. *Adv Energy Mater.* 2023;13(36):2300716.
- [264] Jian Z, Yang N, Vogel M, *et al.* Tunable photoelectrochemistry of patterned TiO<sub>2</sub>/BDD heterojunctions. *Small Methods.* 2020;4:2000257.
- [265] Partridge PG, May PW, Rega CA, *et al.* Potential for diamond fibres and diamond fibre composites. *Mater Sci Technol.* 1994;10(6):505–512.
- [266] May PW, Portman R, Rosser KN. Thermal conductivity of CVD diamond fibres and diamond fibre reinforced epoxy composites. *Diam Relat Mater.* 2005;14(3–7):598–603.
- [267] Zaitsev AM. In: Prelas MA, G. Popovici, L.K. Bigelow, editors. Handbook of industrial diamonds and diamond films. New York (NY); Basel; Hong Kong): Marcel Dekker Inc.; 1998. chapter 7: Optical Properties.
- [268] Koidl P, Klages C-P. Optical applications of polycrystalline diamond. *Diam Relat Mater.* 1992;1(10–11):1065–1074.
- [269] Shvyd'ko Y, Blank V, Terentyev S. Diamond X-ray optics: transparent, resilient, high-resolution, and wave-front preserving. *MRS Bull.* 2017;42(06):437–444.
- [270] Dodson JM, Brandon JR, Dhillon HK, *et al.* Single crystal and polycrystalline CVD diamond for demanding optical applications. In: Tustison RW, editor. Proceedings of SPIE 8016 80160L-1, Window and Dome Technologies and Materials XII; 2011.
- [271] *ii-iv.com (coherent lasers)*. Available from: <https://ii-iv.com/product/cvd-diamond-optics/>
- [272] *Diamond Materials*. Available from: <https://www.diamond-materials.com/en/>
- [273] Dore P, Nucara A, Cannavò D, *et al.* Infrared properties of chemical-vapor deposition polycrystalline diamond windows. *Appl Opt.* 1998;37(24):5731–5736.
- [274] Liehr M, Wieder S, Dieguez-Campo M. Large area microwave coating technology. *Thin Solid Films.* 2006;502(1–2):9–14.
- [275] Mehedi H-A, Achard J, Rats D, *et al.* Low temperature and large area deposition of nanocrystalline diamond films with distributed antenna array microwave-plasma reactor. *Diam Relat Mater.* 2014;47:58–65.
- [276] Kim J, Tsugawa K, Ishihara M, *et al.* Large-area surface wave plasmas using microwave multi-slot antennas for nanocrystalline diamond film deposition. *Plasma Sources Sci Technol.* 2010;19(1):015003.
- [277] Mahi C, Brinza O, Issaoui R, *et al.* Synthesis of high quality transparent nanocrystalline diamond films on glass substrates using a distributed antenna array microwave system. *Coatings.* 2022;12(10):1375.
- [278] Schuelke T, Grotjohn TA. Diamond polishing. *Diam Relat Mater.* 2013;32:17–26.
- [279] U.S. Government Accountability Office. Science & tech spotlight: directed energy weapons; 2023 [cited 2024 Feb 4]. <https://www.gao.gov/products/gao-23-106717#:~:text=What%20is%20it%3F,and%20high%20power%20microwave%20weapons>
- [280] Bennett A, Anokin E, Vrolijk B. Mid-infrared optics: CVD diamond IR optics enable EUV lithography. *Laser Focus World.* 2013;49:43–46.
- [281] Raut HK, Ganesh VA, Nair AS, *et al.* Anti-reflective coatings: a critical, in-depth review. *Energy Environ Sci.* 2011;10:3779–3804.

- [282] Sittinger V, Baron S, Höfer M, *et al.* Hot-filament CVD diamond coatings for optical applications. *Surf Coat Technol.* 2023;457:129287.
- [283] Ying X, Xu X, Luo J, *et al.* A near-infrared diamond anti-reflective filter window. *Diam Relat Mater.* 2000;9(9–10):1730–1733.
- [284] Chan KLA, Tay FH, Poulter G, *et al.* Chemical imaging with variable angles of incidence using a diamond attenuated total reflection accessory. *Appl Spectrosc.* 2008;62(10):1102–1107.
- [285] Mollart TP. The development of CVD infrared optics from planar windows to missile domes. *Proceedings of SPIE 5078, Window and Dome Technologies VIII*; 2003.
- [286] Sounds like a Diamond. E6 technologies capabilities brochure. Available from: [https://e6cvd.com/media/catalog/category/E6\\_Technologies\\_Capabilities\\_Brochure.pdf](https://e6cvd.com/media/catalog/category/E6_Technologies_Capabilities_Brochure.pdf)
- [287] Reilly S, Savitski VG, Liu H, *et al.* Monolithic diamond Raman laser. *Opt Lett.* 2015;40(6):930–933.
- [288] Bennett A, Dhillon H. Optical materials: CVD diamond extends Raman laser capabilities. *Laser Focus World.* 2015;51:57.
- [289] Echarri DT, Chrysalidis K, Fedosseev VN, *et al.* Enabling the use of Raman lasers for spectroscopy: continuous tunability, narrow linewidth and efficient cascading in diamond. 14th Pacific Rim Conference on Lasers and Electro-Optics (CLEO PR 2020), OSA Technical Digest, paper C6A\_3. Optica Publishing Group; 2020.
- [290] Demetriou G, Kemp AJ, Savitski V. 100 kW peak power external cavity diamond Raman laser at 2.52  $\mu\text{m}$ . *Opt Express.* 2019;27(7):10296–10303.
- [291] Shaw RW, Davis VA, Potter RN, *et al.* Corrugated thin diamond foils for SNS H-injection stripping. *Proceedings of 2005 Particle Accelerator Conference*; Knoxville, TN, USA. IEEE; 2005.
- [292] Degenhardt M, Aprigliano G, Schulte-Schrepping H, *et al.* CVD diamond screens for photon beam imaging at PETRA III. *J Phys Conf Ser.* 2013;425(19):192022.
- [293] Alianelli L, Sawhney KJS, Malik A, *et al.* A planar refractive X-ray lens made of nanocrystalline diamond. *J Appl Phys.* 2010;108(12):123107.
- [294] Kobayashi M, Yoshihashi S, Ogawa K, *et al.* A comprehensive evaluation of the thermal neutron detection efficiency by a single crystal CVD diamond detector with a LiF thermal neutron converter. *Fusion Eng Des.* 2022;179:113117.
- [295] Akino Y, Gautam A, Coutinho L, *et al.* Characterization of a new commercial single crystal diamond detector for photon- and proton-beam dosimetry. *J Radiat Res.* 2015;56(6):912–918.
- [296] Dueñas JA, de la J, Pérez T, *et al.* Diamond detector for alpha-particle spectrometry. *Appl Radiat Isot.* 2014;90:177–180.
- [297] Tchakoua Tchouaso M, Kasiwattanawut H, Prelas MA. Energy response of diamond sensor to beta radiation. *Appl Radiat Isot.* 2018;139:66–69.
- [298] Mackenzie GR, Kaluvan S, Martin PG, *et al.* A diamond gammadoltaic cell utilizing surface conductivity and its response to different photon interaction mechanisms. *Mater Today Energy.* 2021;21:100688.
- [299] Girolami M, Serpente V, Mastellone M, *et al.* Self-powered solar-blind ultrafast UV-C diamond detectors with asymmetric Schottky contacts. *Carbon.* 2022;189:27–36.
- [300] Bohon J, Muller E, Smedley J. Development of diamond-based X-ray detection for high-flux beamline diagnostics. *J Synchrotron Rad.* 2010;17(6):711–718.
- [301] Shimaoka T, Koizumi S, Kaneko JH. Recent progress in diamond radiation detectors. *Funct Diam.* 2021;1(1):205–220.
- [302] Tapper RJ. Diamond detectors in particle physics. *Rep Prog Phys.* 2000;63(8):1273–1316.
- [303] Kania DR, Landstrass MI, Plano MA, *et al.* Diamond radiation detectors. *Diam Relat Mater.* 1993;2(5–7):1012–1019.
- [304] Isberg J, Hammersberg J, Johansson E, *et al.* High carrier mobility in single-crystal plasma-deposited diamond. *Science.* 2002;297(5587):1670–1672.
- [305] Meier D, Adam W, Bauer C, *et al.* Proton irradiation of CVD diamond detectors for high-luminosity experiments at the LHC. *Nucl Instr Methods Phys Res A.* 1999;426(1):173–180.
- [306] Artemev KK, Rodionov NB, Amosov VN, *et al.* Development of a diamond detector for the ITER diamond neutral-particle spectrometer. *Instrum Exp Tech.* 2019;62(3):360–365.
- [307] Bergonzo P, Tromson D, Mer C, *et al.* Particle and radiation detectors based on diamond. *Phys Status Solidi A.* 2001;185(1):167–181.
- [308] Whitehead AJ, Airey R, Buttar CM, *et al.* CVD diamond for medical dosimetry applications. *Nucl Instr Methods Phys Res A.* 2001;460(1):20–26.
- [309] Davis JA, Petasecca M, Guatelli S, *et al.* Evolution of diamond based microdosimetry. *J Phys Conf Ser.* 2019;1154:012007.
- [310] Ravichandran R, Binukumar JP, Amri IA, *et al.* Diamond detector in absorbed dose measurements in high-energy linear accelerator photon and electron beams. *J Appl Clin Med Phys.* 2016;17(2):291–303.
- [311] Haas O, Burnham K, Skworcow P, *et al.* Methods and advanced equipment for simulation and treatment in radiation oncology. *Project Report.* University of Coventry; 2009. Available from: <https://pureportal.coventry.ac.uk/en/projects/methods-and-advanced-equipment-for-simulation-and-treatment-in-ra>
- [312] Bucciolini M, Borchi E, Bruzzi M, *et al.* Diamond dosimetry: outcomes of the CANDIDO and CONRAD INFN projects. *Nucl Instr Methods Phys Res A.* 2005;552(1–2):189–196.
- [313] Xue Y, Feng X, Roberts SC, *et al.* Diamond and carbon nanostructures for biomedical applications. *Funct Diam.* 2021;1(1):221–242.
- [314] Hauert R, Thorwarth K, Thorwarth G. An overview on diamond-like carbon coatings in medical applications. *Surf Coat Technol.* 2013;233:119–130.
- [315] Amaral M, Maru MM, Rodrigues SP, *et al.* Extremely low wear rates in hip joint bearings coated with nanocrystalline diamond. *Tribol Int.* 2015;89:72–77.
- [316] Mani N, Rifai A, Houshyar S, *et al.* Diamond in medical devices and sensors: an overview of diamond surfaces. *Med Devices Sens.* 2020;3(6):e10127.
- [317] Santos NE, Mendes JC, Braga SS. The gemstone cyborg: how diamond films are creating new platforms for cell regeneration and biointerfacing. *Molecules.* 2023;28(4):1626.
- [318] Thalhammer A, Edgington RJ, Cingolani LA, *et al.* The use of nanodiamond monolayer coatings to promote the formation of functional neuronal networks. *Biomaterials.* 2010;31(8):2097–2104.
- [319] Nistor PA, May PW, Tamagnini F, *et al.* Long-term culture of pluripotent stem cell derived human neurons on diamond – a substrate for neurodegeneration research and therapy. *Biomaterials.* 2015;61:139–149.
- [320] Specht CG, Williams OA, Jackman RB, *et al.* Ordered growth of neurons on diamond. *Biomaterials.* 2004;25(18):4073–4078.

- [321] Fox K, Palamara J, Judge R, *et al.* Diamond as a scaffold for bone growth. *J Mater Sci Mater Med.* 2013;24(4):849–861.
- [322] Catledge SA, Thomas V, Vohra YK. Nanostructured diamond coatings for orthopaedic applications. *Woodhead Publ Ser Biomater.* 2013;2013:105–150.
- [323] Auciello O, Gurman P, Guglielmotti MB, *et al.* Biocompatible ultrananocrystalline diamond coatings for implantable medical devices. *MRS Bull.* 2014;39(7):621–629.
- [324] Aversa R, Petrescu RV, Apicella A, *et al.* Nano-diamond hybrid materials for structural biomedical application. *Am J Biochem Biotechnol.* 2016;13(1):34–41.
- [325] Hébert C, Warnking J, Depaulis A, *et al.* Microfabrication, characterization and *in vivo* MRI compatibility of diamond microelectrodes array for neural interfacing. *Mater Sci Eng C.* 2015;46:25–31.
- [326] Garrett DJ, Saunders AL, McGowan C, *et al.* *In vivo* biocompatibility of boron doped and nitrogen included conductive-diamond for use in medical implants. *J Biomed Mater Res.* 2016;104(1):19–26.
- [327] Bionic Eye Project. University of Melbourne. Available from: <https://biomedical.eng.unimelb.edu.au/neuroengineering/bionic-eye/>
- [328] Hadjinicolaou AE, Leung RT, Garrett DJ, *et al.* Electrical stimulation of retinal ganglion cells with diamond and the development of an all-diamond retinal prosthesis. *Biomaterials.* 2012;33(24):5812–5820.
- [329] Barriga-Rivera A, Bareket L, Goding J, *et al.* Visual prosthesis: interfacing stimulating electrodes with retinal neurons to restore vision. *Front Neurosci.* 2017;11:620.
- [330] Bergonzo P. DREAMS project – final activity report; 2006. Available from: [https://cordis.europa.eu/docs/publications/1235/123542961-6\\_en.pdf](https://cordis.europa.eu/docs/publications/1235/123542961-6_en.pdf)
- [331] Bergonzo P. Final report summary – NEUROCARE (Neuronal NanoCarbon Interfacing Structures); 2015. Available from: <https://cordis.europa.eu/project/rcn/102485/reporting/en>
- [332] Bergonzo P, Bongrain A, Scorsone E, *et al.* 3D shaped mechanically flexible diamond microelectrode arrays for eye implant applications: the MEDINAS project. *IRBM.* 2011;32(2):91–94.
- [333] Varney MW, Aslam DM, Janoudi A, *et al.* Polycrystalline-diamond MEMS biosensors including neural microelectrode-arrays. *Biosensors.* 2011;1(3):118–133.
- [334] Braingate. Available from: <https://www.braingate.org/>
- [335] Ivanova EP, Hasan J, Webb HK, *et al.* Bactericidal activity of black silicon. *Nat Commun.* 2013;4(1):2838.
- [336] Hazell G, May PW, Taylor P, *et al.* Studies of black silicon and black diamond as materials for antibacterial surfaces. *Biomater Sci.* 2018;6(6):1424–1432.
- [337] Dunseath O, Smith EJW, Al-Jeda T, *et al.* Studies of black diamond as an antibacterial surface for gram negative bacteria: the interplay between chemical and mechanical bactericidal activity. *Sci Rep.* 2019;9(1):8815.
- [338] Norouzi N, Woudstra W, Smith E, *et al.* Antimicrobial studies of black silicon and black diamond using Gram-positive bacteria. *Adv Eng Mater.* 2023;25(21):2301031.
- [339] Cumont A, Pitt AR, Lambert PA, *et al.* Properties, mechanism and applications of diamond as an antibacterial material. *Funct Diam.* 2021;1(1):1–28.
- [340] Jayaraman A. Diamond anvil cell and high-pressure physical investigations. *Rev Mod Phys.* 1983;55(1):65–108.
- [341] Bassett WA. Diamond anvil cell, 50th birthday. *High Pressure Res.* 2009;29(2):163–186.
- [342] Irifune T, Hemley RJ. Synthetic diamond opens windows into the deep earth. *EoS Trans.* 2012;93(7):65–66.
- [343] Samudrala G, Qiu W, Catledge SA, *et al.* Growth chemistry for the fabrication of designer diamonds for high pressure research. *High Pressure Res.* 2008;28(1):1–8.
- [344] Yang J, Li M, Zhang H, *et al.* Preparation of W–Ta thin-film thermocouple on diamond anvil cell for *in-situ* temperature measurement under high pressure. *Rev Sci Instrum.* 2011;82(4):045108.
- [345] Matsumoto R, Yamamoto S, Adachi S, *et al.* Diamond anvil cell with boron-doped diamond heater for high-pressure synthesis and *in situ* transport measurements. *Appl Phys Lett.* 2021;119(5):053502.
- [346] Biener J, Ho DD, Wild C, *et al.* Diamond spheres for inertial confinement fusion. *Nucl Fusion.* 2009;49(11):112001.
- [347] King C. The tiny diamond sphere that could unlock clean power. *BBC News*, February; 2023. Available from: <https://www.bbc.co.uk/news/business-64553796>
- [348] Kato H, Yamada H, Ohmagari S, *et al.* Synthesis and characterization of diamond capsules for direct-drive inertial confinement fusion. *Diam Relat. Mater.* 2018;86:15–19.
- [349] Wang T, Wang J, Liu Y, *et al.* High quality hollow diamond shell for inertial confinement fusion. *Diam Relat Mater.* 2023;135:109885.
- [350] Karmakar S, Mudiganti JC. Gyrotron: the most suitable millimeter-wave source for heating of plasma in Tokamak. In: Shahzad A, editor. *Plasma science and technology.* London, UK: IntechOpen; 2022.
- [351] Diamonds for fusion, F4E website; 2015. Available from: <https://fusionforenergy.europa.eu/news/diamonds-for-fusion/>
- [352] Mazzocchi F, Schreck S, Strauss D, *et al.* Diamond windows diagnostics for fusion reactors – updates of the design. *Fusion Eng Des.* 2017;123:820–824.
- [353] Aiello G, Avramidis KA, Gantenbein G, *et al.* Design verification of the gyrotron diamond output window for the upgrade of the ECRH system at W7-X. *Fusion Eng Des.* 2021;165:112262.
- [354] Duffy DM. Modeling plasma facing materials for fusion power. *Mater Today.* 2009;12(11):38–44.
- [355] Porro S, De Temmerman G, Lisgo S, *et al.* Nanocrystalline diamond coating of fusion plasma facing components. *Diam Relat Mater.* 2009;18(5–8):740–744.
- [356] Merola M, Loesser D, Martin A, *et al.* ITER plasma-facing components. *Fusion Eng Des.* 2010;85(10–12):2312–2322.
- [357] Chiang W-H, Mariotti D, Sankaran RM, *et al.* Microplasmas for advanced materials and devices. *Adv Mater.* 2020;32(18):1905508.
- [358] Mitea S, Zeleznik M, Bowden MD, *et al.* Generation of microdischarges in diamond substrates. *Plasma Sources Sci Technol.* 2012;21(2):022001.
- [359] Truscott BS, Turner C, May PW. High-pressure dc glow discharges in hollow diamond cathodes. *Plasma Sources Sci Technol.* 2016;25(2):025005.
- [360] South West Nuclear Hub. The diamond battery. Available from: <https://southwestnuclearhub.ac.uk/research/case-studies/diamond-battery/>
- [361] Gubbi J, Buyya R, Marusic S, *et al.* Internet of things (IoT): a vision, architectural elements, and future directions. *Future Gen Comp Syst.* 2013;29(7):1645–1660.
- [362] Delfaure C, Pomorski M, de Sanoit J, *et al.* Single crystal CVD diamond membranes for betavoltaic cells. *Appl Phys Lett.* 2016;108(25):252105.

- [363] Bormashov VS, Troschiev S, Tarelkin SA, *et al.* High power density nuclear battery proto-type based on diamond Schottky diodes. *Diam Relat Mater.* 2018;84:41–47.
- [364] Croot A, Wan G, Rowan A, *et al.* Beta radiation enhanced thermionic emission from diamond thin films. *Front Mech Eng.* 2017;3:17.
- [365] *Arkenlight, Ltd.* Available from: <https://www.arkenlight.co.uk/>
- [366] Li Y, Yang L, Jiang X, *et al.* Diamond nanostructures at different dimensions: synthesis and applications. *Adv Funct Mater.* 2024;34(30):2314558.
- [367] Toros A, Kiss M, Graziosi T, *et al.* Reactive ion etching of single crystal diamond by inductively coupled plasma: state of the art and catalog of recipes. *Diam Relat Mater.* 2020;108:107839.
- [368] Ohashi T, Sugimoto W, Takasu Y. Catalytic etching of {100}-oriented diamond coating with Fe, Co, Ni, and Pt nanoparticles under hydrogen. *Diam Relat Mater.* 2011;20(8):1165–1170.
- [369] Babchenko O, Kromka A, Hruska K, *et al.* Nanostructuring of diamond films using self-assembled nanoparticles. *Open Phys.* 2009;7(2):310–314.
- [370] Pope I, Payne L, Zorinians G, *et al.* Coherent anti-Stokes Raman scattering microscopy of single nanodiamonds. *Nat Nanotech.* 2014;9(11):940–946.
- [371] Nunn N, Torelli M, McGuire G, *et al.* Nanodiamond: a high impact nanomaterial. *Curr Opin Solid State Mater Sci.* 2017;21(1):1–9.
- [372] Mochalin VN, Shenderova O, Ho D, *et al.* The properties and applications of nanodiamonds. *Nat Nanotech.* 2012;7(1):11–23.
- [373] Dolmatov V, Veretennikova M, Marchukov V, *et al.* Currently available methods of industrial nanodiamond synthesis. *Phys Solid State.* 2004;46(4):611–615.
- [374] Krueger A, Ozawa M, Jarre G, *et al.* Deagglomeration and functionalisation of detonation diamond. *Phys Status Solidi A.* 2007;204(9):2881–2887.
- [375] Barnard AS, Russo SP, Snook IK. Coexistence of bucky diamond with nanodiamond and fullerene carbon phases. *Phys Rev B.* 2003;68(7):073406.
- [376] Krueger A, Lang D. Functionality is key: recent progress in the surface modification of nanodiamond. *Adv Funct Mater.* 2012;22(5):890–906.
- [377] Say JM, van Vreden C, Reilly DJ, *et al.* Luminescent nanodiamonds for biomedical applications. *Biophys Rev.* 2011;3(4):171–184.
- [378] Barnard AS. Diamond standard in diagnostics: nanodiamond biolabels make their mark. *Analyst.* 2009;134(9):1751–1764.
- [379] Ho D, Wang C-HK, Chow EK-H. Nanodiamonds: the intersection of nanotechnology, drug development, and personalized medicine. *Sci Adv.* 2015;1(7):e1500439.
- [380] Mochalin VN, Pentecost A, Li X-M, *et al.* Adsorption of drugs on nanodiamond: toward development of a drug delivery platform. *Mol Pharm.* 2013;10(10):3728–3735.
- [381] Williams O, editor. *Nanodiamond – RSC Nanoscience & Nanotechnology.* London: RSC; 2014.
- [382] Ho D. *Nanodiamonds – applications in biology and nanoscale medicine.* New York (NY): Springer; 2014.